



Observation of gauge boson joint-polarisation states in $W^\pm Z$ production from pp collisions at $\sqrt{s} = 13$ TeV with the ATLAS detector

The ATLAS Collaboration

Measurements of joint-polarisation states of W and Z gauge bosons in $W^\pm Z$ production are presented. The data set used corresponds to an integrated luminosity of 139 fb^{-1} of proton–proton collisions at a centre-of-mass energy of 13 TeV recorded by the ATLAS detector at the CERN Large Hadron Collider. The $W^\pm Z$ candidate events are reconstructed using leptonic decay modes of the gauge bosons into electrons and muons. The simultaneous pair-production of longitudinally polarised vector bosons is measured for the first time with a significance of 7.1 standard deviations. The measured joint helicity fractions integrated over the fiducial region are $f_{00} = 0.067 \pm 0.010$, $f_{0T} = 0.110 \pm 0.029$, $f_{T0} = 0.179 \pm 0.023$ and $f_{TT} = 0.644 \pm 0.032$, in agreement with the next-to-leading-order Standard Model predictions. Individual helicity fractions of the W and Z bosons are also measured and found to be consistent with joint helicity fractions within the expected amounts of correlation. Both the joint and individual helicity fractions are also measured separately in W^+Z and W^-Z events. Inclusive and differential cross sections for several kinematic observables sensitive to polarisation are presented.

1 Introduction

The study of weak boson polarisation provides a way to directly probe the Standard Model (SM) gauge and Higgs sectors and to discriminate between SM and beyond the Standard Model (BSM) signals. The existence of the longitudinally polarised state of weak bosons is a consequence of the non-vanishing mass of the bosons generated by the electroweak (EW) symmetry breaking mechanism. The measurement of the polarisation in diboson production therefore tests both the SM's gauge symmetry structure, through the existence of the triple gauge coupling, and the particular way this symmetry is spontaneously broken, via the longitudinal helicity state. Angular observables can be used to look for new interactions that can lead to different polarisation behaviour than predicted by the SM, to which the $W^\pm Z$ final state would be particularly sensitive [1, 2].

At hadron colliders, the polarisation of the W boson was previously measured in the decay of the top quark by the CDF and DØ [3–5] Collaborations and by the ATLAS [6] and CMS [7] Collaborations, as well as in single W production by ATLAS [8] and CMS [9]. Polarisation and several other related angular coefficient measurements of singly produced Z bosons were published by the CDF [10], CMS [11] and ATLAS [12] Collaborations. The polarisation of W bosons was also measured in ep collisions by the H1 Collaboration [13]. Finally, for dibosons, first measurements of the W polarisation were performed by LEP experiments in W pair production in e^+e^- collisions [14, 15] and were used to set limits on anomalous triple gauge couplings in Ref. [16]. Correlations between polarisation states of W particles were also probed experimentally at LEP [17–19]. Helicity fractions of pair-produced vector bosons were measured independently of each other and for the first time in hadronic collisions at a centre-of-mass energy of $\sqrt{s} = 13$ TeV by the ATLAS Collaboration [20], followed by the CMS Collaboration [21], using integrated luminosities of 36 fb^{-1} and 137 fb^{-1} , respectively. Benefiting from the full ATLAS data set available at $\sqrt{s} = 13$ TeV, combined with novel analysis techniques, observables more difficult to extract from data, such as the correlations between helicity states of the vector bosons, can now be accessed.

This Letter reports on an observation and measurement of joint polarisation states of weak bosons in $W^\pm Z$ production, extending the pioneering work of Ref. [20]. The W and Z bosons are reconstructed using their decay modes into electrons or muons. The pp collision data were collected with the ATLAS detector from 2015 to 2018 at a centre-of-mass energy of $\sqrt{s} = 13$ TeV and correspond to an integrated luminosity of 139 fb^{-1} . The individual and joint boson polarisation state fractions are measured consistently in the detector fiducial region and their relationships are studied. The reported measurements are compared to the recent fixed-order theory calculation of polarised W and Z boson pair production at next-to-leading-order (NLO) accuracy in quantum chromodynamics (QCD) [22, 23]. Additionally, the $W^\pm Z$ production cross section is measured within a fiducial phase space both inclusively and differentially as a function of several angular variables related to the helicity states of the $W^\pm Z$ system.

2 Theoretical framework and measurement phase space

A complete description of the polarisation states of the produced W and Z bosons is given in terms of the two-particle joint spin density matrix $\rho_{\lambda_W \lambda'_W \lambda_Z \lambda'_Z}$ expressed in the basis of joint-helicity states $(\lambda_W \lambda_Z)$ where λ_W and λ_Z are the helicities of the W and Z bosons, respectively. In terms of the $W^\pm Z$ production

helicity amplitudes, $F_{\lambda_W \lambda_Z}^{(\mu_q \mu_{\bar{q}})}$, the spin density matrix elements are defined by

$$\rho_{\lambda_W \lambda'_W \lambda_Z \lambda'_Z} \equiv \frac{1}{C} \times \sum_{\mu_q \mu_{\bar{q}}} F_{\lambda_W \lambda_Z}^{(\mu_q \mu_{\bar{q}})} F_{\lambda'_W \lambda'_Z}^{(\mu_q \mu_{\bar{q}})*}, \text{ where } C = \sum_{\mu_q \mu_{\bar{q}} \lambda_W \lambda_Z} \left| F_{\lambda_W \lambda_Z}^{(\mu_q \mu_{\bar{q}})} \right|^2.$$

The initial-state helicity is averaged in the numerator and denominator with sums running over $\mu_q, \mu_{\bar{q}} = \pm 1/2$. In the denominator the W and Z bosons helicities are summed over λ_i , where $\lambda_i = \pm 1, 0$, to normalise the trace of the matrix to unity. The complete 9×9 joint spin density matrix $\rho_{\lambda_W \lambda'_W \lambda_Z \lambda'_Z}$ cannot yet be measured because of the limited available data sample. Instead, the following four linear combinations of matrix elements are considered

$$\begin{aligned} f_{00} &= \rho_{0000}, \\ f_{\text{TT}} &= \rho_{++--} + \rho_{--++} + \rho_{----} + \rho_{++++}, \\ f_{0\text{T}} &= \rho_{00--} + \rho_{00++}, \\ f_{\text{T}0} &= \rho_{--00} + \rho_{++00}. \end{aligned}$$

The quantities f_{00} , f_{TT} , $f_{0\text{T}}$ and $f_{\text{T}0}$ are composed of diagonal elements of the full matrix and can be interpreted as probabilities of correlated helicity states of the two W and Z bosons. The distinction between the two transverse helicities of the bosons (right-handed, R, and left-handed, L, also indicated with + and -, respectively) is not made.

The single-boson spin density matrix $\rho_{\lambda\lambda'}$ is derived from the joint spin density matrix $\rho_{\lambda_W \lambda'_W \lambda_Z \lambda'_Z}$ by summing over indices of one of the bosons. It provides information about the helicity of one of the bosons regardless of the state of the other. Diagonal elements of the single-boson spin density matrix are the individual helicity fractions f_0 , f_{L} and f_{R} for the longitudinal, transverse left-handed and transverse right-handed helicity states, respectively. The normalisation is defined such that $f_0 + f_{\text{L}} + f_{\text{R}} = 1$.

Helicity fractions are not Lorentz invariant and hence depend on a chosen reference frame. In diboson production a natural frame choice for single-boson helicity fraction measurement is to fix the reference z -axis to the direction of the corresponding boson in the diboson centre-of-mass frame [23]. This definition is called the modified helicity coordinate system and is used for this measurement. The back-to-back kinematics of the bosons in the $W^\pm Z$ centre-of-mass frame implies that the polarisation vectors of the two bosons are defined with respect to the same reference axis, but in opposite directions. This choice also maximises the decorrelation between 00 and TT helicity states.

The relative contributions of joint helicity states can be determined from the absolute value of the cosine of the scattering angle of the W or Z boson in the WZ centre-of-mass frame, $|\cos \theta_V|$, calculated with respect to the beam axis [24, 25]. Events with 00 helicity have $|\cos \theta_V|$ values closer to 0 while events with TT helicity have $|\cos \theta_V|$ values closer to 1.

The polarisation of an individual gauge boson can be determined from the angular distribution of its decay products. At the Born level, the expected angular distribution for massless fermions in the rest frame of the parent W boson is given by [26–29]

$$\frac{1}{\sigma_{W^\pm Z}} \frac{d\sigma_{W^\pm Z}}{d \cos \theta_{\ell^* W}} = \frac{3}{8} f_{\text{L}} [(1 - q_W \cdot \cos \theta_{\ell^* W}^*)^2] + \frac{3}{8} f_{\text{R}} [(1 + q_W \cdot \cos \theta_{\ell^* W}^*)^2] + \frac{3}{4} f_0 \sin^2 \theta_{\ell^* W}^*, \quad (1)$$

where q_W is the charge of the W boson and $\theta_{\ell^* W}^*$ is defined using the modified helicity frame as the decay angle of the charged lepton in the W rest frame relative to the W direction in the $W^\pm Z$ centre-of-mass

frame. All dependencies on the azimuthal angle are integrated over. The expected angular distribution of the lepton decay products of the Z boson is described by the generalisation of Equation (1) [26–28]

$$\frac{1}{\sigma_{W^\pm Z}} \frac{d\sigma_{W^\pm Z}}{d \cos \theta_{\ell Z}^*} = \frac{3}{8} f_L (1 + 2\alpha \cos \theta_{\ell Z}^* + \cos^2 \theta_{\ell Z}^*) + \frac{3}{8} f_R (1 - 2\alpha \cos \theta_{\ell Z}^* + \cos^2 \theta_{\ell Z}^*) + \frac{3}{4} f_0 \sin^2 \theta_{\ell Z}^*, \quad (2)$$

where $\theta_{\ell Z}^*$ is defined using the modified helicity frame as the decay angle of the negatively charged lepton in the Z rest frame relative to the Z direction in the $W^\pm Z$ centre-of-mass frame. The parameter $\alpha = (2c_v c_a)/(c_v^2 + c_a^2) = 0.147$ is expressed in terms of the vector $c_v = -\frac{1}{2} + 2 \sin^2 \theta_W^{\text{eff}}$ and axial-vector $c_a = -\frac{1}{2}$ couplings of the Z boson to leptons, where the effective value of the Weinberg angle $\sin^2 \theta_W^{\text{eff}} = 0.23152$ [30] is used. Equation (2) also holds for the contribution from γ^* and its interference with the Z boson, with appropriate c_v and c_a coefficients.

The reported helicity fractions and cross sections are measured in a fiducial phase space chosen to closely follow the event selection criteria described in Section 5. It is based on the kinematics of particle-level objects as defined in Ref. [31]. These are final-state prompt¹ leptons associated with the W and Z boson decays. The kinematics of final-state prompt leptons is defined before QED final-state radiation (FSR), i.e. Born leptons.

The Born charged leptons from Z and W boson decay must have $|\eta| < 2.5$ and transverse momentum p_T above 15 GeV and 20 GeV, respectively; the invariant mass of the two leptons from the Z boson decay differs by at most 10 GeV from the world average value of the Z boson mass $m_Z^{\text{PDG}} = 91.1876$ GeV [30].

The W transverse mass, defined as $m_T^W = \sqrt{2 \cdot p_T^\nu \cdot p_T^\ell \cdot [1 - \cos \Delta\phi(\ell, \nu)]}$, where $\Delta\phi(\ell, \nu)$ is the angle between the lepton and the neutrino in the transverse plane, and p_T^ℓ and p_T^ν are the transverse momenta of the lepton from W boson decay and of the neutrino, respectively, must be greater than 30 GeV. In addition, it is required that the angular distance ΔR between the charged leptons from the W and Z decay is larger than 0.3, and that ΔR between the two leptons from the Z decay is larger than 0.2.

The contribution from off-shell effects is minimised by the tight invariant mass window of ± 10 GeV around the nominal Z boson mass used for the definition of the fiducial phase space. These contributions are estimated from NLO QCD calculations to amount to 2% at the integrated level and in most of the differential distributions [23]. However, all the helicity fractions presented here are effective fractions and contain the small non-resonant contributions present in the fiducial phase space, including γ^* events. Interferences among helicity states are also expected to be small, amounting to 0.6% according to NLO QCD+EW calculations [32]. Their effect is included in the measured helicity fractions.

A total phase space is also defined by requiring only the invariant mass of the lepton pair associated with the Z boson to be in the range $66 < m_{\ell\ell} < 116$ GeV. This serves for the generation of polarised Monte Carlo (MC) event templates described in Section 7 for which no restrictions should be applied to the phase space of the decay leptons from W and Z bosons.

¹ A prompt lepton is a lepton that is not produced in the decay of a hadron, a τ -lepton, or their descendants.

3 ATLAS detector

The ATLAS experiment [33] at the LHC is a multipurpose particle detector with a forward–backward symmetric cylindrical geometry and a near 4π coverage in solid angle.² It consists of an inner tracking detector (ID) surrounded by a thin superconducting solenoid providing a 2 T axial magnetic field, electromagnetic and hadron calorimeters and a muon spectrometer (MS). The inner tracking detector covers the pseudorapidity range $|\eta| < 2.5$. It consists of silicon pixel, silicon microstrip and transition radiation tracking detectors. Lead/liquid-argon (LAr) sampling calorimeters provide electromagnetic (EM) energy measurements with high granularity. A steel/scintillator-tile hadron calorimeter covers the central pseudorapidity range ($|\eta| < 1.7$). The endcap and forward regions are instrumented with LAr calorimeters for both the EM and hadronic energy measurements up to $|\eta| = 4.9$. The muon spectrometer surrounds the calorimeters and is based on three large superconducting air-core toroidal magnets with eight coils each. The field integral of the toroids ranges between 2.0 and 6.0 T m across most of the detector. The muon spectrometer includes a system of precision tracking chambers and fast detectors for triggering. A two-level trigger system is used to select events. The first-level trigger is implemented in hardware and uses a subset of the detector information to accept events at a rate below 100 kHz. This is followed by a software-based trigger that reduces the accepted event rate to 1 kHz on average depending on the data-taking conditions. An extensive software suite [34] is used in the reconstruction and analysis of real and simulated data, in detector operations, and in the trigger and data acquisition systems of the experiment.

4 Signal and background simulation

MC simulation is used to model signal and most background processes.

An inclusive sample of simulated $W^\pm Z$ events is used to correct the signal yield for detector effects and to compare the measurements with the theoretical predictions. The production of $W^\pm Z$ pairs and the subsequent leptonic decays of the vector bosons were simulated at NLO in QCD and LO in QED using the POWHEG-BOX v2 [35–38] generator, interfaced to PYTHIA 8.210 [39] for simulation of parton showering, hadronisation and the underlying event. Final-state radiation resulting from QED interactions was simulated using PYTHIA 8.210 with the AZNLO [40] set of tuned parameters. The CT10NLO [41] parton distribution function (PDF) set was used for the hard-scattering process, while the CTEQ6L1 [42] PDF set was used for the parton shower. The sample was generated with dynamic renormalisation and factorisation QCD scales, μ_r and μ_f , equal to $m_{WZ}/2$, where m_{WZ} is the invariant mass of the WZ system [20].

For systematic uncertainties studies, two alternative inclusive $W^\pm Z$ signal samples were generated at NLO in QCD. The first alternative sample was generated using MADGRAPH5_AMC@NLO 2.6.5 [43]. Matrix elements containing three leptons, one neutrino and up to two jets in the final state were calculated at NLO QCD and merged with the parton shower from PYTHIA 8.210 using the FxFx scheme [44]. The NNPDF3.0NLO [45] PDF set was used for the hard-scattering process. The default dynamic renormalisation and factorisation scale set by MADGRAPH5_AMC@NLO was used [46]. This MC sample is referred to as MADGRAPH5_AMC@NLO+PYTHIA.

² ATLAS uses a right-handed coordinate system with its origin at the nominal interaction point (IP) in the centre of the detector and the z -axis along the beam pipe. The x -axis points from the IP to the centre of the LHC ring, and the y -axis points upwards. Cylindrical coordinates (r, ϕ) are used in the transverse plane, ϕ being the azimuthal angle around the z -axis. The pseudorapidity is defined in terms of the polar angle θ as $\eta = -\ln \tan(\theta/2)$. Angular distance is measured in units of $\Delta R \equiv \sqrt{(\Delta\eta)^2 + (\Delta\phi)^2}$.

The second alternative $W^\pm Z$ signal sample was generated using the SHERPA 2.2.2 generator [47]. Matrix elements contain all diagrams with four electroweak vertices. They were calculated for up to one parton at NLO and up to three partons at LO using Comix [48] and OPENLOOPS [49], and merged with the SHERPA parton shower [50] according to the ME+PS@NLO prescription [51]. The NNPDF3.0_{NNLO} PDF set was used along with the associated set of tuned parton-shower parameters developed by the SHERPA authors.

Polarised $W^\pm Z$ events were generated at LO in QCD using MADGRAPH5_AMC@NLO 2.7.3 [52] interfaced to PYTHIA 8.244 for simulation of parton showering, hadronisation and the underlying event. The generation of polarised events is not possible at the full NLO QCD accuracy. To account for the real part of NLO corrections, events were simulated with either no jets or one jet in the matrix element at LO, and merged with PYTHIA parton shower using the CKKW-L scheme [53, 54]. The NNPDF3.0_{NLO} PDF set was used for the hard-scattering process. Four separate MC samples were generated corresponding to the four joint helicity states 00, 0T, T0 and TT, respectively. An inclusive MC sample was created by adding the four polarised samples. These MC sets are referred to as MADGRAPH 0,1j@LO.

The background sources in this analysis include processes with two or more electroweak gauge bosons, namely ZZ , WW and VVV ($V = W, Z$); processes with top quarks, such as $t\bar{t}$ and $t\bar{t}V$, single top and tZj ; and processes with gauge bosons associated with jets or photons ($Z + j$ and $Z\gamma$). Electroweak $W^\pm Z$ production, $WZjj$ -EW, arising at the order α_{EW}^6 is also considered as a background and not part of the measured signal. MC simulation is used to estimate the contribution from background processes with three or more prompt leptons. Background processes with at least one misidentified lepton are evaluated using data-driven techniques and simulated events are used to assess the systematic uncertainties of these backgrounds.

The SHERPA 2.2.2 event generator was used to simulate both the $q\bar{q}$ and gg -initiated ZZ processes, including $H \rightarrow ZZ$ production, using the NNPDF3.0_{NNLO} PDF set. It provides a matrix element calculation accurate to NLO in α_s for 0- and 1-jet final states, and LO accuracy for 2- and 3-jet final states. Triboson events were simulated by the SHERPA 2.2.2 event generator at NLO accuracy with 0 additional partons and at LO accuracy with one and two additional partons and using the NNPDF3.0_{NNLO} PDF set.

Both the $t\bar{t}Z$ and $t\bar{t}W$ processes were generated at NLO with the MADGRAPH5_AMC@NLO MC generator, using the NNPDF3.0_{NLO} PDF set, and interfaced to the PYTHIA 8.186 [55] parton shower model.

Finally, the tZj and $WZjj$ -EW processes were generated at LO by the MADGRAPH5_AMC@NLO MC generator interfaced with PYTHIA 8.244 for the modelling of the parton shower, hadronisation and underlying event. The parton distribution function set was NNPDF3.0_{NLO}. In the simulation of the parton shower the NNPDF2.3_{LO} [56] PDF set was used.

All generated MC events were passed through the ATLAS detector simulation [57], based on GEANT4 [58], and processed using the same reconstruction software as used for the data. The event samples include the simulation of additional pp interactions (pile-up) generated with PYTHIA 8.186 using the NNPDF2.3_{LO} PDF set and the A3 [59] set of tuned parameters for the underlying event and parton fragmentation. Simulated events were reweighted to match the pile-up conditions observed in the data. Scale factors were applied to simulated events to correct for small differences in the efficiencies observed in data and predicted by MC simulation for the trigger, reconstruction, identification, isolation and impact parameter requirements of electrons and muons [60, 61]. Furthermore, the electron energy and muon momentum in simulated events were smeared to account for small differences in resolution between data and MC events [60, 62].

5 Event reconstruction and selection

Only data recorded with stable beam conditions and with all relevant detector subsystems operational are considered. Candidate events are selected using triggers [63–65] that require at least one electron or muon. These triggers require leptons to pass different transverse momentum threshold and isolation criteria, which depend on the data-taking run period and the instantaneous luminosity. The combined efficiency of these triggers is 99% for $W^\pm Z$ events satisfying the offline selection criteria. Events are required to have a primary vertex compatible with the LHC luminous region inside the ATLAS detector. The primary vertex is defined as the reconstructed vertex with at least two charged-particle tracks that has the largest sum of the p_T^2 for the associated tracks.

Muon candidates are identified by tracks reconstructed in the MS and matched to tracks reconstructed in the ID. Muons are required to pass a ‘medium’ identification selection, which is based on requirements on the number of hits in the ID and the MS [61, 62]. The efficiency of this selection averaged over p_T and η is larger than 98%. The muon momentum is measured by combining the MS measurement, corrected for the energy deposited in the calorimeters, and the ID measurement. The p_T of the muon must be greater than 15 GeV and its pseudorapidity must satisfy $|\eta| < 2.5$.

Electron candidates are reconstructed from energy clusters in the electromagnetic calorimeter matched to ID tracks. Electrons are identified using a discriminant that is the value of a likelihood function constructed with information about the shape of the electromagnetic showers in the calorimeter, the track properties and the quality of the track-to-cluster matching for the candidate [60]. Electrons must satisfy a ‘medium’ likelihood requirement, which provides an overall identification efficiency of 90%. The electron momentum is computed from the cluster energy and the direction of the track. The p_T of the electron must be greater than 15 GeV and the pseudorapidity of the cluster must satisfy $|\eta| < 1.37$ or $1.52 < |\eta| < 2.47$.

Electron and muon candidates are required to originate from the primary vertex and to be isolated from other particles using both calorimeter-cluster and ID-track information. The isolation efficiency is at least 90% for electrons with $p_T > 25$ GeV and muons with $p_T > 15$ GeV and at least 99% for electrons and muons with $p_T > 60$ GeV [60, 61].

Jets of hadrons are reconstructed using a particle-flow algorithm based on noise-suppressed positive-energy topological clusters in the calorimeter [66]. Energy deposited in the calorimeter by charged particles is subtracted and replaced by the momenta of tracks which are matched to those topological clusters. The jets are clustered using the anti- k_t algorithm [67, 68] with a radius parameter $R = 0.4$. They are calibrated according to in situ measurements of the jet energy scale [69]. All jets must have $p_T > 25$ GeV and be reconstructed in the pseudorapidity range $|\eta| < 4.5$. Jets with p_T below 60 GeV and with $|\eta| < 2.4$ have to pass a requirement on the *jet vertex tagger* [70], a likelihood discriminant that uses a combination of track and vertex information to suppress jets originating from pile-up activity. Jets with $|\eta| < 2.5$ containing a b -hadron are identified with a deep-learning neural network (NN) [71–73] which uses distinctive features of b -hadron decays in terms of the impact parameters of the tracks and the displaced vertices reconstructed in the inner detector. Jets initiated by b -quarks are selected by setting the algorithm’s output threshold such that an 85% b -jet selection efficiency is achieved in simulated $t\bar{t}$ events, with a rejection factor of 40 against light-flavour jets.

The transverse momentum of the neutrino is estimated from the missing transverse momentum in the event, E_T^{miss} , calculated as the negative vector sum of the transverse momentum of all identified hard physics objects (electrons, muons, jets), with a contribution from an additional soft term. This soft term is calculated from ID tracks matched to the primary vertex and not assigned to any of the hard objects [74].

Events are required to contain exactly three lepton candidates satisfying the selection criteria described above. To ensure that the trigger efficiency is well determined, at least one of the candidate leptons is required to have $p_T > 25$ GeV for 2015 and $p_T > 27$ GeV for 2016–2018 data, as well as being geometrically matched to a lepton that was selected by the trigger. No requirement on the number of jets is applied.

In order to suppress background processes with at least four prompt leptons, events with a fourth lepton candidate satisfying looser selection criteria are rejected. For this looser selection, the lepton p_T requirement is lowered to $p_T > 5$ GeV, electrons are allowed to be reconstructed in the region $1.37 < |\eta| < 1.52$ and ‘loose’ identification requirements [60, 61] are used for both the electrons and muons. A less stringent requirement is applied for electron isolation and is based only on ID track information. No dedicated identification algorithm is used to suppress events with electrons and muons originating from the decay of τ -leptons.

Candidate events are required to have at least one pair of leptons with the same flavour and opposite charge, with an invariant mass that is consistent with m_Z^{PDG} to within 10 GeV. This pair is considered to be the Z boson candidate. If more than one pair can be formed, the pair whose invariant mass is closest to the nominal Z boson mass is taken as the Z boson candidate. The remaining third lepton is assigned to the W boson decay. The transverse mass of the W candidate, computed using E_T^{miss} and the p_T of the associated lepton, is required to be greater than 30 GeV.

Backgrounds originating from misidentified leptons are suppressed by requiring the lepton associated with the W boson to satisfy more stringent selection criteria. The transverse momentum of this lepton is therefore required to be greater than 20 GeV. This lepton is also required to pass the ‘tight’ identification requirements, which results in an efficiency between 90% and 98% for muons and an overall efficiency of 85% for electrons.

The main challenge in the reconstruction of the full kinematics of the selected events arises for the W boson from incomplete knowledge of the neutrino momentum. In the previous ATLAS publication [20] the neutrino longitudinal momentum p_z^ν was reconstructed analytically using the W mass constraint. In this analysis a neural network regression is developed to reconstruct p_z^ν . Input variables to the NN are p_T and p_z of the charged lepton from the W boson decay, the E_T^{miss} components perpendicular and parallel to the direction of this charged lepton and the p_z^ν reconstructed analytically. The NN is trained using $W^\pm Z$ POWHEG+PYTHIA MC events at detector level to reconstruct event-by-event the true p_z^ν value in the MC simulation. The compatibility of the reconstructed W boson mass m_W with its generated value is ensured by using as the loss function the sum of the root-mean-square (RMS) of the deviations of m_W and p_z^ν reconstructed values from their generated values. The regression method provides a reasonable estimate of p_z^ν for events for which the analytical method fails³ and reduces the p_z^ν error RMS by 10% thanks to the improved resolution at high p_z^ν . This improvement comes from fact that the NN is trained to account for the full width of the generated W boson, whereas the analytical method imposes a single value of the W boson mass, fixed to its pole mass, for all events. Additionally, the regression method improves the m_W resolution from 41% obtained with the analytical method to 31%. This in turn improves the reconstruction of angular observables in the modified helicity frame.

³ The analytical method relies on a second-order equation which has complex solutions for roughly 30% of the events. In those cases, its imaginary part is set to zero.

6 Background estimation

The background sources are classified into two groups: events where at least one of the candidate leptons is not a prompt lepton (reducible background) and events where all candidates are prompt leptons or are produced in the decay of a τ -lepton (irreducible background). Candidates that are not prompt leptons are also called ‘misidentified’ leptons.

Events in the first group mostly originate from $Z + j$, $Z\gamma$, $t\bar{t}$, and WW production processes and constitute about 5% of all selected events. This reducible background is estimated with a data-driven method based on the inversion of a matrix containing the efficiencies and misidentification probabilities for prompt and misidentified leptons [20, 75–77]. The method exploits the classification of the leptons as loose or tight candidates and the probability that a non-prompt lepton is misidentified as a loose or tight lepton. Tight leptons are leptons passing the selection criteria described in Section 5. Loose leptons are leptons that do not meet the isolation and identification criteria for signal leptons but satisfy only looser criteria. The misidentification probabilities for misidentified leptons are determined from data using dedicated control samples each enriched in misidentified leptons from light- or heavy-flavour jets and from photon conversions, respectively. The lepton efficiencies for prompt leptons are determined as detailed in Refs. [60–62]. The lepton efficiencies and misidentification probabilities are combined with event rates in data samples of $W^\pm Z$ candidate events where at least one and up to three of the leptons are loose. Then, solving a system of linear equations, the number of events with at least one misidentified lepton is obtained, which represents the amount of reducible background in the $W^\pm Z$ sample. About 2% of this background contribution arises from events with two misidentified leptons. The background from events with three misidentified leptons, e.g. from multijet processes, is negligible. The method allows the shape of any kinematic distribution of reducible background events to be estimated. Another independent method of assessing the reducible background was also considered. This method estimates the amount of reducible background using MC simulations scaled to data by process-dependent factors determined from the data-to-MC comparison in dedicated control regions. Agreement within 20% with the matrix method estimate is obtained in both yield and shape of the distributions of irreducible background events.

The events contributing to the second group of background processes represent $\sim 18\%$ of all selected events. They originate from ZZ , $t\bar{t} + V$, VVV (where $V = Z$ or W) and tZj events. Events from $W^\pm Z$ production with at least one τ -lepton decay or from electroweak $WZjj$ –EW production are also considered as backgrounds and not part of the measured signal. The amount of irreducible background is estimated using MC simulations. The dominant contribution in this second group is from ZZ production, where one of the leptons from the ZZ decay falls outside the detector acceptance. It represents about 7.5% of all selected events. The MC-based estimates of the ZZ and $t\bar{t} + V$ backgrounds are validated by comparing the MC expectations with the event yield and several kinematic distributions of data samples enriched in ZZ and $t\bar{t} + V$ events, respectively. The ZZ control sample is selected from events with a Z candidate which meets all of the analysis selection criteria and which is accompanied by two additional leptons, satisfying the lepton criteria described in Section 5. The ZZ MC expectation is rescaled to match the data by combining the $W^\pm Z$ signal region and a single bin containing all of the events from the ZZ control region in the fit detailed in Section 7 and used to extract the helicity fractions. A scaling factor of 1.13 is obtained from the fit for the ZZ MC contribution, in agreement with the ZZ cross-section measurements performed at $\sqrt{s} = 13$ TeV [78]. The $t\bar{t} + V$ control sample is selected by requiring selected $W^\pm Z$ events to have at least two reconstructed b -jets. The observed data event yield in this validation region is matching the $t\bar{t} + V$ MC prediction rescaled by a factor of 1.3. This scaling factor relative to predictions is in line with the $t\bar{t} + Z$ cross-section measurements performed at $\sqrt{s} = 13$ TeV [79]. The contribution of $t\bar{t} + V$

events amounts to $\sim 4\%$ of all selected events. Systematic uncertainties affecting the rescaling of ZZ and $t\bar{t} + V$ MC predictions are discussed in Section 8. Finally, some $W^\pm\gamma^*$ events produced outside of the total phase space can be selected at detector level. The contribution of such events is estimated from the $W^\pm Z$ POWHEG+PYTHIA MC simulation to amount to 0.5% and is subtracted from data.

7 Measurement methodology

7.1 Joint boson polarisation

In the Born-level fiducial phase space, the $|\cos\theta_V|$, $q_W \cdot \cos\theta_{\ell W}^*$ and $\cos\theta_{\ell Z}^*$ angular observables can be used together to separate the joint helicity states from an inclusive MC sample and determine their respective generated fractions. However, when using the same angular observables at detector level, the separation of the different joint helicity states is not sufficient for the measurement of their respective fractions with an expected precision of 5σ . Therefore, a multivariate discriminant exploiting more kinematic observables is used to better separate the four joint helicity states. A deep neural network (DNN) classifier is implemented to exploit kinematic differences between polarisation states in different observables. Keras v2.2.4-tf [80] with the Tensorflow v1.3 [81] backend are used. The DNN is trained and optimised using simulated MADGRAPH 0,1j@LO polarised MC samples. A total of eight variables are used as inputs to the DNN: the transverse momenta of the three leptons and of the neutrino, $p_T^{\ell W}$, $p_T^{\ell Z}$, p_T^{ν} and E_T^{miss} , angular variables as the absolute difference between the rapidities of the Z boson and the lepton from the decay of the W boson, $|y_Z - y_{\ell W}|$, the azimuthal angle difference between the two leptons of each W and Z -boson decay, $\Delta\phi(\ell^W, \nu)$, $\Delta\phi(\ell_1^Z, \ell_2^Z)$, respectively, and the transverse momentum of the WZ system p_T^{WZ} . The DNN classifier is trained such that the components of the vector output, one for each of the four joint-polarisation states, are combined in a single output node in its last layer, used in the analysis for the separation. The optimisation of the combination is part of the DNN training procedure and a sigmoid activation function is applied to the combination output. The output is therefore a continuous score, labelled ‘DNN score,’ ranging from 0 to 1 that takes typical values peaking around 0, 0.5, and 1 for TT, mixed 0T and T0, and 00 helicity states, respectively. The DNN classifier achieves integrals of the receiver operating characteristic (ROC) curves between 0.8 and 0.85 for separating the 00 state from each of the three others joint polarisation states. The sensitivity of the analysis in disentangling the mixed helicity states 0T and T0 is achieved by categorising events depending on the $\cos\theta_{\ell W}^*$ and $\cos\theta_{\ell Z}^*$ observables. Four categories are defined as $(|\cos\theta_{\ell W}^*| < 0.5, |\cos\theta_{\ell Z}^*| < 0.5)$, $(|\cos\theta_{\ell W}^*| > 0.5, |\cos\theta_{\ell Z}^*| < 0.5)$, $(|\cos\theta_{\ell W}^*| < 0.5, |\cos\theta_{\ell Z}^*| > 0.5)$ and $(|\cos\theta_{\ell W}^*| > 0.5, |\cos\theta_{\ell Z}^*| > 0.5)$. A one-dimensional representation of the DNN score variable in the four $(|\cos\theta_{\ell W}^*|, |\cos\theta_{\ell Z}^*|)$ categories, shown in Figure 1 and referred to as the 4-category DNN score, is built.

To measure joint helicity fractions a binned maximum-likelihood fit [82] to data of the four helicity states templates is performed. The binned likelihood function used in the fit consists of a product of Poisson probability terms over bins of the 4-category DNN score distribution in the $W^\pm Z$ signal region and a single-bin integrating over the ZZ control region. Each source of systematic uncertainty is implemented in the likelihood function as a nuisance parameter with a Gaussian constraint, except for the NLO QCD modelling systematic uncertainty described in section 8. Independent parameters of the fit are the particle level helicity fractions f_{00} , f_{T0} , f_{TT} and the integrated fiducial cross section. The fourth joint helicity fraction f_{0T} is obtained using the constraint $f_{00} + f_{0T} + f_{T0} + f_{TT} = 1$. Differences between detector-level and particle-level fractions due to detector efficiencies and QED final-state radiation effects are accounted

for in the fit using independent correction factors applied to each helicity fraction. The factors are obtained from simulation and range from 0.95 to 1.01 depending on the helicity state.

As observed in theory calculations [23], a strong relationship exists between NLO QCD corrections and polarisation effects. Therefore, templates for helicity states generated at LO are insufficient. The MADGRAPH 0,1j@LO MC simulation corrects for the real part of NLO QCD effects but misses virtual corrections that are also important for polarisation measurements. In order to verify that the shapes of the polarised templates are valid, a closure test is performed. Templates are used to fit pseudo-data generated using inclusive MC simulations at NLO QCD accuracy, such as with POWHEG+PYTHIA or MADGRAPH5_AMC@NLO+PYTHIA. The fit is performed on detector-level distributions. Polarisation fractions extracted from the fit are compared with the generated polarisation fractions of the NLO MC samples. Differences from 10% to 50% depending on the polarisation state are observed between extracted and built-in fractions when using polarised templates from the MADGRAPH 0,1j@LO generation. This demonstrates the need for using polarised templates at NLO QCD accuracy for polarisation measurements.

Templates better approaching the NLO QCD accuracy are built using a DNN-based event-by-event reweighting procedure [83]. Four DNNs are trained and each of them is specialised to reweight at particle-level the inclusive MADGRAPH 0,1j@LO events to one of the four joint polarised states. Input variables of the DNNs are those of the polarisation DNN classifier augmented by the invariant mass of the WZ system m_{WZ} , and the angular variables $\cos \theta_{\ell W}^*$, $\cos \theta_{\ell Z}^*$ and $|\cos \theta_V|$. The four DNNs are then applied to reweight the inclusive POWHEG+PYTHIA MC events, creating four polarised MC templates with NLO-like accuracy in QCD. This method provides the best fit closure, with no bias on the extracted polarisation fractions visible within the statistical precision of the closure test.

A second method is used to create NLO QCD accurate polarised templates, based on the available fixed-order parton-level theory predictions [23]. Predicted distributions, including the output score of the DNN classifier, are calculated in the parton-level fiducial phase space [23]. Corrections for parton-shower (PS) effects on the shape of the templates are incorporated by binned factors. The correction factors are calculated per helicity state by comparing MADGRAPH 0,1j@LO predictions at particle and parton level. The templates obtained at particle level are transformed to detector level using a folding procedure to account for detector effects. This method provides a good fit closure, reducing the bias up to $\sim 10\%$. This template creation method is used to estimate systematic uncertainties in the template shapes.

Interference among polarisation states manifests itself as a shape difference between the sum of polarised templates and the inclusive distribution. This difference is expected to be at most 4% for the DNN score observable [23]. The fit procedure adjusts fitted polarisation fractions such that the sum of polarised templates matches the inclusive distribution of data, with increased fit uncertainties. The measured polarisation fractions therefore include interference effects.

7.2 Individual boson polarisation

For individual W and Z boson polarisation states, the helicity parameters f_0 and $f_L - f_R$ are measured using a fit of templates for the three f_0 , f_L and f_R helicity states to the $q_W \cdot \cos \theta_{\ell W}^*$ and $\cos \theta_{\ell Z}^*$ distributions. The equation $f_0 + f_R + f_L = 1$ is used to constrain the independent parameters of the fit to determine f_0 , $f_L - f_R$ and the integrated fiducial cross section. Templates with NLO QCD accuracy are also required for the $q_W \cdot \cos \theta_{\ell W}^*$ and $\cos \theta_{\ell Z}^*$ distributions. Neither such templates at NLO QCD accuracy nor templates for left- and right-handed helicity states of the vector bosons can be produced by the MADGRAPH5_AMC@NLO 2.7.3 MC event generator. The templates for the $q_W \cdot \cos \theta_{\ell W}^*$ and $\cos \theta_{\ell Z}^*$

distributions for each of the three individual helicity states of the W and Z bosons are therefore created from the inclusive POWHEG+PYTHIA MC sample using a reweighting technique [20]. For each of the gauge bosons the predicted helicity fractions of POWHEG+PYTHIA MC events are determined using the moment method [12, 26] in the total phase space. Following the method detailed in Ref. [20], the predicted fractions are used to reweight POWHEG+PYTHIA MC events to represent each of the longitudinal, left- and right-handed states of the W or Z bosons. This creates polarised MC templates at detector level.

7.3 Differential cross section

Independently of polarisation fractions, the inclusive $W^\pm Z$ production cross section is measured differentially within the fiducial phase space defined at particle level and as a function of the variables the most sensitive to polarisation of the vector bosons. Similarly to measurements in Ref. [20], the differential detector-level distributions of background-subtracted data are corrected for detector resolution, efficiencies and QED final-state radiation effects using simulated signal events and an iterative Bayesian unfolding method [84], as implemented in the RooUnfold toolkit [85]. The number of iterations ranges from two to four, depending on the resolution in the unfolded variable and chosen in order to minimise the sum of the expected statistical and unfolding uncertainties in the unfolded distribution. The width of the bins in each distribution is chosen according to the experimental resolution and to the statistical significance of the expected number of events in each bin. The fraction of signal MC events generated in a bin which are reconstructed in the same bin is always greater than 35%. The detector-level distributions are unfolded with a response matrix computed using the POWHEG+PYTHIA MC signal sample that includes all four measured decay channels (eee , $ee\mu$, $\mu\mu e$ and $\mu\mu\mu$) and is divided by four, such that cross sections refer to final states where the W and Z bosons decay in a single leptonic channel with muons or electrons.

8 Systematic uncertainties

Systematic uncertainties affecting the shape and normalisation of the 4-category DNN score distribution for the background contributions, as well as the acceptance of the helicity components and the shape of their templates, are considered.

Uncertainties due to theoretical modelling in the helicity templates for higher order QCD corrections are evaluated by varying in the POWHEG+PYTHIA MC simulation the renormalisation and factorisation scales independently by factors of two and one-half, removing combinations where the variations differ by a factor of four. The uncertainties due to the PDF and the α_s value used in the PDF determination are evaluated using the PDF4LHC prescription [86].

For joint polarisation measurements an uncertainty due to the modelling of NLO QCD is estimated by comparing predictions of the 4-category DNN score distributions for each of the joint-helicity states obtained from the parton-level NLO calculation with the DNN reweighting of the POWHEG+PYTHIA MC simulation. The difference between the predicted shapes from the two methods is considered as an uncertainty. The associated nuisance parameter in the fit is parametrised by a flat constraint in the range between the two template shapes from each of the method, with steeply vanishing constraints outside of this range, defined using a double Fermi distribution. A specific uncertainty is attributed to the DNN reweighting method. It is estimated by applying the reweighting method to inclusive MADGRAPH 0,1j@LO

MC events and comparing the obtained distributions with those of polarised MADGRAPH 0,1j@LO MC events. The difference between the shapes is treated as an uncertainty.

For individual boson polarisation measurements a modelling uncertainty in the helicity templates is estimated by comparing predictions of the $q_W \cdot \cos \theta_{\ell W}^*$ and $\cos \theta_{\ell Z}^*$ distributions from the POWHEG+PYTHIA event generator with those of SHERPA. The difference between the predicted shapes from the two generators is considered as an uncertainty. An uncertainty is attributed to the reweighting method used to create templates with individually polarised bosons from inclusive POWHEG+PYTHIA MC events. It is estimated in the same way as for the joint polarisation measurement.

Uncertainties in differential cross-section measurements arising from imperfect description of the data by the POWHEG+PYTHIA MC simulation are evaluated using a data-driven method [87]. Each MC differential distribution is corrected to match the data distribution and the resulting weighted MC distribution at detector level is unfolded with the response matrix used in the actual data unfolding. The new unfolded distribution is compared with the weighted MC distribution at particle level and the difference is taken as the systematic uncertainty. An additional uncertainty is derived to account for more subtle differences between the POWHEG+PYTHIA and MADGRAPH5_AMC@NLO+PYTHIA generators (e.g. hadronisation models, additional soft objects, mis-modelling in other kinematic variables). The MADGRAPH5_AMC@NLO+PYTHIA generator is used to unfold the data and deviation from the nominal result is taken as the uncertainty. In order to remove effects already accounted for in the data-driven method, the MADGRAPH5_AMC@NLO+PYTHIA distributions were first reweighted to match POWHEG+PYTHIA distributions at particle level.

Systematic uncertainties affecting the reconstruction and energy calibration of electrons, muons and jets are propagated through the analysis. The uncertainties due to lepton reconstruction, identification, isolation requirements and trigger efficiencies as well as in the lepton momentum scale and resolution are assessed using tag-and-probe methods in $Z \rightarrow \ell\ell$ events [60–62]. The uncertainties in the jet energy scale and resolution are based on their respective measurements in data [88]. The uncertainty in E_T^{miss} is estimated by propagating the uncertainties in the transverse momenta of reconstructed objects and by applying momentum scale and resolution uncertainties to the track-based soft term [74]. A variation in the pile-up reweighting of MC events is included in order to cover the uncertainty in the ratio of the predicted and measured pp inelastic cross sections [89]. For the measurements of the W charge-dependent polarisation fractions, an uncertainty arising from the charge misidentification of electrons is also considered.

The uncertainty in the amount of background from misidentified leptons takes into account the limited number of events in the control regions as well as the difference in background composition between the control region used to determine the lepton misidentification rate and the control regions used to estimate the yield in the signal region. This results in an uncertainty of about 25% in the total misidentified-lepton background yield and in the shape of the differential distributions of the reducible background events.

Uncertainties due to the theoretical modelling of ZZ generated events are considered. They arise from higher-order QCD corrections and the PDFs and are evaluated in the same way as for $W^\pm Z$ events. The uncertainty due to irreducible background sources other than ZZ is evaluated by propagating the uncertainty in their MC cross sections. These are 30% for VVV [90], 25% for $WZjj$ -EW [91] and 15% for tZj [92] and $t\bar{t} + V$ [79, 93]. The contribution of events from $W^\pm Z$ production with at least one τ -lepton decay is linked in the fit to the measured $W^\pm Z$ production cross section for electron and muon decays. A normalisation uncertainty of 10% is attributed to this contribution to account for a possible mis-modelling in the MC simulation of the efficiency to select $W^\pm Z$ events with a τ -lepton decay.

The uncertainty in the combined 2015–2018 integrated luminosity is 1.7% [94], obtained using the LUCID-2 detector [95] for the primary luminosity measurements. It is applied to the signal normalisation as well as to all background contributions that are estimated using only MC simulations.

The effect of the systematic uncertainties on the final results after the maximum-likelihood fit is shown in Table 3 where the breakdown of the contributions to the uncertainties in the measured joint polarisation fractions is presented.

9 Results

9.1 Joint boson polarisation measurements

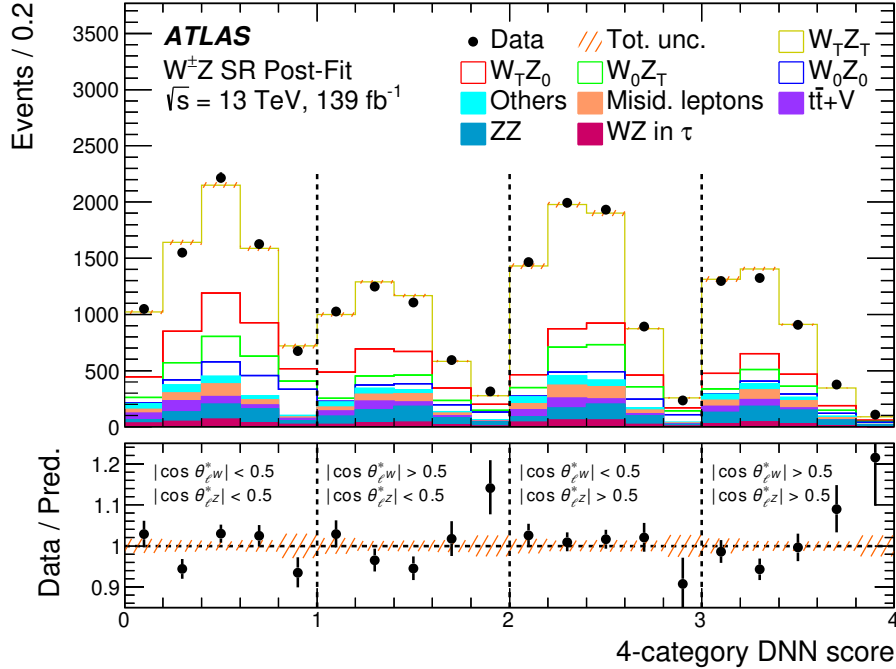


Figure 1: Post-fit distribution of the 4-category DNN score in $W^\pm Z$ events at detector level in the signal region (SR). The 4-category DNN score is defined for each event as the sum of the DNN score and of the category number ranging from 0 to 3. Respective contributions of the $W^\pm Z$ joint-helicity states 00, 0T, T0 and TT and backgrounds are normalised to the expected number of events after the fit. The sum of background events containing misidentified leptons is labelled ‘Misid. leptons’. The sum of VVV , $WZjj$ –EW and tZj background events is labelled ‘Others’. The uncertainty band around the expectation includes all systematic uncertainties as obtained from the fit.

The distribution of the 4-category DNN score in the $W^\pm Z$ signal region with background normalisations, signal normalisation and nuisance parameters adjusted by the profile-likelihood fit is shown in Figure 1. The corresponding pre-fit and post-fit yields in the signal region and in the ZZ control region are detailed in Table 1.

The measurements of f_{00} , f_{0T} , f_{T0} and f_{TT} are summarised in Table 2. The hypotheses of having no events in each of the joint helicity states are tested. In $W^\pm Z$ events, the presence of a pair of W and Z bosons with

Table 1: Expected and observed numbers of events in the $W^\pm Z$ signal region (left) and in the ZZ control region (right). Numbers are presented before and after a fit to the 4-category DNN score distribution in $W^\pm Z$ events. The sum of background events containing misidentified leptons is labelled ‘Misid. leptons’. The sum of VVV , $WZjj$ -EW and tZj background events is labelled ‘Others’. The pre-fit uncertainties quoted are of statistical and systematic origin but do not take into account correlations between parameters of the fit. The post-fit uncertainties quoted are of statistical and systematic origin and take into account the correlations between the various parameters of the fit. For the $W^\pm Z$ signal templates, the correlations arising from the relationship $f_{00} + f_{0T} + f_{T0} + f_{TT} = 1$ explain the larger post-fit uncertainties compared to the pre-fit ones.

	Signal Region		ZZ Control Region	
	Pre-fit	Post-fit	Pre-fit	Post-fit
WZ in τ	620 \pm 60	630 \pm 60		
ZZ	1420 \pm 120	1630 \pm 50		
$t\bar{t} + V$	870 \pm 130	820 \pm 120	WZ unpol.	35.6 \pm 1.9
Misid. leptons	1170 \pm 230	1010 \pm 220	ZZ	2030 \pm 150
Others	800 \pm 90	780 \pm 90	$t\bar{t} + V$	153 \pm 23
$W_0 Z_0$	920 \pm 40	1190 \pm 160	Misid. leptons	14 \pm 4
$W_0 Z_T$	2670 \pm 50	1900 \pm 500	Others	32 \pm 8
$W_T Z_0$	2670 \pm 60	3100 \pm 400	Total MC	2260 \pm 150
$W_T Z_T$	10200 \pm 230	10900 \pm 600	Data	—
Total MC	21400 \pm 500	21950 \pm 170		2554
Data	—	21936		

a simultaneous longitudinal polarisation (f_{00}) is observed with a significance of 7.1σ , compared to 6.2σ expected. The other joint helicity fractions f_{0T} , f_{T0} and f_{TT} are also measured with observed (expected) significances of 3.4σ (5.4σ), 7.1σ (6.6σ) and 11σ (9.7σ), respectively. The joint helicity fractions are also measured in W^+Z and W^-Z events separately, with observed significances for f_{00} of 6.9σ and 4.1σ , respectively. Table 3 shows the main sources of uncertainty in the measurement of the joint helicity fractions. Uncertainties related to data statistics and to QCD effects, namely the QCD scale and modelling uncertainties, make similar contributions to the precision of the measurements. The modelling uncertainty is dominated by the uncertainties in the shape of the distributions of polarised $W^\pm Z$ events due to NLO QCD corrections. Among them, the uncertainty from the DNN reweighting method is dominant, except for f_{00} where the uncertainty from the template generation method is of equal size. Different correlation schemes between bins and between helicity states are tested for this latter modelling uncertainty. All yield consistent results. Uncertainties in the energy scale and reconstruction of jets are dominant among detector uncertainties, showing how observables for joint polarisation are linked to jet emissions. The values of f_{00} , f_{0T} , f_{T0} and f_{TT} measured in $W^\pm Z$ events are shown in Figure 2. The global level of agreement between the four measured joint helicity fractions with the fixed-order predictions at NLO QCD [23] is observed to be 1.4σ . A similar level of agreement is observed with respect to POWHEG+PYTHIA predictions. The impact of EW corrections on the joint helicity fractions is negligible, smaller than 3% [32].

9.2 Individual boson polarisation measurements

The distributions of $q_W \cdot \cos \theta_{\ell W}^*$ and $\cos \theta_{\ell Z}^*$ with background normalisations, signal normalisation and nuisance parameters, adjusted by the profile-likelihood fit, are shown in Figure 3. The post-fit event yields in the $W^\pm Z$ signal region and in the ZZ control region are compatible with those obtained in the fit to the 4-category DNN score distribution.

Table 2: Measured joint helicity fractions f_{00} , f_{0T} , f_{T0} and f_{TT} in the fiducial phase space, for $W^\pm Z$, W^+Z and W^-Z events. The total uncertainties in the measurements are reported. The measurements are compared with predictions from POWHEG+PYTHIA and from NLO QCD fixed-order calculations [23]. The uncertainties in the POWHEG+PYTHIA prediction include statistical, PDF and QCD scale uncertainties; the uncertainties in the NLO QCD fixed-order prediction include QCD scale uncertainties.

	Data	POWHEG+PYTHIA	NLO QCD
$W^\pm Z$			
f_{00}	0.067 ± 0.010	0.0590 ± 0.0009	0.058 ± 0.002
f_{0T}	0.110 ± 0.029	0.1515 ± 0.0017	0.159 ± 0.003
f_{T0}	0.179 ± 0.023	0.1465 ± 0.0017	0.149 ± 0.003
f_{TT}	0.644 ± 0.032	0.6431 ± 0.0021	0.628 ± 0.004
W^+Z			
f_{00}	0.072 ± 0.016	0.0583 ± 0.0012	0.057 ± 0.002
f_{0T}	0.119 ± 0.034	0.1484 ± 0.0022	0.155 ± 0.003
f_{T0}	0.152 ± 0.033	0.1461 ± 0.0022	0.147 ± 0.003
f_{TT}	0.66 ± 0.04	0.6472 ± 0.0026	0.635 ± 0.004
W^-Z			
f_{00}	0.063 ± 0.016	0.0600 ± 0.0014	0.059 ± 0.002
f_{0T}	0.11 ± 0.04	0.1560 ± 0.0027	0.166 ± 0.003
f_{T0}	0.21 ± 0.04	0.1470 ± 0.0027	0.152 ± 0.003
f_{TT}	0.62 ± 0.05	0.6370 ± 0.0033	0.618 ± 0.004

The measurements of f_0 and $f_L - f_R$ are summarised in Table 4 where they are compared with the predictions from POWHEG+PYTHIA and, for f_0 , from an NLO QCD fixed-order calculation [23]. Good agreement of the measured helicity fractions of both the W and Z bosons with the predictions from POWHEG+PYTHIA is observed. Measured f_0 values agree within 1σ with the prediction, while $f_L - f_R$ values agree within 1.5σ , except for W^-Z events where the level of agreement deteriorates to 2.3σ . Table 5 shows the main sources of uncertainty in the measurement of the individual helicity fractions. The measurements are dominated by statistical uncertainties, except for the f_0 measurement of the W boson where the modelling uncertainty is equally important. The values of f_0 and $f_L - f_R$ measured in $W^\pm Z$ events are shown in Figure 4 for the W and Z bosons.

The compatibility of the measured joint and individual helicity fractions is tested. Ignoring the interference between polarisations, which should represent only 0.6%–0.8% of the events according to NLO QCD and NLO QCD+EW fixed-order predictions [23, 32], the following relationships ensue

$$f_{0T} = f_0^W - f_{00}, \quad f_{T0} = f_0^Z - f_{00} \quad \text{and} \quad f_{TT} = 1 + f_{00} - f_0^W - f_0^Z.$$

Using these relationships, joint f_{00} and individual f_0^W , f_0^Z helicity fractions can be measured simultaneously from a fit to the 4-category DNN score observable. The fractions f_0^W and f_0^Z measured in this procedure agree within less than 1σ of their own uncertainties alone with the f_0^W and f_0^Z values obtained via individual $\cos\theta_{\ell W}^*$ and $\cos\theta_{\ell Z}^*$ distributions. This represents a consistency test of the joint helicity measurement procedure.

The spin-correlation between longitudinal W and Z bosons is tested by comparing joint and individual

Table 3: Summary of the relative uncertainties in the joint helicity fractions f_{00} , f_{0T} , f_{T0} , and f_{TT} measured in $W^\pm Z$ events. The uncertainties are reported as percentages.

	f_{00}	f_{0T}	f_{T0}	f_{TT}
Relative uncertainty [%]				
e energy scale and id. efficiency	0.34	0.6	0.8	0.31
μ energy scale and id. efficiency	0.8	0.23	0.23	0.13
E_T^{miss} and jets	3.3	1.3	1.2	0.4
Pile-up	0.6	0.17	0.4	0.15
Misidentified lepton background	2.3	1.6	0.8	0.26
ZZ background	0.9	0.17	0.32	0.07
Other backgrounds	3.0	1.6	1.3	0.4
Parton Distribution Function	0.5	1.8	0.09	0.5
QCD scale	0.19	8	0.9	2.0
Modelling	9	4	2.9	1.2
Total systematic uncertainty	14	15	8	4
Luminosity	0.35	0.24	0.15	0.05
Statistical uncertainty	13	10	12	3.0
Total	19	18	14	5

Table 4: Individual helicity fractions f_0 and $f_L - f_R$ of the W and Z bosons measured in the fiducial phase space for $W^\pm Z$, $W^+ Z$ and $W^- Z$ events. The total uncertainties in the measurements are reported. The measurements are compared with predictions from POWHEG+PYTHIA and, for f_0 , from NLO QCD fixed-order calculations [23]. The uncertainties in the POWHEG+PYTHIA prediction include statistical, PDF and QCD scale uncertainties; the uncertainties in the NLO QCD fixed-order prediction include QCD scale uncertainties.

	f_0			$f_L - f_R$	
	Data	POWHEG+PYTHIA	NLO QCD	Data	POWHEG+PYTHIA
W in $W^+ Z$	0.23 ± 0.05	0.2044 ± 0.0024	0.211 ± 0.002	0.071 ± 0.023	0.0990 ± 0.0015
W in $W^- Z$	0.19 ± 0.05	0.217 ± 0.004	0.225 ± 0.001	0.026 ± 0.027	-0.0491 ± 0.0020
W in $W^\pm Z$	0.21 ± 0.04	0.2094 ± 0.0016	0.217 ± 0.001	0.059 ± 0.016	0.0390 ± 0.0011
Z in $W^+ Z$	0.223 ± 0.025	0.1971 ± 0.0019	0.206 ± 0.002	-0.20 ± 0.10	-0.217 ± 0.006
Z in $W^- Z$	0.241 ± 0.029	0.2065 ± 0.0023	0.211 ± 0.001	0.10 ± 0.13	0.092 ± 0.007
Z in $W^\pm Z$	0.231 ± 0.019	0.2009 ± 0.0014	0.208 ± 0.001	-0.10 ± 0.08	-0.092 ± 0.005

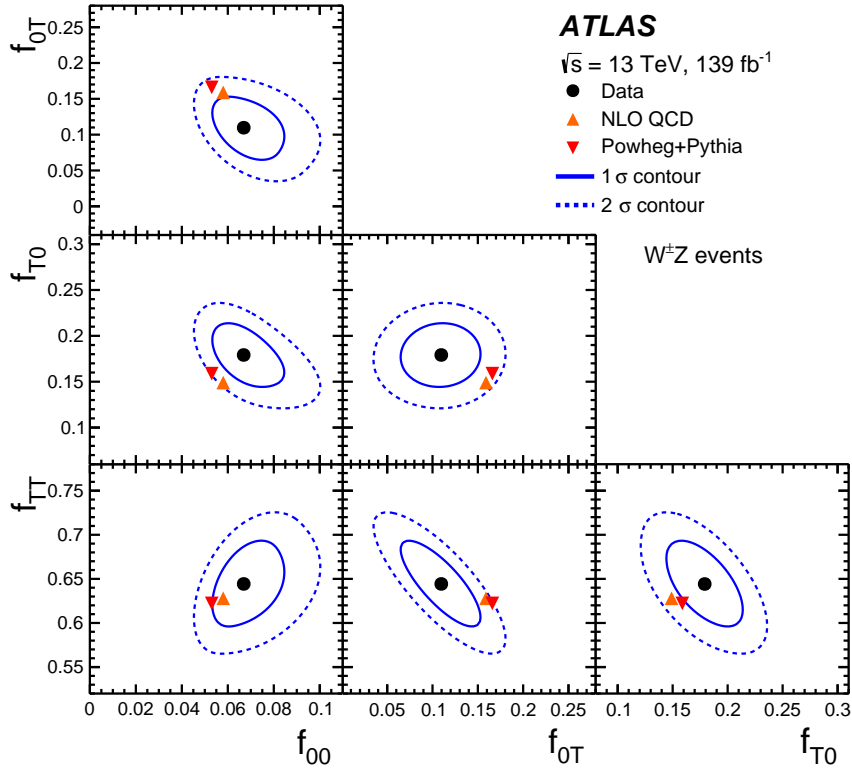


Figure 2: Measured joint helicity fractions f_{00} , f_{0T} , f_{T0} and f_{TT} of the W and Z bosons in $W^\pm Z$ events, compared with NLO QCD fixed-order predictions [23] (upward pointing triangle) and to MC predictions from POWHEG+PYTHIA (downward pointing triangle). The effect of PDF and QCD scale uncertainties on the POWHEG+PYTHIA and NLO QCD fixed-order predictions are of the same size as the respective markers. The full and dashed ellipses around the data points correspond to one and two standard deviations, respectively.

helicity fractions and measuring the ratio $R_c = f_{00}/(f_0^W f_0^Z)$. In the absence of spin correlations, neglecting interference effects, R_c is equal to 1. A value of $R_c = 1.3$ is predicted by NLO QCD fixed-order calculations, indicating the presence of correlation between polarisation states of the bosons. The ratio R_c is extracted from data by a simultaneous fit to the 4-category DNN score observable of f_{00} , f_0^W and f_0^Z . It is measured in $W^\pm Z$ events to be $R_c = 1.54 \pm 0.35$. The observed significance relative to the no spin-correlations hypothesis, i.e. $R_c = 1$, is 1.6σ .

9.3 Differential cross-section measurements

The inclusive cross section of $W^\pm Z$ production in the fiducial region for leptonic decay modes (electrons or muons) is determined simultaneously to the joint helicity fractions. It is measured to be $\sigma_{W^\pm Z \rightarrow \ell' \nu \ell \ell}^{\text{fid.}} = 64.6 \pm 0.5$ (stat.) ± 1.8 (syst.) ± 1.1 (lumi.) fb, where the uncertainties correspond to statistical uncertainties, experimental and modelling systematic uncertainties, and luminosity uncertainties. The corresponding SM NNLO QCD prediction from MATRIX [96] is $64.0_{-1.3}^{+1.5}$ fb, where the uncertainty corresponds to the QCD scale uncertainty.

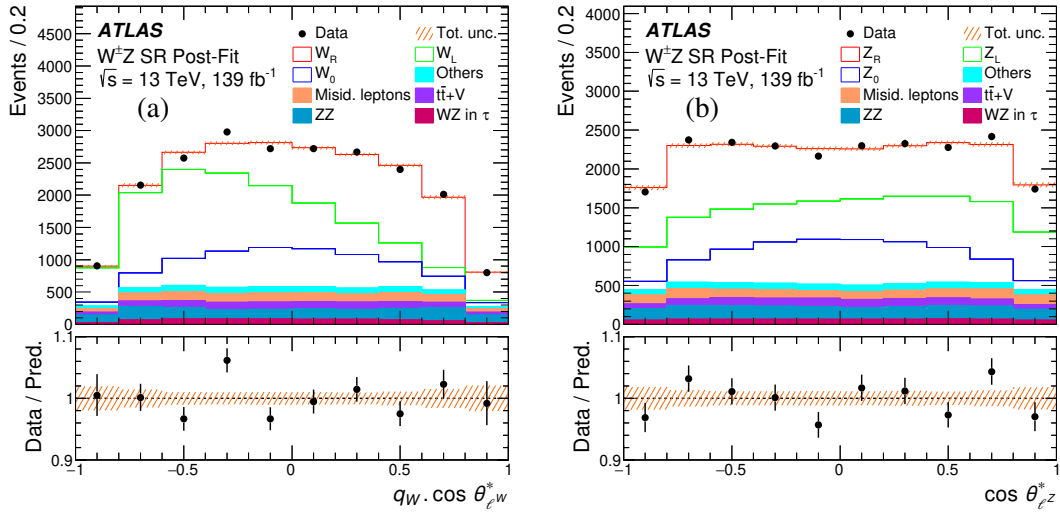


Figure 3: Post-fit distributions of (a) $q_W \cdot \cos \theta_{eW}^*$ and (b) $\cos \theta_{eZ}^*$ in $W^\pm Z$ events at detector level in the signal region (SR). Respective contributions of the $W^\pm Z$ individual helicity states 0, L and R of the W and Z bosons and backgrounds are normalised to the expected number of events after the fit. The sum of background events containing misidentified leptons is labelled ‘Misid. leptons’. The sum of VVV , $WZjj$ –EW and tZj background events is labelled ‘Others’. The uncertainty band around the expectation includes all systematic uncertainties as obtained from the fit.

Table 5: Summary of the relative uncertainties in the polarisation fractions f_0 and $f_L - f_R$ measured in $W^\pm Z$ events for W and Z bosons. The uncertainties are reported as percentages.

	W^\pm in $W^\pm Z$		Z in $W^\pm Z$	
	f_0	$f_L - f_R$	f_0	$f_L - f_R$
Relative uncertainty [%]				
e energy scale and id. efficiency	1.4	0.8	1.3	0.7
μ energy scale and id. efficiency	2.1	5	0.8	0.5
E_T^{miss} and jets	1.9	2.8	0.28	3.0
Pile-up	1.4	4	1.2	3.1
Misidentified lepton background	3.4	0.8	1.6	1.2
ZZ background	0.7	0.6	0.6	2.5
Other backgrounds	0.9	1.3	0.7	1.3
Parton Distribution Function	0.5	2.9	0.05	0.5
QCD scale	6	6	0.22	5
Modelling	12	3.1	2.2	19
Total systematic uncertainty	14	11	3.5	21
Luminosity	0.25	0.09	0.06	0.19
Statistical uncertainty	13	40	9	90
Total	19	40	10	90

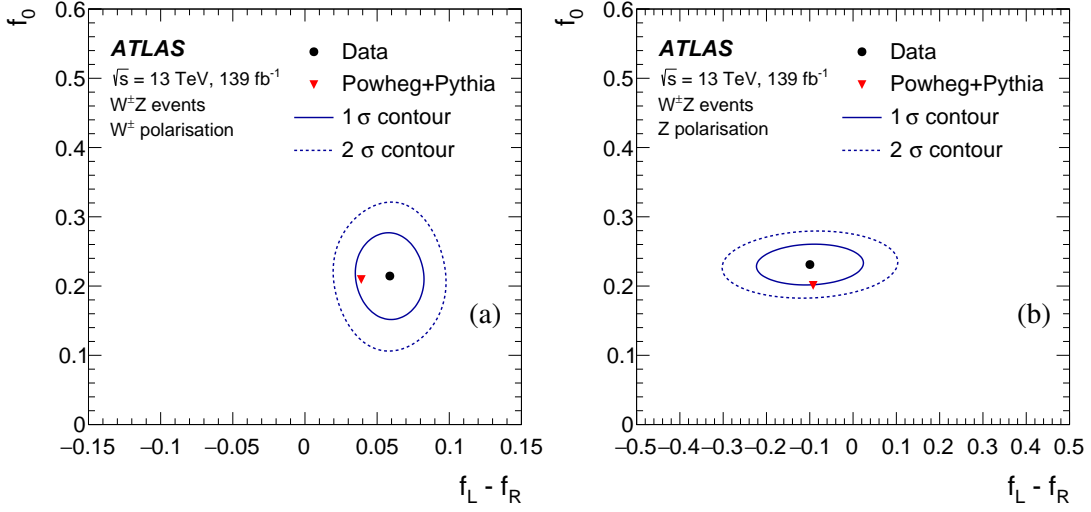


Figure 4: Individual helicity fractions f_0 and $f_L - f_R$ measured for the (a) W and (b) Z bosons in $W^\pm Z$ events, compared with predictions from POWHEG+PYTHIA with $\sin^2 \theta_W = 0.23152$ (downward pointing triangle). The effect of PDF and QCD scale uncertainties on the POWHEG+PYTHIA prediction are of the same size as the triangle marker. The full and dashed ellipses around the data points correspond to one and two standard deviations, respectively.

The $W^\pm Z$ production cross section is measured as a function of several variables sensitive to the individual and joint boson polarisation: $q_W \cdot \cos \theta_{\ell W}^*$, $\cos \theta_{\ell Z}^*$, $|\cos \theta_V|$ and the DNN score. The measured differential cross sections in Figure 5 are compared with the Born-level predictions at NLO in QCD from the POWHEG+PYTHIA, MADGRAPH5_AMC@NLO+PYTHIA MC generators and to the sum of the polarised MADGRAPH 0,1j@LO LO predictions. The Born-level DNN score prediction is evaluated using the same DNN as trained at detector level and evaluated using Born-level input observables. The predicted integrated fiducial cross sections of the three MC generators are rescaled to the NNLO cross section from MATRIX [96], as indicated in Figure 5. Good agreement of the shapes of the measured distributions with the NLO QCD predictions is observed. The MADGRAPH 0,1j@LO LO prediction exhibits larger differences from the measured cross section for the $|\cos \theta_V|$ distribution. This is expected as the $|\cos \theta_V|$ distribution is particularly sensitive to NLO QCD corrections [23] and the MADGRAPH 0,1j@LO LO prediction only includes their real parts. The measured cross sections and the Rivet [97] routine for this measurement, including for the evaluation of the DNN classifier score, are published on HEPData [98]⁴.

⁴ In the HEPData entry, two sets of cross section measurements are provided, determined using both dressed and Born leptons, respectively.

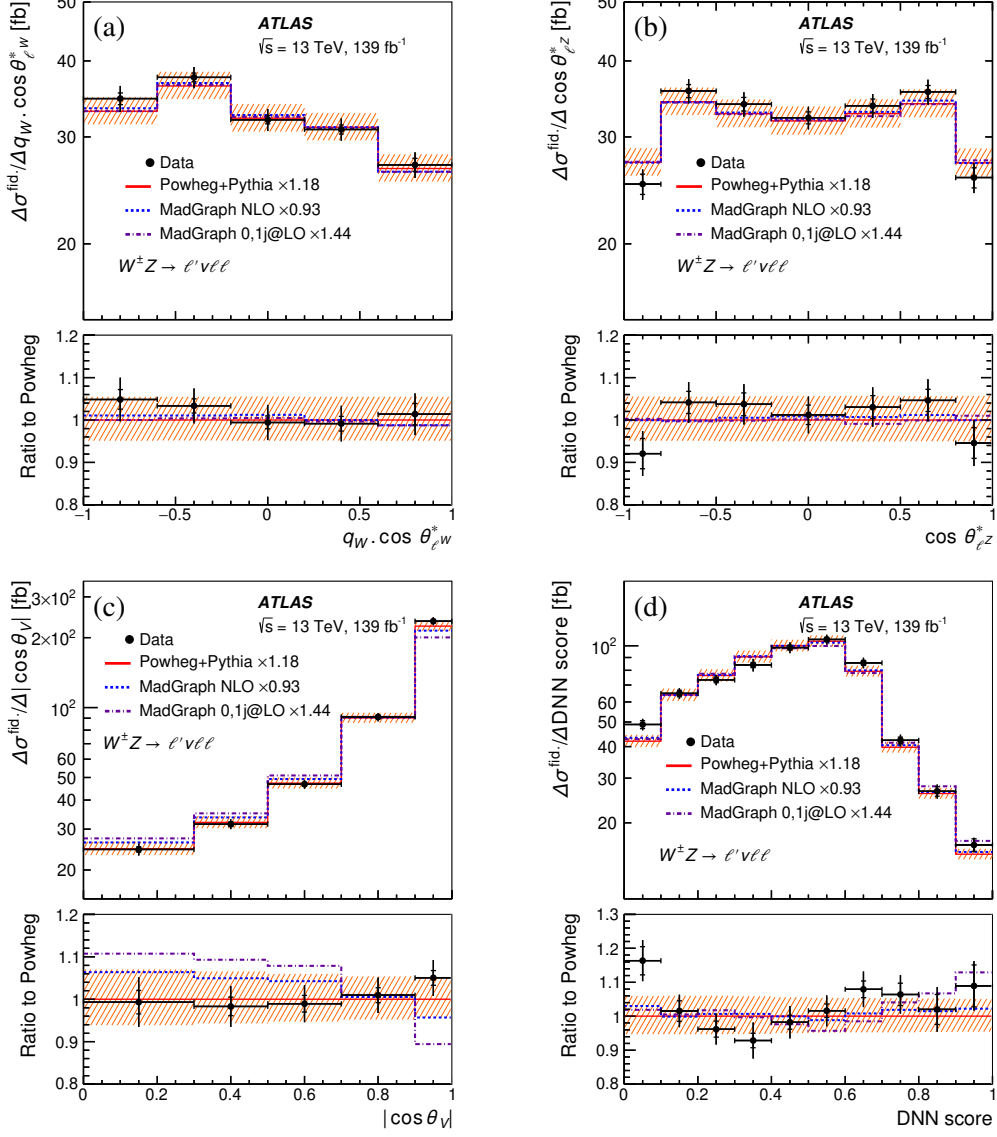


Figure 5: The measured $W^\pm Z$ differential cross section in the fiducial phase space as a function of (a) $q_W \cdot \cos \theta_{\ell^*W}^*$, (b) $\cos \theta_{\ell^*Z}^*$, (c) $|\cos \theta_V|$ and (d) DNN score. The total cross section integrated over each bin and divided by the bin width is represented. The inner and outer error bars on the data points represent the statistical and total uncertainties, respectively. The measurements are compared with the NLO prediction from POWHEG+PYTHIA (solid line). The dashed band shows how the sum of QCD scale and PDF uncertainties affects the POWHEG+PYTHIA NLO prediction. The predictions from the MADGRAPH 0,1j@LO and MADGRAPH5_AMC@NLO+PYTHIA MC generators are also indicated by dotted-dashed and dashed lines, respectively. All predictions have been scaled to the NNLO QCD integrated cross section predicted by MATRIX.

10 Conclusion

Measurements of gauge boson polarisation states from $W^\pm Z$ production in $\sqrt{s} = 13$ TeV pp collisions at the LHC are presented. The data analysed were collected with the ATLAS detector during the years 2015–2018 and correspond to an integrated luminosity of 139 fb^{-1} . The measurements use leptonic decay modes of the gauge bosons to electrons or muons and are performed in a fiducial phase space closely matching the detector acceptance.

Using neural-network-based advanced analysis techniques, joint helicity fractions of pair-produced vector bosons are measured. For the first time, the presence of a W boson and a Z boson with a simultaneous longitudinal polarisation is measured with observed and expected significances of 7.1 and 6.2 standard deviations, respectively. Integrated over the fiducial region, the fractions of the W and Z bosons both longitudinally or transversely polarised are measured in $W^\pm Z$ events to be $f_{00} = 0.067 \pm 0.010$ and $f_{\text{TT}} = 0.644 \pm 0.032$, respectively, in agreement with the SM predictions at NLO in QCD. The impact of EW corrections is negligible. The measured fractions of mixed polarisation modes are $f_{0\text{T}} = 0.110 \pm 0.029$ and $f_{\text{T}0} = 0.179 \pm 0.023$. Joint helicity fractions are also measured separately for $W^+ Z$ and $W^- Z$ events.

Individual helicity fractions f_0 and $f_L - f_R$ of the W and Z bosons are measured. The measured values agree with the SM predictions and are consistent with the measured joint helicity fractions when neglecting interference among polarisation states, which from NLO QCD+EW calculations are expected to be smaller than the uncertainty of the present measurement.

Furthermore, the inclusive cross section of $W^\pm Z$ production in the fiducial region for leptonic decay modes is measured to be $\sigma_{W^\pm Z \rightarrow \ell' \nu \ell \ell}^{\text{fid.}} = 64.6 \pm 2.1 \text{ fb}$, in agreement with the NNLO SM expectation of $64.0^{+1.5}_{-1.3} \text{ fb}$. The $W^\pm Z$ production cross section is measured as a function of several kinematic variables sensitive to polarisation and compared with SM predictions at NLO in QCD from the POWHEG+PYTHIA and MADGRAPH5_AMC@NLO+PYTHIA MC event generators. In particular, the variable related to the output of the deep neural network classifier used for the joint helicity measurement is unfolded in order to remove detector effects. The differential cross-section distributions are well described by the NLO MC predictions.

Acknowledgements

We thank CERN for the very successful operation of the LHC, as well as the support staff from our institutions without whom ATLAS could not be operated efficiently.

We acknowledge the support of ANPCyT, Argentina; YerPhI, Armenia; ARC, Australia; BMWFW and FWF, Austria; ANAS, Azerbaijan; CNPq and FAPESP, Brazil; NSERC, NRC and CFI, Canada; CERN; ANID, Chile; CAS, MOST and NSFC, China; Minciencias, Colombia; MEYS CR, Czech Republic; DNRF and DNSRC, Denmark; IN2P3-CNRS and CEA-DRF/IRFU, France; SRNSFG, Georgia; BMBF, HGF and MPG, Germany; GSRI, Greece; RGC and Hong Kong SAR, China; ISF and Benoziyo Center, Israel; INFN, Italy; MEXT and JSPS, Japan; CNRST, Morocco; NWO, Netherlands; RCN, Norway; MEiN, Poland; FCT, Portugal; MNE/IFA, Romania; MESTD, Serbia; MSSR, Slovakia; ARRS and MIZŠ, Slovenia; DSI/NRF, South Africa; MICINN, Spain; SRC and Wallenberg Foundation, Sweden; SERI, SNSF and Cantons of Bern and Geneva, Switzerland; MOST, Taiwan; TENMAK, Türkiye; STFC, United Kingdom; DOE and NSF, United States of America. In addition, individual groups and members have received support from BCKDF, CANARIE, Compute Canada and CRC, Canada; PRIMUS 21/SCI/017 and UNCE SCI/013,

Czech Republic; COST, ERC, ERDF, Horizon 2020 and Marie Skłodowska-Curie Actions, European Union; Investissements d’Avenir Labex, Investissements d’Avenir Idex and ANR, France; DFG and AvH Foundation, Germany; Herakleitos, Thales and Aristeia programmes co-financed by EU-ESF and the Greek NSRF, Greece; BSF-NSF and MINERVA, Israel; Norwegian Financial Mechanism 2014-2021, Norway; NCN and NAWA, Poland; La Caixa Banking Foundation, CERCA Programme Generalitat de Catalunya and PROMETEO and GenT Programmes Generalitat Valenciana, Spain; Göran Gustafssons Stiftelse, Sweden; The Royal Society and Leverhulme Trust, United Kingdom.

The crucial computing support from all WLCG partners is acknowledged gratefully, in particular from CERN, the ATLAS Tier-1 facilities at TRIUMF (Canada), NDGF (Denmark, Norway, Sweden), CC-IN2P3 (France), KIT/GridKA (Germany), INFN-CNAF (Italy), NL-T1 (Netherlands), PIC (Spain), ASGC (Taiwan), RAL (UK) and BNL (USA), the Tier-2 facilities worldwide and large non-WLCG resource providers. Major contributors of computing resources are listed in Ref. [99].

References

- [1] A. Azatov, J. Elias-Miro, Y. Reyimuaji and E. Venturini, *Novel measurements of anomalous triple gauge couplings for the LHC*, [JHEP **10** \(2017\) 027](#), arXiv: [1707.08060 \[hep-ph\]](#).
- [2] G. Panico, F. Riva and A. Wulzer, *Diboson interference resurrection*, [Phys. Lett. B **776** \(2018\) 473](#), arXiv: [1708.07823 \[hep-ph\]](#).
- [3] CDF and D0 Collaborations, *Combination of CDF and D0 measurements of the W boson helicity in top quark decays*, [Phys. Rev. D **85** \(2012\) 071106](#), arXiv: [1202.5272 \[hep-ex\]](#).
- [4] CDF Collaboration, *Measurement of W-Boson Polarization in Top-Quark Decay in $p\bar{p}$ Collisions at $\sqrt{s} = 1.96$ TeV*, [Phys. Rev. Lett. **105** \(2010\) 042002](#), arXiv: [1003.0224 \[hep-ex\]](#).
- [5] D0 Collaboration, *Measurement of the W boson helicity in top quark decays using 5.4 fb^{-1} of $p\bar{p}$ collision data*, [Phys. Rev. D **83** \(2011\) 032009](#), arXiv: [1011.6549 \[hep-ex\]](#).
- [6] ATLAS Collaboration, *Measurement of the W boson polarization in top quark decays with the ATLAS detector*, [JHEP **06** \(2012\) 088](#), arXiv: [1205.2484 \[hep-ex\]](#).
- [7] CMS Collaboration, *Measurement of the W boson helicity fractions in the decays of top quark pairs to lepton + jets final states produced in pp collisions at $\sqrt{s} = 8\text{TeV}$* , [Phys. Lett. B **762** \(2016\) 512](#), arXiv: [1605.09047 \[hep-ex\]](#).
- [8] ATLAS Collaboration, *Measurement of the polarisation of W bosons produced with large transverse momentum in pp collisions at $\sqrt{s} = 7$ TeV with the ATLAS experiment*, [Eur. Phys. J. C **72** \(2012\) 2001](#), arXiv: [1203.2165 \[hep-ex\]](#).
- [9] CMS Collaboration, *Measurement of the Polarization of W Bosons with Large Transverse Momenta in W+jets Events at the LHC*, [Phys. Rev. Lett. **107** \(2011\) 021802](#), arXiv: [1104.3829 \[hep-ex\]](#).
- [10] CDF Collaboration, *First Measurement of the Angular Coefficients of Drell-Yan e^+e^- Pairs in the Z Mass Region from $p\bar{p}$ Collisions at $\sqrt{s} = 1.96$ TeV*, [Phys. Rev. Lett. **106** \(2011\) 241801](#), arXiv: [1103.5699 \[hep-ex\]](#).

- [11] CMS Collaboration, *Angular coefficients of Z bosons produced in pp collisions at $\sqrt{s} = 8$ TeV and decaying to $\mu^+\mu^-$ as a function of transverse momentum and rapidity*, *Phys. Lett. B* **750** (2015) 154, arXiv: [1504.03512 \[hep-ex\]](#).
- [12] ATLAS Collaboration, *Measurement of the angular coefficients in Z-boson events using electron and muon pairs from data taken at $\sqrt{s} = 8$ TeV with the ATLAS detector*, *JHEP* **08** (2016) 159, arXiv: [1606.00689 \[hep-ex\]](#).
- [13] H1 Collaboration, *Events with isolated leptons and missing transverse momentum and measurement of W production at HERA*, *Eur. Phys. J. C* **64** (2009) 251, arXiv: [0901.0488 \[hep-ex\]](#).
- [14] L3 Collaboration, *Measurement of W polarisation at LEP*, *Phys. Lett. B* **557** (2003) 147, arXiv: [hep-ex/0301027](#).
- [15] OPAL Collaboration, *W boson polarization at LEP2*, *Phys. Lett. B* **585** (2004) 223, arXiv: [hep-ex/0312047](#).
- [16] DELPHI Collaboration, *Study of W-boson polarisations and triple gauge boson couplings in the reaction $e^+e^- \rightarrow W^+W^-$ at LEP 2*, *Eur. Phys. J. C* **54** (2008) 345, arXiv: [0801.1235 \[hep-ex\]](#).
- [17] OPAL Collaboration, *Measurement of W boson polarizations and CP violating triple gauge couplings from W^+W^- production at LEP*, *Eur. Phys. J. C* **19** (2001) 229, arXiv: [hep-ex/0009021](#).
- [18] L3 Collaboration, *Study of spin and decay-plane correlations of W bosons in the $e^+e^- \rightarrow W^+W^-$ process at LEP*, *Eur. Phys. J. C* **40** (2005) 333, arXiv: [hep-ex/0501036](#).
- [19] DELPHI Collaboration, *Correlations between Polarisation States of W Particles in the Reaction $e^+e^- \rightarrow W^-W^+$ at LEP2 Energies 189-GeV - 209-GeV*, *Eur. Phys. J. C* **63** (2009) 611, arXiv: [0908.1023 \[hep-ex\]](#).
- [20] ATLAS Collaboration, *Measurement of $W^\pm Z$ production cross sections and gauge boson polarisation in pp collisions at $\sqrt{s} = 13$ TeV with the ATLAS detector*, *Eur. Phys. J. C* **79** (2019) 535, arXiv: [1902.05759 \[hep-ex\]](#).
- [21] CMS Collaboration, *Measurement of the inclusive and differential WZ production cross sections, polarization angles, and triple gauge couplings in pp collisions at $\sqrt{s} = 13$ TeV*, (2021), arXiv: [2110.11231 \[hep-ex\]](#).
- [22] A. Denner and G. Pelliccioli, *Polarized electroweak bosons in W^+W^- production at the LHC including NLO QCD effects*, *JHEP* **09** (2020) 164, arXiv: [2206.14867 \[hep-ph\]](#).
- [23] A. Denner and G. Pelliccioli, *NLO QCD predictions for doubly-polarized WZ production at the LHC*, *Phys. Lett. B* **814** (2020) 136107, arXiv: [2010.07149 \[hep-ph\]](#),
(We would like to thank Ansgar Denner and Giovanni Pelliccioli for fruitful discussions and for providing us with the NLO QCD predictions for the specific deep-neural network classifier output used in the analysis and for both W^+Z and W^-Z events.)
- [24] U. Baur, T. Han and J. Ohnemus, *Amplitude zeros in $W^{+/-}Z$ production*, *Phys. Rev. Lett.* **72** (1994) 3941, arXiv: [hep-ph/9403248](#).
- [25] R. Franceschini, G. Panico, A. Pomarol, F. Riva and A. Wulzer, *Electroweak precision tests in high-energy diboson processes*, *JHEP* **02** (2018) 111, arXiv: [1712.01310 \[hep-ph\]](#).

- [26] E. Mirkes and J. Ohnemus, *W and Z polarization effects in hadronic collisions*, *Phys. Rev. D* **50** (1994) 5692, arXiv: [hep-ph/9406381](#).
- [27] S. Groote, J. G. Korner and P. Tuvike, *$O(\alpha_s)$ corrections to the decays of polarized W^\pm and Z bosons into massive quark pairs*, *Eur. Phys. J. C* **72** (2012) 2177, arXiv: [1204.5295 \[hep-ph\]](#).
- [28] W. J. Stirling and E. Vryonidou, *Electroweak gauge boson polarisation at the LHC*, *JHEP* **07** (2012) 124, arXiv: [1204.6427 \[hep-ph\]](#).
- [29] G. Gounaris, J. Layssac, G. Moultaqa and F. M. Renard, *Analytic expressions of cross-sections, asymmetries and W density matrices for $e^+ e^- \rightarrow W^+ W^-$ with general three boson couplings*, *Int. J. Mod. Phys. A* **8** (1993) 3285.
- [30] Particle Data Group, *Review of Particle Physics*, *Phys. Rev. D* **98** (2018) 030001.
- [31] ATLAS Collaboration, *Proposal for truth particle observable definitions in physics measurements*, tech. rep. ATL-PHYS-PUB-2015-013, CERN, 2015, URL: <https://cds.cern.ch/record/2022743>.
- [32] D. N. Le and J. Baglio, *Doubly-polarized WZ hadronic cross sections at NLO QCD+EW accuracy*, (2022), arXiv: [2203.01470 \[hep-ph\]](#).
- [33] ATLAS Collaboration, *The ATLAS Experiment at the CERN Large Hadron Collider*, *JINST* **3** (2008) S08003.
- [34] ATLAS Collaboration, *The ATLAS Collaboration Software and Firmware*, ATL-SOFT-PUB-2021-001, 2021, URL: <https://cds.cern.ch/record/2767187>.
- [35] P. Nason, *A New method for combining NLO QCD with shower Monte Carlo algorithms*, *JHEP* **11** (2004) 040, arXiv: [hep-ph/0409146](#).
- [36] S. Frixione, P. Nason and C. Oleari, *Matching NLO QCD computations with parton shower simulations: the POWHEG method*, *JHEP* **11** (2007) 070, arXiv: [0709.2092 \[hep-ph\]](#).
- [37] S. Alioli, P. Nason, C. Oleari and E. Re, *A general framework for implementing NLO calculations in shower Monte Carlo programs: the POWHEG BOX*, *JHEP* **06** (2010) 043, arXiv: [1002.2581 \[hep-ph\]](#).
- [38] T. Melia, P. Nason, R. Röntsch and G. Zanderighi, *W^+W^- , WZ and ZZ production in the POWHEG BOX*, *JHEP* **11** (2011) 078, arXiv: [1107.5051 \[hep-ph\]](#).
- [39] T. Sjöstrand et al., *An introduction to PYTHIA 8.2*, *Comput. Phys. Commun.* **191** (2015) 159, arXiv: [1410.3012 \[hep-ph\]](#).
- [40] ATLAS Collaboration, *Measurement of the Z/ γ^* boson transverse momentum distribution in pp collisions at $\sqrt{s} = 7$ TeV with the ATLAS detector*, *JHEP* **09** (2014) 145, arXiv: [1406.3660 \[hep-ex\]](#).
- [41] H.-L. Lai et al., *New parton distributions for collider physics*, *Phys. Rev. D* **82** (2010) 074024, arXiv: [1007.2241 \[hep-ph\]](#).
- [42] J. Pumplin et al., *New Generation of Parton Distributions with Uncertainties from Global QCD Analysis*, *JHEP* **07** (2002) 012, arXiv: [hep-ph/0201195](#).

- [43] J. Alwall et al., *The automated computation of tree-level and next-to-leading order differential cross sections, and their matching to parton shower simulations*, *JHEP* **07** (2014) 079, arXiv: [1405.0301 \[hep-ph\]](#).
- [44] R. Frederix and S. Frixione, *Merging meets matching in MC@NLO*, *JHEP* **12** (2012) 061, arXiv: [1209.6215 \[hep-ph\]](#).
- [45] R. D. Ball et al., *Parton distributions for the LHC run II*, *JHEP* **04** (2015) 040, arXiv: [1410.8849 \[hep-ph\]](#).
- [46] V. Hirschi and O. Mattelaer, *Automated event generation for loop-induced processes*, *JHEP* **10** (2015) 146, arXiv: [1507.00020 \[hep-ph\]](#).
- [47] E. Bothmann et al., *Event Generation with Sherpa 2.2*, *SciPost Phys.* **7** (2019) 034, arXiv: [1905.09127 \[hep-ph\]](#).
- [48] T. Gleisberg and S. Hoeche, *Comix, a new matrix element generator*, *JHEP* **12** (2008) 039, arXiv: [0808.3674 \[hep-ph\]](#).
- [49] F. Cascioli, P. Maierhöfer and S. Pozzorini, *Scattering Amplitudes with Open Loops*, *Phys. Rev. Lett.* **108** (2012) 111601, arXiv: [1111.5206 \[hep-ph\]](#).
- [50] S. Schumann and F. Krauss, *A Parton shower algorithm based on Catani-Seymour dipole factorisation*, *JHEP* **03** (2008) 038, arXiv: [0709.1027 \[hep-ph\]](#).
- [51] S. Hoeche, F. Krauss, M. Schonherr and F. Siegert, *QCD matrix elements + parton showers: The NLO case*, *JHEP* **04** (2013) 027, arXiv: [1207.5030 \[hep-ph\]](#).
- [52] D. Buarque Franzosi, O. Mattelaer, R. Ruiz and S. Shil, *Automated predictions from polarized matrix elements*, *JHEP* **04** (2020) 082, arXiv: [1912.01725 \[hep-ph\]](#).
- [53] L. Lönnblad, *Correcting the Colour-Dipole Cascade Model with Fixed Order Matrix Elements*, *JHEP* **05** (2002) 046, arXiv: [hep-ph/0112284](#).
- [54] L. Lönnblad and S. Prestel, *Matching tree-level matrix elements with interleaved showers*, *JHEP* **03** (2012) 019, arXiv: [1109.4829 \[hep-ph\]](#).
- [55] T. Sjöstrand, S. Mrenna and P. Skands, *A brief introduction to PYTHIA 8.1*, *Comput. Phys. Commun.* **178** (2008) 852, arXiv: [0710.3820 \[hep-ph\]](#).
- [56] R. D. Ball et al., *Parton distributions with LHC data*, *Nucl. Phys. B* **867** (2013) 244, arXiv: [1207.1303 \[hep-ph\]](#).
- [57] ATLAS Collaboration, *The ATLAS Simulation Infrastructure*, *Eur. Phys. J. C* **70** (2010) 823, arXiv: [1005.4568 \[physics.ins-det\]](#).
- [58] S. Agostinelli et al., *GEANT4 – a simulation toolkit*, *Nucl. Instrum. Meth. A* **506** (2003) 250.
- [59] ATLAS Collaboration, *The Pythia 8 A3 tune description of ATLAS minimum bias and inelastic measurements incorporating the Donnachie-Landshoff diffractive model*, tech. rep., CERN, 2016, URL: <https://cds.cern.ch/record/2206965>.
- [60] ATLAS Collaboration, *Electron and photon performance measurements with the ATLAS detector using the 2015–2017 LHC proton-proton collision data*, *JINST* **14** (2019) P12006, arXiv: [1908.00005 \[hep-ex\]](#).

- [61] ATLAS Collaboration, *Muon reconstruction and identification efficiency in ATLAS using the full Run 2 pp collision data set at $\sqrt{s} = 13$ TeV*, *Eur. Phys. J. C* **81** (2021) 578, arXiv: [2012.00578 \[hep-ex\]](#).
- [62] ATLAS Collaboration, *Muon reconstruction performance of the ATLAS detector in proton–proton collision data at $\sqrt{s} = 13$ TeV*, *Eur. Phys. J. C* **76** (2016) 292, arXiv: [1603.05598 \[hep-ex\]](#).
- [63] ATLAS Collaboration, *Performance of the ATLAS trigger system in 2015*, *Eur. Phys. J. C* **77** (2017) 317, arXiv: [1611.09661 \[hep-ex\]](#).
- [64] ATLAS Collaboration, *Performance of electron and photon triggers in ATLAS during LHC Run 2*, *Eur. Phys. J. C* **80** (2020) 47, arXiv: [1909.00761 \[hep-ex\]](#).
- [65] ATLAS Collaboration, *Performance of the ATLAS muon triggers in Run 2*, *JINST* **15** (2020) P09015, arXiv: [2004.13447 \[physics.ins-det\]](#).
- [66] ATLAS Collaboration, *Jet reconstruction and performance using particle flow with the ATLAS Detector*, *Eur. Phys. J. C* **77** (2017) 466, arXiv: [1703.10485 \[hep-ex\]](#).
- [67] M. Cacciari, G. P. Salam and G. Soyez, *The anti- k_t jet clustering algorithm*, *JHEP* **04** (2008) 063, arXiv: [0802.1189 \[hep-ph\]](#).
- [68] M. Cacciari, G. P. Salam and G. Soyez, *FastJet user manual*, *Eur. Phys. J. C* **72** (2012) 1896, arXiv: [1111.6097 \[hep-ph\]](#).
- [69] ATLAS Collaboration, *Jet energy scale and resolution measured in proton–proton collisions at $\sqrt{s} = 13$ TeV with the ATLAS detector*, *Eur. Phys. J. C* **81** (2021) 689, arXiv: [2007.02645 \[hep-ex\]](#).
- [70] ATLAS Collaboration, *Performance of pile-up mitigation techniques for jets in pp collisions at $\sqrt{s} = 8$ TeV using the ATLAS detector*, *Eur. Phys. J. C* **76** (2016) 581, arXiv: [1510.03823 \[hep-ex\]](#).
- [71] ATLAS Collaboration, *ATLAS b-jet identification performance and efficiency measurement with $t\bar{t}$ events in pp collisions at $\sqrt{s} = 13$ TeV*, *Eur. Phys. J. C* **79** (2019) 970, arXiv: [1907.05120 \[hep-ex\]](#).
- [72] ATLAS Collaboration, *Identification of Jets Containing b-Hadrons with Recurrent Neural Networks at the ATLAS Experiment*, tech. rep. ATL-PHYS-PUB-2017-003, CERN, 2017, URL: <https://cds.cern.ch/record/2255226>.
- [73] ATLAS Collaboration, *Optimisation and performance studies of the ATLAS b-tagging algorithms for the 2017-18 LHC run*, tech. rep. ATL-PHYS-PUB-2017-013, CERN, 2017, URL: <https://cds.cern.ch/record/2273281>.
- [74] ATLAS Collaboration, *Performance of missing transverse momentum reconstruction with the ATLAS detector using proton-proton collisions at $\sqrt{s} = 13$ TeV*, *Eur. Phys. J. C* **78** (2018) 903, arXiv: [1802.08168 \[hep-ex\]](#).
- [75] ATLAS Collaboration, *Measurements of $W^\pm Z$ production cross sections in pp collisions at $\sqrt{s} = 8$ TeV with the ATLAS detector and limits on anomalous gauge boson self-couplings*, *Phys. Rev. D* **93** (2016) 092004, arXiv: [1603.02151 \[hep-ex\]](#).
- [76] ATLAS Collaboration, *Search for supersymmetry at $\sqrt{s}=8$ TeV in final states with jets and two same-sign leptons or three leptons with the ATLAS detector*, *JHEP* **06** (2014) 035, arXiv: [1404.2500 \[hep-ex\]](#).

- [77] ATLAS Collaboration, *Tools for estimating fake/non-prompt lepton backgrounds with the ATLAS detector at the LHC*, submitted to JINST. (2022), arXiv: [2211.16178 \[hep-ex\]](#).
- [78] ATLAS Collaboration, *ZZ $\rightarrow \ell^+\ell^-\ell'^+\ell'^-$ cross-section measurements and search for anomalous triple gauge couplings in 13 TeV pp collisions with the ATLAS detector*, *Phys. Rev. D* **97** (2018) 032005, arXiv: [1709.07703 \[hep-ex\]](#).
- [79] ATLAS Collaboration, *Measurements of the inclusive and differential production cross sections of a top-quark–antiquark pair in association with a Z boson at $\sqrt{s} = 13$ TeV with the ATLAS detector*, *Eur. Phys. J. C* **81** (2021) 737, arXiv: [2103.12603 \[hep-ex\]](#).
- [80] F. Chollet et al., *Keras*, 2015, URL: <https://github.com/fchollet/keras>.
- [81] Martin Abadi et al., *TensorFlow: Large-Scale Machine Learning on Heterogeneous Systems*, Software available from tensorflow.org, 2015, arXiv: [1603.04467](#), URL: <https://www.tensorflow.org/>.
- [82] K. Cranmer, G. Lewis, L. Moneta, A. Shibata and W. Verkerke, *HistFactory: A tool for creating statistical models for use with RooFit and RooStats*, tech. rep., New York U., 2012, URL: <https://cds.cern.ch/record/1456844>.
- [83] A. Andreassen and B. Nachman, *Neural networks for full phase-space reweighting and parameter tuning*, *Phys. Rev. D* **101** (2020) 091901, arXiv: [1907.08209 \[hep-ph\]](#).
- [84] G. D’Agostini, *A multidimensional unfolding method based on Bayes’ theorem*, *Nucl. Instrum. Meth. A* **362** (1995) 487.
- [85] T. Adye, *Unfolding algorithms and tests using RooUnfold*, (2011) 313, arXiv: [1105.1160 \[physics.data-an\]](#).
- [86] J. Butterworth et al., *PDF4LHC recommendations for LHC Run II*, *J. Phys.* **G43** (2016) 023001, arXiv: [1510.03865 \[hep-ph\]](#).
- [87] B. Malaescu, *An Iterative, Dynamically Stabilized(IDS) Method of Data Unfolding*, Proceedings of the PHYSTAT 2011 Workshop, CERN, Geneva, Switzerland (2011) 271, arXiv: [1106.3107 \[physics.data-an\]](#).
- [88] ATLAS Collaboration, *Jet energy scale measurements and their systematic uncertainties in proton-proton collisions at $\sqrt{s} = 13$ TeV with the ATLAS detector*, *Phys. Rev. D* **96** (2017) 072002, arXiv: [1703.09665 \[hep-ex\]](#).
- [89] ATLAS Collaboration, *Measurement of the Inelastic Proton-Proton Cross Section at $\sqrt{s} = 13$ TeV with the ATLAS Detector at the LHC*, *Phys. Rev. Lett.* **117** (2016) 182002, arXiv: [1606.02625 \[hep-ex\]](#).
- [90] ATLAS Collaboration, *Multi-Boson Simulation for 13 TeV ATLAS Analyses*, ATL-PHYS-PUB-2016-002, 2016, URL: <https://cds.cern.ch/record/2119986>.
- [91] ATLAS Collaboration, *Observation of electroweak $W^\pm Z$ boson pair production in association with two jets in pp collisions at $\sqrt{s} = 13$ TeV with the ATLAS detector*, *Phys. Lett. B* **793** (2019) 469, arXiv: [1812.09740 \[hep-ex\]](#).
- [92] ATLAS Collaboration, *Observation of the associated production of a top quark and a Z boson in pp collisions at $\sqrt{s} = 13$ TeV with the ATLAS detector*, *JHEP* **07** (2020) 124, arXiv: [2002.07546 \[hep-ex\]](#).

- [93] ATLAS Collaboration, *Modelling of the $t\bar{t}H$ and $t\bar{t}V$ ($V = W, Z$) processes for $\sqrt{s} = 13$ TeV ATLAS analyses*, tech. rep. ATL-PHYS-PUB-2016-005, CERN, 2016, URL: <https://cds.cern.ch/record/2120826>.
- [94] ATLAS Collaboration, *Luminosity determination in pp collisions at $\sqrt{s} = 13$ TeV using the ATLAS detector at the LHC*, tech. rep. ATLAS-CONF-2019-021, CERN, 2019, URL: <https://cds.cern.ch/record/2677054>.
- [95] G. Avoni et al., *The new LUCID-2 detector for luminosity measurement and monitoring in ATLAS*, *JINST* **13** (2018) P07017.
- [96] M. Grazzini, S. Kallweit, D. Rathlev and M. Wiesemann, *$W^\pm Z$ production at the LHC: fiducial cross sections and distributions in NNLO QCD*, *JHEP* **05** (2017) 139, arXiv: [1703.09065](https://arxiv.org/abs/1703.09065) [[hep-ph](https://arxiv.org/abs/1703.09065)].
- [97] C. Bierlich et al., *Robust Independent Validation of Experiment and Theory: Rivet version 3*, *SciPost Phys.* **8** (2020) 026, arXiv: [1912.05451](https://arxiv.org/abs/1912.05451) [[hep-ph](https://arxiv.org/abs/1912.05451)].
- [98] E. Maguire, L. Heinrich and G. Watt, *HEPData: a repository for high energy physics data*, *J. Phys. Conf. Ser.* **898** (2017) 102006, ed. by R. Mount and C. Tull, arXiv: [1704.05473](https://arxiv.org/abs/1704.05473) [[hep-ex](https://arxiv.org/abs/1704.05473)].
- [99] ATLAS Collaboration, *ATLAS Computing Acknowledgements*, ATL-SOFT-PUB-2021-003, 2021, URL: <https://cds.cern.ch/record/2776662>.

The ATLAS Collaboration

G. Aad ¹⁰¹, B. Abbott ¹¹⁹, D.C. Abbott ¹⁰², K. Abeling ⁵⁵, S.H. Abidi ²⁹, A. Aboulhorma ^{35e}, H. Abramowicz ¹⁵⁰, H. Abreu ¹⁴⁹, Y. Abulaiti ¹¹⁶, A.C. Abusleme Hoffman ^{136a}, B.S. Acharya ^{68a,68b,p}, B. Achkar ⁵⁵, C. Adam Bourdarios ⁴, L. Adamczyk ^{84a}, L. Adamek ¹⁵⁴, S.V. Addepalli ²⁶, J. Adelman ¹¹⁴, A. Adiguzel ^{21c}, S. Adorni ⁵⁶, T. Adye ¹³³, A.A. Affolder ¹³⁵, Y. Afik ³⁶, M.N. Agaras ¹³, J. Agarwala ^{72a,72b}, A. Aggarwal ⁹⁹, C. Agheorghiesei ^{27c}, J.A. Aguilar-Saavedra ^{129f}, A. Ahmad ³⁶, F. Ahmadov ^{38,z}, W.S. Ahmed ¹⁰³, S. Ahuja ⁹⁴, X. Ai ⁴⁸, G. Aielli ^{75a,75b}, I. Aizenberg ¹⁶⁸, M. Akbiyik ⁹⁹, T.P.A. Åkesson ⁹⁷, A.V. Akimov ³⁷, K. Al Khoury ⁴¹, G.L. Alberghi ^{23b}, J. Albert ¹⁶⁴, P. Albicocco ⁵³, S. Alderweireldt ⁵², M. Aleksa ³⁶, I.N. Aleksandrov ³⁸, C. Alexa ^{27b}, T. Alexopoulos ¹⁰, A. Alfonsi ¹¹³, F. Alfonsi ^{23b}, M. Alhroob ¹¹⁹, B. Ali ¹³¹, S. Ali ¹⁴⁷, M. Aliev ³⁷, G. Alimonti ^{70a}, W. Alkakhri ⁵⁵, C. Allaire ⁶⁶, B.M.M. Allbrooke ¹⁴⁵, P.P. Allport ²⁰, A. Aloisio ^{71a,71b}, F. Alonso ⁸⁹, C. Alpigiani ¹³⁷, E. Alunno Camelia ^{75a,75b}, M. Alvarez Estevez ⁹⁸, M.G. Alvigi ^{71a,71b}, M. Aly ¹⁰⁰, Y. Amaral Coutinho ^{81b}, A. Ambler ¹⁰³, C. Amelung ³⁶, M. Amerl ¹, C.G. Ames ¹⁰⁸, D. Amidei ¹⁰⁵, S.P. Amor Dos Santos ^{129a}, S. Amoroso ⁴⁸, K.R. Amos ¹⁶², V. Ananiev ¹²⁴, C. Anastopoulos ¹³⁸, T. Andeen ¹¹, J.K. Anders ³⁶, S.Y. Andrean ^{47a,47b}, A. Andreatza ^{70a,70b}, S. Angelidakis ⁹, A. Angerami ^{41,ac}, A.V. Anisenkov ³⁷, A. Annovi ^{73a}, C. Antel ⁵⁶, M.T. Anthony ¹³⁸, E. Antipov ¹²⁰, M. Antonelli ⁵³, D.J.A. Antrim ^{17a}, F. Anulli ^{74a}, M. Aoki ⁸², T. Aoki ¹⁵², J.A. Aparisi Pozo ¹⁶², M.A. Aparo ¹⁴⁵, L. Aperio Bella ⁴⁸, C. Appelt ¹⁸, N. Aranzabal ³⁶, V. Araujo Ferraz ^{81a}, C. Arcangeletti ⁵³, A.T.H. Arce ⁵¹, E. Arena ⁹¹, J-F. Arguin ¹⁰⁷, S. Argyropoulos ⁵⁴, J.-H. Arling ⁴⁸, A.J. Armbruster ³⁶, O. Arnaez ¹⁵⁴, H. Arnold ¹¹³, Z.P. Arrubarrena Tame ¹⁰⁸, G. Artoni ^{74a,74b}, H. Asada ¹¹⁰, K. Asai ¹¹⁷, S. Asai ¹⁵², N.A. Asbah ⁶¹, J. Assahsah ^{35d}, K. Assamagan ²⁹, R. Astalos ^{28a}, R.J. Atkin ^{33a}, M. Atkinson ¹⁶¹, N.B. Atlay ¹⁸, H. Atmani ^{62b}, P.A. Atmasiddha ¹⁰⁵, K. Augsten ¹³¹, S. Auricchio ^{71a,71b}, A.D. Auriol ²⁰, V.A. Austrup ¹⁷⁰, G. Avner ¹⁴⁹, G. Avolio ³⁶, K. Axiotis ⁵⁶, M.K. Ayoub ^{14c}, G. Azuelos ^{107,ah}, D. Babal ^{28a}, H. Bachacou ¹³⁴, K. Bachas ^{151,s}, A. Bachiu ³⁴, F. Backman ^{47a,47b}, A. Badea ⁶¹, P. Bagnaia ^{74a,74b}, M. Bahmani ¹⁸, A.J. Bailey ¹⁶², V.R. Bailey ¹⁶¹, J.T. Baines ¹³³, C. Bakalis ¹⁰, O.K. Baker ¹⁷¹, P.J. Bakker ¹¹³, E. Bakos ¹⁵, D. Bakshi Gupta ⁸, S. Balaji ¹⁴⁶, R. Balasubramanian ¹¹³, E.M. Baldin ³⁷, P. Balek ¹³², E. Ballabene ^{70a,70b}, F. Balli ¹³⁴, L.M. Baltes ^{63a}, W.K. Balunas ³², J. Balz ⁹⁹, E. Banas ⁸⁵, M. Bandieramonte ¹²⁸, A. Bandyopadhyay ²⁴, S. Bansal ²⁴, L. Barak ¹⁵⁰, E.L. Barberio ¹⁰⁴, D. Barberis ^{57b,57a}, M. Barbero ¹⁰¹, G. Barbour ⁹⁵, K.N. Barends ^{33a}, T. Barillari ¹⁰⁹, M-S. Barisits ³⁶, T. Barklow ¹⁴², R.M. Barnett ^{17a}, P. Baron ¹²¹, D.A. Baron Moreno ¹⁰⁰, A. Baroncelli ^{62a}, G. Barone ²⁹, A.J. Barr ¹²⁵, L. Barranco Navarro ^{47a,47b}, F. Barreiro ⁹⁸, J. Barreiro Guimarães da Costa ^{14a}, U. Barron ¹⁵⁰, M.G. Barros Teixeira ^{129a}, S. Barsov ³⁷, F. Bartels ^{63a}, R. Bartoldus ¹⁴², A.E. Barton ⁹⁰, P. Bartos ^{28a}, A. Basalae ⁴⁸, A. Basan ⁹⁹, M. Baselga ⁴⁹, I. Bashta ^{76a,76b}, A. Bassalat ^{66,b}, M.J. Basso ¹⁵⁴, C.R. Basson ¹⁰⁰, R.L. Bates ⁵⁹, S. Batlamous ^{35e}, J.R. Batley ³², B. Batool ¹⁴⁰, M. Battaglia ¹³⁵, D. Battulga ¹⁸, M. Bauge ^{74a,74b}, P. Bauer ²⁴, A. Bayirli ^{21a}, J.B. Beacham ⁵¹, T. Beau ¹²⁶, P.H. Beauchemin ¹⁵⁷, F. Becherer ⁵⁴, P. Bechtel ²⁴, H.P. Beck ^{19,r}, K. Becker ¹⁶⁶, A.J. Beddall ^{21d}, V.A. Bednyakov ³⁸, C.P. Bee ¹⁴⁴, L.J. Beemster ¹⁵, T.A. Beermann ³⁶, M. Begalli ^{81d}, M. Begel ²⁹, A. Behera ¹⁴⁴, J.K. Behr ⁴⁸, C. Beirao Da Cruz E Silva ³⁶, J.F. Beirer ^{55,36}, F. Beisiegel ²⁴, M. Belfkir ¹⁵⁸, G. Bella ¹⁵⁰, L. Bellagamba ^{23b}, A. Bellerive ³⁴, P. Bellos ²⁰, K. Beloborodov ³⁷, K. Belotskiy ³⁷, N.L. Belyaev ³⁷, D. Benckekroun ^{35a}, F. Bendebba ^{35a}, Y. Benhammou ¹⁵⁰, D.P. Benjamin ²⁹,

M. Benoit ²⁹, J.R. Bensinger ²⁶, S. Bentvelsen ¹¹³, L. Beresford ³⁶, M. Beretta ⁵³, D. Berge ¹⁸,
E. Bergeaas Kuutmann ¹⁶⁰, N. Berger ⁴, B. Bergmann ¹³¹, J. Beringer ^{17a}, S. Berlendis ⁷,
G. Bernardi ⁵, C. Bernius ¹⁴², F.U. Bernlochner ²⁴, T. Berry ⁹⁴, P. Berta ¹³², A. Berthold ⁵⁰,
I.A. Bertram ⁹⁰, S. Bethke ¹⁰⁹, A. Betti ^{74a,74b}, A.J. Bevan ⁹³, M. Bhamjee ^{33c}, S. Bhatta ¹⁴⁴,
D.S. Bhattacharya ¹⁶⁵, P. Bhattarai ²⁶, V.S. Bhopatkar ¹²⁰, R. Bi ^{29,ak}, R.M. Bianchi ¹²⁸,
O. Biebel ¹⁰⁸, R. Bielski ¹²², M. Biglietti ^{76a}, T.R.V. Billoud ¹³¹, M. Bindi ⁵⁵, A. Bingul ^{21b},
C. Bini ^{74a,74b}, S. Biondi ^{23b,23a}, A. Biondini ⁹¹, C.J. Birch-sykes ¹⁰⁰, G.A. Bird ^{20,133},
M. Birman ¹⁶⁸, T. Bisanz ³⁶, E. Bisceglie ^{43b,43a}, D. Biswas ^{169,1}, A. Bitadze ¹⁰⁰, K. Bjørke ¹²⁴,
I. Bloch ⁴⁸, C. Blocker ²⁶, A. Blue ⁵⁹, U. Blumenschein ⁹³, J. Blumenthal ⁹⁹, G.J. Bobbink ¹¹³,
V.S. Bobrovnikov ³⁷, M. Boehler ⁵⁴, D. Bogavac ³⁶, A.G. Bogdanchikov ³⁷, C. Bohm ^{47a},
V. Boisvert ⁹⁴, P. Bokan ⁴⁸, T. Bold ^{84a}, M. Bomben ⁵, M. Bona ⁹³, M. Boonekamp ¹³⁴,
C.D. Booth ⁹⁴, A.G. Borbély ⁵⁹, H.M. Borecka-Bielska ¹⁰⁷, L.S. Borgna ⁹⁵, G. Borissov ⁹⁰,
D. Bortoletto ¹²⁵, D. Boscherini ^{23b}, M. Bosman ¹³, J.D. Bossio Sola ³⁶, K. Bouaouda ^{35a},
N. Bouchhar ¹⁶², J. Boudreau ¹²⁸, E.V. Bouhova-Thacker ⁹⁰, D. Boumediene ⁴⁰, R. Bouquet ⁵,
A. Boveia ¹¹⁸, J. Boyd ³⁶, D. Boye ²⁹, I.R. Boyko ³⁸, J. Bracinik ²⁰, N. Brahimi ^{62d},
G. Brandt ¹⁷⁰, O. Brandt ³², F. Braren ⁴⁸, B. Brau ¹⁰², J.E. Brau ¹²², K. Brendlinger ⁴⁸,
R. Brenner ¹⁶⁸, L. Brenner ¹¹³, R. Brenner ¹⁶⁰, S. Bressler ¹⁶⁸, B. Brickwedde ⁹⁹, D. Britton ⁵⁹,
D. Britzger ¹⁰⁹, I. Brock ²⁴, G. Brooijmans ⁴¹, W.K. Brooks ^{136f}, E. Brost ²⁹, T.L. Bruckler ¹²⁵,
P.A. Bruckman de Renstrom ⁸⁵, B. Brüers ⁴⁸, D. Bruncko ^{28b,*}, A. Bruni ^{23b}, G. Bruni ^{23b},
M. Bruschi ^{23b}, N. Bruscinò ^{74a,74b}, L. Bryngemark ¹⁴², T. Buanes ¹⁶, Q. Buat ¹³⁷,
P. Buchholz ¹⁴⁰, A.G. Buckley ⁵⁹, I.A. Budagov ^{38,*}, M.K. Bugge ¹²⁴, O. Bulekov ³⁷,
B.A. Bullard ⁶¹, S. Burdin ⁹¹, C.D. Burgard ⁴⁸, A.M. Burger ⁴⁰, B. Burghgrave ⁸, J.T.P. Burr ³²,
C.D. Burton ¹¹, J.C. Burzynski ¹⁴¹, E.L. Busch ⁴¹, V. Büscher ⁹⁹, P.J. Bussey ⁵⁹, J.M. Butler ²⁵,
C.M. Buttar ⁵⁹, J.M. Butterworth ⁹⁵, W. Buttinger ¹³³, C.J. Buxo Vazquez ¹⁰⁶, A.R. Buzykaev ³⁷,
G. Cabras ^{23b}, S. Cabrera Urbán ¹⁶², D. Caforio ⁵⁸, H. Cai ¹²⁸, Y. Cai ^{14a,14d}, V.M.M. Cairo ³⁶,
O. Cakir ^{3a}, N. Calace ³⁶, P. Calafiura ^{17a}, G. Calderini ¹²⁶, P. Calfayan ⁶⁷, G. Callea ⁵⁹,
L.P. Caloba ^{81b}, D. Calvet ⁴⁰, S. Calvet ⁴⁰, T.P. Calvet ¹⁰¹, M. Calvetti ^{73a,73b},
R. Camacho Toro ¹²⁶, S. Camarda ³⁶, D. Camarero Munoz ²⁶, P. Camarri ^{75a,75b},
M.T. Camerlingo ^{76a,76b}, D. Cameron ¹²⁴, C. Camincher ¹⁶⁴, M. Campanelli ⁹⁵, A. Camplani ⁴²,
V. Canale ^{71a,71b}, A. Canesse ¹⁰³, M. Cano Bret ⁷⁹, J. Cantero ¹⁶², Y. Cao ¹⁶¹, F. Capocasa ²⁶,
M. Capua ^{43b,43a}, A. Carbone ^{70a,70b}, R. Cardarelli ^{75a}, J.C.J. Cardenas ⁸, F. Cardillo ¹⁶²,
T. Carli ³⁶, G. Carlino ^{71a}, J.I. Carlotto ¹³, B.T. Carlson ^{128,t}, E.M. Carlson ^{164,155a},
L. Carminati ^{70a,70b}, M. Carnesale ^{74a,74b}, S. Caron ¹¹², E. Carquin ^{136f}, S. Carrá ^{70a,70b},
G. Carratta ^{23b,23a}, F. Carri Argos ^{33g}, J.W.S. Carter ¹⁵⁴, T.M. Carter ⁵², M.P. Casado ^{13,i},
A.F. Casha ¹⁵⁴, E.G. Castiglia ¹⁷¹, F.L. Castillo ^{63a}, L. Castillo Garcia ¹³, V. Castillo Gimenez ¹⁶²,
N.F. Castro ^{129a,129e}, A. Catinaccio ³⁶, J.R. Catmore ¹²⁴, V. Cavaliere ²⁹, N. Cavalli ^{23b,23a},
V. Cavasinni ^{73a,73b}, E. Celebi ^{21a}, F. Celli ¹²⁵, M.S. Centonze ^{69a,69b}, K. Cerny ¹²¹,
A.S. Cerqueira ^{81a}, A. Cerri ¹⁴⁵, L. Cerrito ^{75a,75b}, F. Cerutti ^{17a}, A. Cervelli ^{23b}, S.A. Cetin ^{21d},
Z. Chadi ^{35a}, D. Chakraborty ¹¹⁴, M. Chala ^{129f}, J. Chan ¹⁶⁹, W.Y. Chan ¹⁵², J.D. Chapman ³²,
B. Chargeishvili ^{148b}, D.G. Charlton ²⁰, T.P. Charman ⁹³, M. Chatterjee ¹⁹, S. Chekanov ⁶,
S.V. Chekulaev ^{155a}, G.A. Chelkov ^{38,a}, A. Chen ¹⁰⁵, B. Chen ¹⁵⁰, B. Chen ¹⁶⁴, H. Chen ^{14c},
H. Chen ²⁹, J. Chen ^{62c}, J. Chen ²⁶, S. Chen ¹⁵², S.J. Chen ^{14c}, X. Chen ^{62c}, X. Chen ^{14b,ag},
Y. Chen ^{62a}, C.L. Cheng ¹⁶⁹, H.C. Cheng ^{64a}, S. Cheong ¹⁴², A. Cheplakov ³⁸,
E. Cheremushkina ⁴⁸, E. Cherepanova ¹¹³, R. Cherkaoui El Moursli ^{35e}, E. Cheu ⁷, K. Cheung ⁶⁵,
L. Chevalier ¹³⁴, V. Chiarella ⁵³, G. Chiarelli ^{73a}, N. Chiedde ¹⁰¹, G. Chiodini ^{69a},
A.S. Chisholm ²⁰, A. Chitan ^{27b}, M. Chitishvili ¹⁶², Y.H. Chiu ¹⁶⁴, M.V. Chizhov ³⁸, K. Choi ¹¹,
A.R. Chomont ^{74a,74b}, Y. Chou ¹⁰², E.Y.S. Chow ¹¹³, T. Chowdhury ^{33g}, L.D. Christopher ^{33g},

K.L. Chu^{64a}, M.C. Chu^{64a}, X. Chu^{14a,14d}, J. Chudoba¹³⁰, J.J. Chwastowski⁸⁵, D. Cieri¹⁰⁹,
 K.M. Ciesla^{84a}, V. Cindro⁹², A. Ciocio^{17a}, F. Cirotto^{71a,71b}, Z.H. Citron^{168,m}, M. Citterio^{70a},
 D.A. Ciubotaru^{27b}, B.M. Ciungu¹⁵⁴, A. Clark⁵⁶, P.J. Clark⁵², J.M. Clavijo Columbie⁴⁸,
 S.E. Clawson¹⁰⁰, C. Clement^{47a,47b}, J. Clercx⁴⁸, L. Clissa^{23b,23a}, Y. Coadou¹⁰¹,
 M. Cobal^{68a,68c}, A. Coccaro^{57b}, R.F. Coelho Barrue^{129a}, R. Coelho Lopes De Sa¹⁰²,
 S. Coelli^{70a}, H. Cohen¹⁵⁰, A.E.C. Coimbra^{70a,70b}, B. Cole⁴¹, J. Collot⁶⁰,
 P. Conde Muiño^{129a,129g}, M.P. Connell^{33c}, S.H. Connell^{33c}, I.A. Connelly⁵⁹, E.I. Conroy¹²⁵,
 F. Conventi^{71a,ai}, H.G. Cooke²⁰, A.M. Cooper-Sarkar¹²⁵, F. Cormier¹⁶³, L.D. Corpe³⁶,
 M. Corradi^{74a,74b}, E.E. Corrigan⁹⁷, F. Corriveau^{103,x}, A. Cortes-Gonzalez¹⁸, M.J. Costa¹⁶²,
 F. Costanza⁴, D. Costanzo¹³⁸, B.M. Cote¹¹⁸, G. Cowan⁹⁴, J.W. Cowley³², K. Cranmer¹¹⁶,
 S. Crépe-Renaudin⁶⁰, F. Crescioli¹²⁶, M. Cristinziani¹⁴⁰, M. Cristoforetti^{77a,77b,d}, V. Croft¹⁵⁷,
 G. Crosetti^{43b,43a}, A. Cueto³⁶, T. Cuhadar Donszelmann¹⁵⁹, H. Cui^{14a,14d}, Z. Cui⁷,
 A.R. Cukierman¹⁴², W.R. Cunningham⁵⁹, F. Curcio^{43b,43a}, P. Czodrowski³⁶, M.M. Czurylo^{63b},
 M.J. Da Cunha Sargedas De Sousa^{62a}, J.V. Da Fonseca Pinto^{81b}, C. Da Via¹⁰⁰, W. Dabrowski^{84a},
 T. Dado⁴⁹, S. Dahbi^{33g}, T. Dai¹⁰⁵, C. Dallapiccola¹⁰², M. Dam⁴², G. D'amen²⁹,
 V. D'Amico¹⁰⁸, J. Damp⁹⁹, J.R. Dandoy¹²⁷, M.F. Daneri³⁰, M. Danninger¹⁴¹, V. Dao³⁶,
 G. Darbo^{57b}, S. Darmora⁶, S.J. Das^{29,ak}, S. D'Auria^{70a,70b}, C. David^{155b}, T. Davidek¹³²,
 D.R. Davis⁵¹, B. Davis-Purcell³⁴, I. Dawson⁹³, K. De⁸, R. De Asmundis^{71a},
 M. De Beurs¹¹³, N. De Biase⁴⁸, S. De Castro^{23b,23a}, N. De Groot¹¹², P. de Jong¹¹³,
 H. De la Torre¹⁰⁶, A. De Maria^{14c}, A. De Salvo^{74a}, U. De Sanctis^{75a,75b}, A. De Santo¹⁴⁵,
 J.B. De Vivie De Regie⁶⁰, D.V. Dedovich³⁸, J. Degens¹¹³, A.M. Deiana⁴⁴, F. Del Corso^{23b,23a},
 J. Del Peso⁹⁸, F. Del Rio^{63a}, F. Deliot¹³⁴, C.M. Delitzsch⁴⁹, M. Della Pietra^{71a,71b},
 D. Della Volpe⁵⁶, A. Dell'Acqua³⁶, L. Dell'Asta^{70a,70b}, M. Delmastro⁴, P.A. Delsart⁶⁰,
 S. Demers¹⁷¹, M. Demichev³⁸, S.P. Denisov³⁷, L. D'Eramo¹¹⁴, D. Derendarz⁸⁵,
 F. Derue¹²⁶, P. Dervan⁹¹, K. Desch²⁴, K. Dette¹⁵⁴, C. Deutsch²⁴, P.O. Deviveiros³⁶,
 F.A. Di Bello^{57b,57a}, A. Di Ciaccio^{75a,75b}, L. Di Ciaccio⁴, A. Di Domenico^{74a,74b},
 C. Di Donato^{71a,71b}, A. Di Girolamo³⁶, G. Di Gregorio⁵, A. Di Luca^{77a,77b}, B. Di Micco^{76a,76b},
 R. Di Nardo^{76a,76b}, C. Diaconu¹⁰¹, F.A. Dias¹¹³, T. Dias Do Vale¹⁴¹, M.A. Diaz^{136a,136b},
 F.G. Diaz Capriles²⁴, M. Didenko¹⁶², E.B. Diehl¹⁰⁵, L. Diehl⁵⁴, S. Díez Cornell⁴⁸,
 C. Diez Pardos¹⁴⁰, C. Dimitriadi^{24,160}, A. Dimitrievska^{17a}, W. Ding^{14b}, J. Dingfelder²⁴,
 I-M. Dinu^{27b}, S.J. Dittmeier^{63b}, F. Dittus³⁶, F. Djama¹⁰¹, T. Djobava^{148b}, J.I. Djuvsland¹⁶,
 C. Doglioni^{100,97}, J. Dolejsi¹³², Z. Dolezal¹³², M. Donadelli^{81c}, B. Dong^{62c}, J. Donini⁴⁰,
 A. D'Onofrio^{14c}, M. D'Onofrio⁹¹, J. Dopke¹³³, A. Doria^{71a}, M.T. Dova⁸⁹, A.T. Doyle⁵⁹,
 M.A. Draguet¹²⁵, E. Drechsler¹⁴¹, E. Dreyer¹⁶⁸, I. Drivas-koulouris¹⁰, A.S. Drobac¹⁵⁷,
 M. Drozdova⁵⁶, D. Du^{62a}, T.A. du Pree¹¹³, F. Dubinin³⁷, M. Dubovsky^{28a}, E. Duchovni¹⁶⁸,
 G. Duckeck¹⁰⁸, O.A. Ducu^{27b}, D. Duda¹⁰⁹, A. Dudarev³⁶, M. D'uffizi¹⁰⁰, L. Duflot⁶⁶,
 M. Dührssen³⁶, C. Dülsen¹⁷⁰, A.E. Dumitriu^{27b}, M. Dunford^{63a}, S. Dungs⁴⁹,
 K. Dunne^{47a,47b}, A. Duperrin¹⁰¹, H. Duran Yildiz^{3a}, M. Düren⁵⁸, A. Durglishvili^{148b},
 B.L. Dwyer¹¹⁴, G.I. Dyckes^{17a}, M. Dyndal^{84a}, S. Dysch¹⁰⁰, B.S. Dziedzic⁸⁵,
 Z.O. Earnshaw¹⁴⁵, B. Eckerova^{28a}, M.G. Eggleston⁵¹, E. Egidio Purcino De Souza^{81b},
 L.F. Ehrke⁵⁶, G. Eigen¹⁶, K. Einsweiler^{17a}, T. Ekelof¹⁶⁰, P.A. Ekman⁹⁷, Y. El Ghazali^{35b},
 H. El Jarrari^{35e,147}, A. El Moussaouy^{35a}, V. Ellajosyula¹⁶⁰, M. Ellert¹⁶⁰, F. Ellinghaus¹⁷⁰,
 A.A. Elliot⁹³, N. Ellis³⁶, J. Elmsheuser²⁹, M. Elsing³⁶, D. Emelianov¹³³, A. Emerman⁴¹,
 Y. Enari¹⁵², I. Ene^{17a}, S. Epari¹³, J. Erdmann^{49,ae}, A. Ereditato¹⁹, P.A. Erland⁸⁵,
 M. Errenst¹⁷⁰, M. Escalier⁶⁶, C. Escobar¹⁶², E. Etzion¹⁵⁰, G. Evans^{129a}, H. Evans⁶⁷,
 M.O. Evans¹⁴⁵, A. Ezhilov³⁷, S. Ezzarqtouni^{35a}, F. Fabbri⁵⁹, L. Fabbri^{23b,23a}, G. Facini⁹⁵,
 V. Fadeyev¹³⁵, R.M. Fakhrutdinov³⁷, S. Falciano^{74a}, P.J. Falke²⁴, S. Falke³⁶, J. Faltova¹³²,

Y. Fan [id^{14a}](#), Y. Fang [id^{14a,14d}](#), G. Fanourakis [id⁴⁶](#), M. Fanti [id^{70a,70b}](#), M. Faraj [id^{68a,68b}](#), Z. Farazpay [id⁹⁶](#),
 A. Farbin [id⁸](#), A. Farilla [id^{76a}](#), T. Farooque [id¹⁰⁶](#), S.M. Farrington [id⁵²](#), F. Fassi [id^{35e}](#), D. Fassouliotis [id⁹](#),
 M. Faucci Giannelli [id^{75a,75b}](#), W.J. Fawcett [id³²](#), L. Fayard [id⁶⁶](#), P. Federicova [id¹³⁰](#), O.L. Fedin [id^{37,a}](#),
 G. Fedotov [id³⁷](#), M. Feickert [id¹⁶⁹](#), L. Feligioni [id¹⁰¹](#), A. Fell [id¹³⁸](#), D.E. Fellers [id¹²²](#), C. Feng [id^{62b}](#),
 M. Feng [id^{14b}](#), Z. Feng [id¹¹³](#), M.J. Fenton [id¹⁵⁹](#), A.B. Fenyuk [id³⁷](#), L. Ferencz [id⁴⁸](#), S.W. Ferguson [id⁴⁵](#),
 J. Ferrando [id⁴⁸](#), A. Ferrari [id¹⁶⁰](#), P. Ferrari [id^{113,112}](#), R. Ferrari [id^{72a}](#), D. Ferrere [id⁵⁶](#), C. Ferretti [id¹⁰⁵](#),
 F. Fiedler [id⁹⁹](#), A. Filipčič [id⁹²](#), E.K. Filmer [id¹](#), F. Filthaut [id¹¹²](#), M.C.N. Fiolhais [id^{129a,129c,c}](#),
 L. Fiorini [id¹⁶²](#), F. Fischer [id¹⁴⁰](#), W.C. Fisher [id¹⁰⁶](#), T. Fitschen [id¹⁰⁰](#), I. Fleck [id¹⁴⁰](#), P. Fleischmann [id¹⁰⁵](#),
 T. Flick [id¹⁷⁰](#), L. Flores [id¹²⁷](#), M. Flores [id^{33d,ad}](#), L.R. Flores Castillo [id^{64a}](#), F.M. Follega [id^{77a,77b}](#),
 N. Fomin [id¹⁶](#), J.H. Foo [id¹⁵⁴](#), B.C. Forland [id⁶⁷](#), A. Formica [id¹³⁴](#), A.C. Forti [id¹⁰⁰](#), E. Fortin [id¹⁰¹](#),
 A.W. Fortman [id⁶¹](#), M.G. Foti [id^{17a}](#), L. Fountas [id^{9j}](#), D. Fournier [id⁶⁶](#), H. Fox [id⁹⁰](#), P. Francavilla [id^{73a,73b}](#),
 S. Francescato [id⁶¹](#), S. Franchellucci [id⁵⁶](#), M. Franchini [id^{23b,23a}](#), S. Franchino [id^{63a}](#), D. Francis [id³⁶](#),
 L. Franco [id¹¹²](#), L. Franconi [id¹⁹](#), M. Franklin [id⁶¹](#), G. Frattari [id²⁶](#), A.C. Freegard [id⁹³](#), P.M. Freeman [id²⁰](#),
 W.S. Freund [id^{81b}](#), N. Fritzsche [id⁵⁰](#), A. Froch [id⁵⁴](#), D. Froidevaux [id³⁶](#), J.A. Frost [id¹²⁵](#), Y. Fu [id^{62a}](#),
 M. Fujimoto [id¹¹⁷](#), E. Fullana Torregrosa [id^{162,*}](#), J. Fuster [id¹⁶²](#), A. Gabrielli [id^{23b,23a}](#), A. Gabrielli [id¹⁵⁴](#),
 P. Gadow [id⁴⁸](#), G. Gagliardi [id^{57b,57a}](#), L.G. Gagnon [id^{17a}](#), G.E. Gallardo [id¹²⁵](#), E.J. Gallas [id¹²⁵](#),
 B.J. Gallop [id¹³³](#), R. Gamboa Goni [id⁹³](#), K.K. Gan [id¹¹⁸](#), S. Ganguly [id¹⁵²](#), J. Gao [id^{62a}](#), Y. Gao [id⁵²](#),
 F.M. Garay Walls [id^{136a,136b}](#), B. Garcia [id^{29,ak}](#), C. García [id¹⁶²](#), J.E. García Navarro [id¹⁶²](#),
 J.A. García Pascual [id^{14a}](#), M. Garcia-Sciveres [id^{17a}](#), R.W. Gardner [id³⁹](#), D. Garg [id⁷⁹](#), R.B. Garg [id^{142,q}](#),
 S. Gargiulo [id⁵⁴](#), C.A. Garner [id¹⁵⁴](#), V. Garonne [id²⁹](#), S.J. Gasiorowski [id¹³⁷](#), P. Gaspar [id^{81b}](#), G. Gaudio [id^{72a}](#),
 V. Gautam [id¹³](#), P. Gauzzi [id^{74a,74b}](#), I.L. Gavrilenko [id³⁷](#), A. Gavrilyuk [id³⁷](#), C. Gay [id¹⁶³](#), G. Gaycken [id⁴⁸](#),
 E.N. Gazis [id¹⁰](#), A.A. Geanta [id^{27b,27e}](#), C.M. Gee [id¹³⁵](#), J. Geisen [id⁹⁷](#), M. Geisen [id⁹⁹](#), C. Gemme [id^{57b}](#),
 M.H. Genest [id⁶⁰](#), S. Gentile [id^{74a,74b}](#), S. George [id⁹⁴](#), W.F. George [id²⁰](#), T. Geralis [id⁴⁶](#), L.O. Gerlach [id⁵⁵](#),
 P. Gessinger-Befurt [id³⁶](#), M. Ghasemi Bostanabad [id¹⁶⁴](#), M. Ghneimat [id¹⁴⁰](#), K. Ghorbanian [id⁹³](#),
 A. Ghosal [id¹⁴⁰](#), A. Ghosh [id¹⁵⁹](#), A. Ghosh [id⁷](#), B. Giacobbe [id^{23b}](#), S. Giagu [id^{74a,74b}](#),
 N. Giangiacomi [id¹⁵⁴](#), P. Giannetti [id^{73a}](#), A. Giannini [id^{62a}](#), S.M. Gibson [id⁹⁴](#), M. Gignac [id¹³⁵](#),
 D.T. Gil [id^{84b}](#), A.K. Gilbert [id^{84a}](#), B.J. Gilbert [id⁴¹](#), D. Gillberg [id³⁴](#), G. Gilles [id¹¹³](#), N.E.K. Gillwald [id⁴⁸](#),
 L. Ginabat [id¹²⁶](#), D.M. Gingrich [id^{2,ah}](#), M.P. Giordani [id^{68a,68c}](#), P.F. Giraud [id¹³⁴](#), G. Giugliarelli [id^{68a,68c}](#),
 D. Giugni [id^{70a}](#), F. Giuli [id³⁶](#), I. Gkialas [id^{9,j}](#), L.K. Gladilin [id³⁷](#), C. Glasman [id⁹⁸](#), G.R. Gledhill [id¹²²](#),
 M. Glisic [id¹²²](#), I. Gnesi [id^{43b,f}](#), Y. Go [id^{29,ak}](#), M. Goblirsch-Kolb [id²⁶](#), B. Gocke [id⁴⁹](#), D. Godin [id¹⁰⁷](#),
 S. Goldfarb [id¹⁰⁴](#), T. Golling [id⁵⁶](#), M.G.D. Gololo [id^{33g}](#), D. Golubkov [id³⁷](#), J.P. Gombas [id¹⁰⁶](#),
 A. Gomes [id^{129a,129b}](#), G. Gomes Da Silva [id¹⁴⁰](#), A.J. Gomez Delegido [id¹⁶²](#), R. Goncalves Gama [id⁵⁵](#),
 R. Gonçalves [id^{129a,129c}](#), G. Gonella [id¹²²](#), L. Gonella [id²⁰](#), A. Gongadze [id³⁸](#), F. Gonnella [id²⁰](#),
 J.L. Gonski [id⁴¹](#), R.Y. González Andana [id⁵²](#), S. González de la Hoz [id¹⁶²](#), S. Gonzalez Fernandez [id¹³](#),
 R. Gonzalez Lopez [id⁹¹](#), C. Gonzalez Renteria [id^{17a}](#), R. Gonzalez Suarez [id¹⁶⁰](#), S. Gonzalez-Sevilla [id⁵⁶](#),
 G.R. Gonzalvo Rodriguez [id¹⁶²](#), L. Goossens [id³⁶](#), N.A. Gorasia [id²⁰](#), P.A. Gorbounov [id³⁷](#), B. Gorini [id³⁶](#),
 E. Gorini [id^{69a,69b}](#), A. Gorišek [id⁹²](#), A.T. Goshaw [id⁵¹](#), M.I. Gostkin [id³⁸](#), C.A. Gottardo [id³⁶](#),
 M. Goughri [id^{35b}](#), V. Goumarre [id⁴⁸](#), A.G. Goussiou [id¹³⁷](#), N. Govender [id^{33c}](#), C. Goy [id⁴](#),
 I. Grabowska-Bold [id^{84a}](#), K. Graham [id³⁴](#), E. Gramstad [id¹²⁴](#), S. Grancagnolo [id¹⁸](#), M. Grandi [id¹⁴⁵](#),
 V. Gratchev [id^{37,*}](#), P.M. Gravila [id^{27f}](#), F.G. Gravili [id^{69a,69b}](#), H.M. Gray [id^{17a}](#), M. Greco [id^{69a,69b}](#),
 C. Grefe [id²⁴](#), I.M. Gregor [id⁴⁸](#), P. Grenier [id¹⁴²](#), C. Grieco [id¹³](#), A.A. Grillo [id¹³⁵](#), K. Grimm [id^{31,n}](#),
 S. Grinstein [id^{13,v}](#), J.-F. Grivaz [id⁶⁶](#), E. Gross [id¹⁶⁸](#), J. Grosse-Knetter [id⁵⁵](#), C. Grud [id¹⁰⁵](#), A. Grummer [id¹¹¹](#),
 J.C. Grundy [id¹²⁵](#), L. Guan [id¹⁰⁵](#), W. Guan [id¹⁶⁹](#), C. Gubbels [id¹⁶³](#), J.G.R. Guerrero Rojas [id¹⁶²](#),
 G. Guerrieri [id^{68a,68b}](#), F. Guescini [id¹⁰⁹](#), R. Gugel [id⁹⁹](#), J.A.M. Guhit [id¹⁰⁵](#), A. Guida [id⁴⁸](#), T. Guillemain [id⁴](#),
 E. Guilloton [id^{166,133}](#), S. Guindon [id³⁶](#), F. Guo [id^{14a,14d}](#), J. Guo [id^{62c}](#), L. Guo [id⁶⁶](#), Y. Guo [id¹⁰⁵](#),
 R. Gupta [id⁴⁸](#), S. Gurbuz [id²⁴](#), S.S. Gurdasani [id⁵⁴](#), G. Gustavino [id³⁶](#), M. Guth [id⁵⁶](#), P. Gutierrez [id¹¹⁹](#),
 L.F. Gutierrez Zagazeta [id¹²⁷](#), C. Gutschow [id⁹⁵](#), C. Guyot [id¹³⁴](#), C. Gwenlan [id¹²⁵](#), C.B. Gwilliam [id⁹¹](#),

E.S. Haaland ¹²⁴, A. Haas ¹¹⁶, M. Habedank ⁴⁸, C. Haber ^{17a}, H.K. Hadavand ⁸, A. Hadeif ⁹⁹,
 S. Hadzic ¹⁰⁹, E.H. Haines ⁹⁵, M. Haleem ¹⁶⁵, J. Haley ¹²⁰, J.J. Hall ¹³⁸, G.D. Hallelwell ¹⁰¹,
 L. Halser ¹⁹, K. Hamano ¹⁶⁴, H. Hamdaoui ^{35e}, M. Hamer ²⁴, G.N. Hamity ⁵², J. Han ^{62b},
 K. Han ^{62a}, L. Han ^{14c}, L. Han ^{62a}, S. Han ^{17a}, Y.F. Han ¹⁵⁴, K. Hanagaki ⁸², M. Hance ¹³⁵,
 D.A. Hangal ^{41,ac}, H. Hanif ¹⁴¹, M.D. Hank ³⁹, R. Hankache ¹⁰⁰, J.B. Hansen ⁴²,
 J.D. Hansen ⁴², P.H. Hansen ⁴², K. Hara ¹⁵⁶, D. Harada ⁵⁶, T. Harenberg ¹⁷⁰, S. Harkusha ³⁷,
 Y.T. Harris ¹²⁵, N.M. Harrison ¹¹⁸, P.F. Harrison ¹⁶⁶, N.M. Hartman ¹⁴², N.M. Hartmann ¹⁰⁸,
 Y. Hasegawa ¹³⁹, A. Hasib ⁵², S. Haug ¹⁹, R. Hauser ¹⁰⁶, M. Havranek ¹³¹, C.M. Hawkes ²⁰,
 R.J. Hawkings ³⁶, S. Hayashida ¹¹⁰, D. Hayden ¹⁰⁶, C. Hayes ¹⁰⁵, R.L. Hayes ¹⁶³, C.P. Hays ¹²⁵,
 J.M. Hays ⁹³, H.S. Hayward ⁹¹, F. He ^{62a}, Y. He ¹⁵³, Y. He ¹²⁶, M.P. Heath ⁵², V. Hedberg ⁹⁷,
 A.L. Heggelund ¹²⁴, N.D. Hehir ⁹³, C. Heidegger ⁵⁴, K.K. Heidegger ⁵⁴, W.D. Heidorn ⁸⁰,
 J. Heilmann ³⁴, S. Heim ⁴⁸, T. Heim ^{17a}, J.G. Heinlein ¹²⁷, J.J. Heinrich ¹²², L. Heinrich ^{109,af},
 J. Hejbal ¹³⁰, L. Helary ⁴⁸, A. Held ¹⁶⁹, S. Hellesund ¹²⁴, C.M. Helling ¹⁶³, S. Hellman ^{47a,47b},
 C. Helsens ³⁶, R.C.W. Henderson ⁹⁰, L. Henkelmann ³², A.M. Henriques Correia ³⁶, H. Herde ⁹⁷,
 Y. Hernández Jiménez ¹⁴⁴, L.M. Herrmann ²⁴, M.G. Herrmann ¹⁰⁸, T. Herrmann ⁵⁰, G. Herten ⁵⁴,
 R. Hertenberger ¹⁰⁸, L. Hervas ³⁶, N.P. Hesse ^{155a}, H. Hibi ⁸³, E. Higón-Rodríguez ¹⁶²,
 S.J. Hillier ²⁰, I. Hinchliffe ^{17a}, F. Hinterkeuser ²⁴, M. Hirose ¹²³, S. Hirose ¹⁵⁶,
 D. Hirschbuehl ¹⁷⁰, T.G. Hitchings ¹⁰⁰, B. Hiti ⁹², J. Hobbs ¹⁴⁴, R. Hobincu ^{27e}, N. Hod ¹⁶⁸,
 M.C. Hodgkinson ¹³⁸, B.H. Hodgkinson ³², A. Hoecker ³⁶, J. Hofer ⁴⁸, D. Hohn ⁵⁴, T. Holm ²⁴,
 M. Holzbock ¹⁰⁹, L.B.A.H. Hommels ³², B.P. Honan ¹⁰⁰, J. Hong ^{62c}, T.M. Hong ¹²⁸,
 J.C. Honig ⁵⁴, A. Hönle ¹⁰⁹, B.H. Hooberman ¹⁶¹, W.H. Hopkins ⁶, Y. Horii ¹¹⁰, S. Hou ¹⁴⁷,
 A.S. Howard ⁹², J. Howarth ⁵⁹, J. Hoya ⁶, M. Hrabovsky ¹²¹, A. Hrynevich ⁴⁸, T. Hryn'ova ⁴,
 P.J. Hsu ⁶⁵, S.-C. Hsu ¹³⁷, Q. Hu ^{41,ac}, Y.F. Hu ^{14a,14d,aj}, D.P. Huang ⁹⁵, S. Huang ^{64b},
 X. Huang ^{14c}, Y. Huang ^{62a}, Y. Huang ^{14a}, Z. Huang ¹⁰⁰, Z. Hubacek ¹³¹, M. Huebner ²⁴,
 F. Huegging ²⁴, T.B. Huffman ¹²⁵, M. Huhtinen ³⁶, S.K. Huiberts ¹⁶, R. Hulskén ¹⁰³,
 N. Huseynov ^{12,a}, J. Huston ¹⁰⁶, J. Huth ⁶¹, R. Hyneman ¹⁴², S. Hyrych ^{28a}, G. Iacobucci ⁵⁶,
 G. Iakovidis ²⁹, I. Ibragimov ¹⁴⁰, L. Iconomidou-Fayard ⁶⁶, P. Iengo ^{71a,71b}, R. Iguchi ¹⁵²,
 T. Iizawa ⁵⁶, Y. Ikegami ⁸², A. Ilg ¹⁹, N. Ilic ¹⁵⁴, H. Imam ^{35a}, T. Ingebretsen Carlson ^{47a,47b},
 G. Introzzi ^{72a,72b}, M. Iodice ^{76a}, V. Ippolito ^{74a,74b}, M. Ishino ¹⁵², W. Islam ¹⁶⁹, C. Issever ^{18,48},
 S. Istin ^{21a,am}, H. Ito ¹⁶⁷, J.M. Iturbe Ponce ^{64a}, R. Iuppa ^{77a,77b}, A. Ivina ¹⁶⁸, J.M. Izen ⁴⁵,
 V. Izzo ^{71a}, P. Jacka ^{130,131}, P. Jackson ¹, R.M. Jacobs ⁴⁸, B.P. Jaeger ¹⁴¹, C.S. Jagfeld ¹⁰⁸,
 G. Jäkel ¹⁷⁰, K. Jakobs ⁵⁴, T. Jakoubek ¹⁶⁸, J. Jamieson ⁵⁹, K.W. Janas ^{84a}, G. Jarlskog ⁹⁷,
 A.E. Jaspan ⁹¹, M. Javurkova ¹⁰², F. Jeanneau ¹³⁴, L. Jeanty ¹²², J. Jejelava ^{148a,aa}, P. Jenni ^{54,g},
 C.E. Jessiman ³⁴, S. Jézéquel ⁴, J. Jia ¹⁴⁴, X. Jia ⁶¹, X. Jia ^{14a,14d}, Z. Jia ^{14c}, Y. Jiang ^{62a},
 S. Jiggins ⁵², J. Jimenez Pena ¹⁰⁹, S. Jin ^{14c}, A. Jinaru ^{27b}, O. Jinnouchi ¹⁵³, P. Johansson ¹³⁸,
 K.A. Johns ⁷, D.M. Jones ³², E. Jones ¹⁶⁶, P. Jones ³², R.W.L. Jones ⁹⁰, T.J. Jones ⁹¹,
 R. Joshi ¹¹⁸, J. Jovicevic ¹⁵, X. Ju ^{17a}, J.J. Junggeburth ³⁶, A. Juste Rozas ^{13,v}, S. Kabana ^{136e},
 A. Kaczmarska ⁸⁵, M. Kado ^{74a,74b}, H. Kagan ¹¹⁸, M. Kagan ¹⁴², A. Kahn ⁴¹, A. Kahn ¹²⁷,
 C. Kahra ⁹⁹, T. Kaji ¹⁶⁷, E. Kajomovitz ¹⁴⁹, N. Kakati ¹⁶⁸, C.W. Kalderon ²⁹,
 A. Kamenshchikov ¹⁵⁴, S. Kanayama ¹⁵³, N.J. Kang ¹³⁵, Y. Kano ¹¹⁰, D. Kar ^{33g}, K. Karava ¹²⁵,
 M.J. Kareem ^{155b}, E. Karentzos ⁵⁴, I. Karkanas ¹⁵¹, S.N. Karpov ³⁸, Z.M. Karpova ³⁸,
 V. Kartvelishvili ⁹⁰, A.N. Karyukhin ³⁷, E. Kasimi ¹⁵¹, C. Kato ^{62d}, J. Katzy ⁴⁸, S. Kaur ³⁴,
 K. Kawade ¹³⁹, K. Kawagoe ⁸⁸, T. Kawamoto ¹³⁴, G. Kawamura ⁵⁵, E.F. Kay ¹⁶⁴, F.I. Kaya ¹⁵⁷,
 S. Kazakos ¹³, V.F. Kazanin ³⁷, Y. Ke ¹⁴⁴, J.M. Keaveney ^{33a}, R. Keeler ¹⁶⁴, G.V. Kehris ⁶¹,
 J.S. Keller ³⁴, A.S. Kelly ⁹⁵, D. Kelsey ¹⁴⁵, J.J. Kempster ²⁰, K.E. Kennedy ⁴¹, P.D. Kennedy ⁹⁹,
 O. Kepka ¹³⁰, B.P. Kerridge ¹⁶⁶, S. Kersten ¹⁷⁰, B.P. Kerševan ⁹², S. Keshri ⁶⁶,
 L. Keszeghova ^{28a}, S. Ketabchi Haghghat ¹⁵⁴, M. Khandoga ¹²⁶, A. Khanov ¹²⁰,

A.G. Kharlamov ³⁷, T. Kharlamova ³⁷, E.E. Khoda ¹³⁷, T.J. Khoo ¹⁸, G. Khoriauli ¹⁶⁵,
 J. Khubua ^{148b}, Y.A.R. Khwaira ⁶⁶, M. Kiehn ³⁶, A. Kilgallon ¹²², D.W. Kim ^{47a,47b},
 E. Kim ¹⁵³, Y.K. Kim ³⁹, N. Kimura ⁹⁵, A. Kirchhoff ⁵⁵, D. Kirchmeier ⁵⁰, C. Kirfel ²⁴,
 J. Kirk ¹³³, A.E. Kiryunin ¹⁰⁹, T. Kishimoto ¹⁵², D.P. Kisliuk ¹⁵⁴, C. Kitsaki ¹⁰, O. Kivernyk ²⁴,
 M. Klassen ^{63a}, C. Klein ³⁴, L. Klein ¹⁶⁵, M.H. Klein ¹⁰⁵, M. Klein ⁹¹, S.B. Klein ⁵⁶,
 U. Klein ⁹¹, P. Klimek ³⁶, A. Klimentov ²⁹, F. Klimpel ¹⁰⁹, T. Klingl ²⁴, T. Klioutchnikova ³⁶,
 F.F. Klitzner ¹⁰⁸, P. Kluit ¹¹³, S. Kluth ¹⁰⁹, E. Kneringer ⁷⁸, T.M. Knight ¹⁵⁴, A. Knue ⁵⁴,
 D. Kobayashi⁸⁸, R. Kobayashi ⁸⁶, M. Kocian ¹⁴², P. Kodyš ¹³², D.M. Koeck ¹⁴⁵, P.T. Koenig ²⁴,
 T. Koffas ³⁴, M. Kolb ¹³⁴, I. Koletsou ⁴, T. Komarek ¹²¹, K. Köneke ⁵⁴, A.X.Y. Kong ¹,
 T. Kono ¹¹⁷, N. Konstantinidis ⁹⁵, B. Konya ⁹⁷, R. Kopeliansky ⁶⁷, S. Koperny ^{84a}, K. Korcyl ⁸⁵,
 K. Kordas ¹⁵¹, G. Koren ¹⁵⁰, A. Korn ⁹⁵, S. Korn ⁵⁵, I. Korolkov ¹³, N. Korotkova ³⁷,
 B. Kortman ¹¹³, O. Kortner ¹⁰⁹, S. Kortner ¹⁰⁹, W.H. KostECKa ¹¹⁴, V.V. Kostyukhin ¹⁴⁰,
 A. Kotsokchagia ¹³⁴, A. Kotwal ⁵¹, A. Koulouris ³⁶, A. Kourkoumeli-Charalampidi ^{72a,72b},
 C. Kourkoumelis ⁹, E. Kourlitis ⁶, O. Kovanda ¹⁴⁵, R. Kowalewski ¹⁶⁴, W. Kozanecki ¹³⁴,
 A.S. Kozhin ³⁷, V.A. Kramarenko ³⁷, G. Kramberger ⁹², P. Kramer ⁹⁹, M.W. Krasny ¹²⁶,
 A. Krasznahorkay ³⁶, J.A. Kremer ⁹⁹, T. Kresse ⁵⁰, J. Kretzschmar ⁹¹, K. Kreul ¹⁸,
 P. Krieger ¹⁵⁴, F. Krieter ¹⁰⁸, S. Krishnamurthy ¹⁰², A. Krishnan ^{63b}, M. Krivos ¹³²,
 K. Krizka ^{17a}, K. Kroeninger ⁴⁹, H. Kroha ¹⁰⁹, J. Kroll ¹³⁰, J. Kroll ¹²⁷, K.S. Krowpman ¹⁰⁶,
 U. Kruchonak ³⁸, H. Krüger ²⁴, N. Krumnack⁸⁰, M.C. Kruse ⁵¹, J.A. Krzysiak ⁸⁵,
 O. Kuchinskaia ³⁷, S. Kuday ^{3a}, D. Kuechler ⁴⁸, J.T. Kuechler ⁴⁸, S. Kuehn ³⁶, T. Kuhl ⁴⁸,
 V. Kukhtin ³⁸, Y. Kulchitsky ^{37,a}, S. Kuleshov ^{136d,136b}, M. Kumar ^{33g}, N. Kumari ¹⁰¹,
 A. Kupco ¹³⁰, T. Kupfer⁴⁹, A. Kupich ³⁷, O. Kuprash ⁵⁴, H. Kurashige ⁸³, L.L. Kurchaninov ^{155a},
 Y.A. Kurochkin ³⁷, A. Kurova ³⁷, M. Kuze ¹⁵³, A.K. Kvam ¹⁰², J. Kvita ¹²¹, T. Kwan ¹⁰³,
 K.W. Kwok ^{64a}, N.G. Kyriacou ¹⁰⁵, L.A.O. Laatu ¹⁰¹, C. Lacasta ¹⁶², F. Lacava ^{74a,74b},
 H. Lacker ¹⁸, D. Lacour ¹²⁶, N.N. Lad ⁹⁵, E. Ladygin ³⁸, B. Laforge ¹²⁶, T. Lagouri ^{136e},
 S. Lai ⁵⁵, I.K. Lakomic ^{84a}, N. Lalloue ⁶⁰, J.E. Lambert ¹¹⁹, S. Lammers ⁶⁷, W. Lampl ⁷,
 C. Lampoudis ¹⁵¹, A.N. Lancaster ¹¹⁴, E. Lançon ²⁹, U. Landgraf ⁵⁴, M.P.J. Landon ⁹³,
 V.S. Lang ⁵⁴, R.J. Langenberg ¹⁰², A.J. Lankford ¹⁵⁹, F. Lanni ³⁶, K. Lantzsch ²⁴, A. Lanza ^{72a},
 A. Lapertosa ^{57b,57a}, J.F. Laporte ¹³⁴, T. Lari ^{70a}, F. Lasagni Manghi ^{23b}, M. Lassnig ³⁶,
 V. Latonova ¹³⁰, T.S. Lau ^{64a}, A. Laudrain ⁹⁹, A. Laurier ³⁴, S.D. Lawlor ⁹⁴, Z. Lawrence ¹⁰⁰,
 M. Lazzaroni ^{70a,70b}, B. Le¹⁰⁰, B. Leban ⁹², A. Lebedev ⁸⁰, M. LeBlanc ³⁶, T. LeCompte ⁶,
 F. Ledroit-Guillon ⁶⁰, A.C.A. Lee⁹⁵, G.R. Lee ¹⁶, L. Lee ⁶¹, S.C. Lee ¹⁴⁷, S. Lee ^{47a,47b},
 T.F. Lee ⁹¹, L.L. Leeuw ^{33c}, H.P. Lefebvre ⁹⁴, M. Lefebvre ¹⁶⁴, C. Leggett ^{17a}, K. Lehmann ¹⁴¹,
 G. Lehmann Miotto ³⁶, M. Leigh ⁵⁶, W.A. Leight ¹⁰², A. Leisos ^{151,u}, M.A.L. Leite ^{81c},
 C.E. Leitgeb ⁴⁸, R. Leitner ¹³², K.J.C. Leney ⁴⁴, T. Lenz ²⁴, S. Leone ^{73a}, C. Leonidopoulos ⁵²,
 A. Leopold ¹⁴³, C. Leroy ¹⁰⁷, R. Les ¹⁰⁶, C.G. Lester ³², M. Levchenko ³⁷, J. Levêque ⁴,
 D. Levin ¹⁰⁵, L.J. Levinson ¹⁶⁸, M.P. Lewicki ⁸⁵, D.J. Lewis ⁴, A. Li ⁵, B. Li ^{14b}, B. Li ^{62b},
 C. Li^{62a}, C-Q. Li ^{62c}, H. Li ^{62a}, H. Li ^{62b}, H. Li ^{14c}, H. Li ^{62b}, J. Li ^{62c}, K. Li ¹³⁷, L. Li ^{62c},
 M. Li ^{14a,14d}, Q.Y. Li ^{62a}, S. Li ^{14a,14d}, S. Li ^{62d,62c,e}, T. Li ^{62b}, X. Li ¹⁰³, Z. Li ^{62b}, Z. Li ¹²⁵,
 Z. Li ¹⁰³, Z. Li ⁹¹, Z. Li ^{14a,14d}, Z. Liang ^{14a}, M. Liberatore ⁴⁸, B. Liberti ^{75a}, K. Lie ^{64c},
 J. Lieber Marin ^{81b}, K. Lin ¹⁰⁶, R.A. Linck ⁶⁷, R.E. Lindley ⁷, J.H. Lindon ², A. Linss ⁴⁸,
 E. Lipeles ¹²⁷, A. Lipniacka ¹⁶, A. Lister ¹⁶³, J.D. Little ⁴, B. Liu ^{14a}, B.X. Liu ¹⁴¹,
 D. Liu ^{62d,62c}, J.B. Liu ^{62a}, J.K.K. Liu ³², K. Liu ^{62d,62c}, M. Liu ^{62a}, M.Y. Liu ^{62a}, P. Liu ^{14a},
 Q. Liu ^{62d,137,62c}, X. Liu ^{62a}, Y. Liu ⁴⁸, Y. Liu ^{14c,14d}, Y.L. Liu ¹⁰⁵, Y.W. Liu ^{62a},
 M. Livan ^{72a,72b}, J. Llorente Merino ¹⁴¹, S.L. Lloyd ⁹³, E.M. Lobodzinska ⁴⁸, P. Loch ⁷,
 S. Loffredo ^{75a,75b}, T. Lohse ¹⁸, K. Lohwasser ¹³⁸, M. Lokajicek ^{130,*}, J.D. Long ¹⁶¹,
 I. Longarini ^{74a,74b}, L. Longo ^{69a,69b}, R. Longo ¹⁶¹, I. Lopez Paz ³⁶, A. Lopez Solis ⁴⁸,



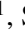
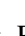

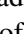
J. Lorenz ^{id108}, N. Lorenzo Martinez ^{id4}, A.M. Lory ^{id108}, A. Lösle ^{id54}, X. Lou ^{id47a,47b}, X. Lou ^{id14a,14d},
 A. Lounis ^{id66}, J. Love ^{id6}, P.A. Love ^{id90}, J.J. Lozano Bahilo ^{id162}, G. Lu ^{id14a,14d}, M. Lu ^{id79},
 S. Lu ^{id127}, Y.J. Lu ^{id65}, H.J. Lubatti ^{id137}, C. Luci ^{id74a,74b}, F.L. Lucio Alves ^{id14c}, A. Lucotte ^{id60},
 F. Luehring ^{id67}, I. Luise ^{id144}, O. Lukianchuk ^{id66}, O. Lundberg ^{id143}, B. Lund-Jensen ^{id143},
 N.A. Luongo ^{id122}, M.S. Lutz ^{id150}, D. Lynn ^{id29}, H. Lyons⁹¹, R. Lysak ^{id130}, E. Lytken ^{id97}, F. Lyu ^{id14a},
 V. Lyubushkin ^{id38}, T. Lyubushkina ^{id38}, H. Ma ^{id29}, L.L. Ma ^{id62b}, Y. Ma ^{id95}, D.M. Mac Donell ^{id164},
 G. Maccarrone ^{id53}, J.C. MacDonald ^{id138}, R. Madar ^{id40}, W.F. Mader ^{id50}, J. Maeda ^{id83}, T. Maeno ^{id29},
 M. Maerker ^{id50}, V. Magerl ^{id54}, H. Maguire ^{id138}, D.J. Mahon ^{id41}, C. Maidantchik ^{id81b},
 A. Maio ^{id129a,129b,129d}, K. Maj ^{id84a}, O. Majersky ^{id28a}, S. Majewski ^{id122}, N. Makovec ^{id66},
 V. Maksimovic ^{id15}, B. Malaescu ^{id126}, Pa. Malecki ^{id85}, V.P. Maleev ^{id37}, F. Malek ^{id60},
 D. Malito ^{id43b,43a}, U. Mallik ^{id79}, C. Malone ^{id32}, S. Maltezos¹⁰, S. Malyukov³⁸, J. Mamuzic ^{id13},
 G. Mancini ^{id53}, G. Manco ^{id72a,72b}, J.P. Mandalia ^{id93}, I. Mandić ^{id92},
 L. Manhaes de Andrade Filho ^{id81a}, I.M. Maniatis ^{id151}, M. Manisha ^{id134}, J. Manjarres Ramos ^{id50},
 D.C. Mankad ^{id168}, A. Mann ^{id108}, B. Mansoulie ^{id134}, S. Manzoni ^{id36}, A. Marantis ^{id151,u},
 G. Marchiori ^{id5}, M. Marcisovsky ^{id130}, L. Marcoccia ^{id75a,75b}, C. Marcon ^{id70a,70b}, M. Marinescu ^{id20},
 M. Marjanovic ^{id119}, E.J. Marshall ^{id90}, Z. Marshall ^{id17a}, S. Marti-Garcia ^{id162}, T.A. Martin ^{id166},
 V.J. Martin ^{id52}, B. Martin dit Latour ^{id16}, L. Martinelli ^{id74a,74b}, M. Martinez ^{id13,v},
 P. Martinez Agullo ^{id162}, V.I. Martinez Outschoorn ^{id102}, P. Martinez Suarez ^{id13}, S. Martin-Haugh ^{id133},
 V.S. Martoiu ^{id27b}, A.C. Martyniuk ^{id95}, A. Marzin ^{id36}, S.R. Maschek ^{id109}, L. Masetti ^{id99},
 T. Mashimo ^{id152}, J. Masik ^{id100}, A.L. Maslennikov ^{id37}, L. Massa ^{id23b}, P. Massarotti ^{id71a,71b},
 P. Mastrandrea ^{id73a,73b}, A. Mastroberardino ^{id43b,43a}, T. Masubuchi ^{id152}, T. Mathisen ^{id160},
 N. Matsuzawa¹⁵², J. Maurer ^{id27b}, B. Maček ^{id92}, D.A. Maximov ^{id37}, R. Mazini ^{id147}, I. Maznas ^{id151},
 M. Mazza ^{id106}, S.M. Mazza ^{id135}, C. Mc Ginn ^{id29,ak}, J.P. Mc Gowan ^{id103}, S.P. Mc Kee ^{id105},
 W.P. McCormack ^{id17a}, E.F. McDonald ^{id104}, A.E. McDougall ^{id113}, J.A. Mcfayden ^{id145},
 G. Mchedlidze ^{id148b}, R.P. Mckenzie ^{id33g}, T.C. Mclachlan ^{id48}, D.J. Mclaughlin ^{id95}, K.D. McLean ^{id164},
 S.J. McMahan ^{id133}, P.C. McNamara ^{id104}, C.M. Mccpartland ^{id91}, R.A. McPherson ^{id164,x}, T. Megy ^{id40},
 S. Mehlhase ^{id108}, A. Mehta ^{id91}, B. Meirose ^{id45}, D. Melini ^{id149}, B.R. Mellado Garcia ^{id33g},
 A.H. Melo ^{id55}, F. Meloni ^{id48}, E.D. Mendes Gouveia ^{id129a}, A.M. Mendes Jacques Da Costa ^{id20},
 H.Y. Meng ^{id154}, L. Meng ^{id90}, S. Menke ^{id109}, M. Mentink ^{id36}, E. Meoni ^{id43b,43a}, C. Merlassino ^{id125},
 L. Merola ^{id71a,71b}, C. Meroni ^{id70a}, G. Merz¹⁰⁵, O. Meshkov ^{id37}, J.K.R. Meshreki ^{id140}, J. Metcalfe ^{id6},
 A.S. Mete ^{id6}, C. Meyer ^{id67}, J-P. Meyer ^{id134}, M. Michetti ^{id18}, R.P. Middleton ^{id133}, L. Mijović ^{id52},
 G. Mikenberg ^{id168}, M. Mikesikova ^{id130}, M. Mikuž ^{id92}, H. Mildner ^{id138}, A. Milic ^{id36},
 C.D. Milke ^{id44}, D.W. Miller ^{id39}, L.S. Miller ^{id34}, A. Milov ^{id168}, D.A. Milstead^{47a,47b}, T. Min^{14c},
 A.A. Minaenko ^{id37}, I.A. Minashvili ^{id148b}, L. Mince ^{id59}, A.I. Mincer ^{id116}, B. Mindur ^{id84a},
 M. Mineev ^{id38}, Y. Mino ^{id86}, L.M. Mir ^{id13}, M. Miralles Lopez ^{id162}, M. Mironova ^{id125},
 M.C. Missio ^{id112}, T. Mitani ^{id167}, A. Mitra ^{id166}, V.A. Mitsou ^{id162}, O. Miu ^{id154}, P.S. Miyagawa ^{id93},
 Y. Miyazaki⁸⁸, A. Mizukami ^{id82}, J.U. Mjörnmark ^{id97}, T. Mkrtchyan ^{id63a}, T. Mlinarevic ^{id95},
 M. Mlynarikova ^{id36}, T. Moa ^{id47a,47b}, S. Mobius ^{id55}, K. Mochizuki ^{id107}, P. Moder ^{id48}, P. Mogg ^{id108},
 A.F. Mohammed ^{id14a,14d}, S. Mohapatra ^{id41}, G. Mokgatitwane ^{id33g}, B. Mondal ^{id140}, S. Mondal ^{id131},
 K. Mönig ^{id48}, E. Monnier ^{id101}, L. Monsonis Romero¹⁶², J. Montejo Berlingen ^{id36}, M. Montella ^{id118},
 F. Monticelli ^{id89}, N. Morange ^{id66}, A.L. Moreira De Carvalho ^{id129a}, M. Moreno Llácer ^{id162},
 C. Moreno Martinez ^{id56}, P. Morettini ^{id57b}, S. Morgenstern ^{id166}, M. Morii ^{id61}, M. Morinaga ^{id152},
 A.K. Morley ^{id36}, F. Morodei ^{id74a,74b}, L. Morvaj ^{id36}, P. Moschovakos ^{id36}, B. Moser ^{id36},
 M. Mosidze^{148b}, T. Moskalets ^{id54}, P. Moskvitina ^{id112}, J. Moss ^{id31,o}, E.J.W. Moyse ^{id102},
 S. Muanza ^{id101}, J. Mueller ^{id128}, D. Muenstermann ^{id90}, R. Müller ^{id19}, G.A. Mullier ^{id97}, J.J. Mullin¹²⁷,
 D.P. Mungo ^{id154}, J.L. Munoz Martinez ^{id13}, D. Munoz Perez ^{id162}, F.J. Munoz Sanchez ^{id100},
 M. Murin ^{id100}, W.J. Murray ^{id166,133}, A. Murrone ^{id70a,70b}, J.M. Muse ^{id119}, M. Muškinja ^{id17a},

C. Mwewa ²⁹, A.G. Myagkov ^{37,a}, A.J. Myers ⁸, A.A. Myers ¹²⁸, G. Myers ⁶⁷, M. Myska ¹³¹,
 B.P. Nachman ^{17a}, O. Nackenhorst ⁴⁹, A. Nag ⁵⁰, K. Nagai ¹²⁵, K. Nagano ⁸², J.L. Nagle ^{29,ak},
 E. Nagy ¹⁰¹, A.M. Nairz ³⁶, Y. Nakahama ⁸², K. Nakamura ⁸², H. Nanjo ¹²³, R. Narayan ⁴⁴,
 E.A. Narayanan ¹¹¹, I. Naryshkin ³⁷, M. Naseri ³⁴, C. Nass ²⁴, G. Navarro ^{22a},
 J. Navarro-Gonzalez ¹⁶², R. Nayak ¹⁵⁰, A. Nayaz ¹⁸, P.Y. Nechaeva ³⁷, F. Nechansky ⁴⁸,
 L. Nedic ¹²⁵, T.J. Neep ²⁰, A. Negri ^{72a,72b}, M. Negrini ^{23b}, C. Nellist ¹¹², C. Nelson ¹⁰³,
 K. Nelson ¹⁰⁵, S. Nemecek ¹³⁰, M. Nessi ^{36,h}, M.S. Neubauer ¹⁶¹, F. Neuhaus ⁹⁹,
 J. Neundorff ⁴⁸, R. Newhouse ¹⁶³, P.R. Newman ²⁰, C.W. Ng ¹²⁸, Y.S. Ng ¹⁸, Y.W.Y. Ng ⁴⁸,
 B. Ngair ^{35e}, H.D.N. Nguyen ¹⁰⁷, R.B. Nickerson ¹²⁵, R. Nicolaidou ¹³⁴, J. Nielsen ¹³⁵,
 M. Niemeyer ⁵⁵, N. Nikiforou ³⁶, V. Nikolaenko ^{37,a}, I. Nikolic-Audit ¹²⁶, K. Nikolopoulos ²⁰,
 P. Nilsson ²⁹, H.R. Nindhito ⁵⁶, A. Nisati ^{74a}, N. Nishu ², R. Nisius ¹⁰⁹, J-E. Nitschke ⁵⁰,
 E.K. Nkadimeng ^{33g}, S.J. Noacco Rosende ⁸⁹, T. Nobe ¹⁵², D.L. Noel ³², Y. Noguchi ⁸⁶,
 T. Nommensen ¹⁴⁶, M.A. Nomura ²⁹, M.B. Norfolk ¹³⁸, R.R.B. Norisam ⁹⁵, B.J. Norman ³⁴,
 J. Novak ⁹², T. Novak ⁴⁸, O. Novgorodova ⁵⁰, L. Novotny ¹³¹, R. Novotny ¹¹¹, L. Nozka ¹²¹,
 K. Ntekas ¹⁵⁹, N.M.J. Nunes De Moura Junior ^{81b}, E. Nurse ⁹⁵, F.G. Oakham ^{34,ah}, J. Ocariz ¹²⁶,
 A. Ochi ⁸³, I. Ochoa ^{129a}, S. Oerdek ¹⁶⁰, A. Ogrodnik ^{84a}, A. Oh ¹⁰⁰, C.C. Ohm ¹⁴³,
 H. Oide ⁸², R. Oishi ¹⁵², M.L. Ojeda ⁴⁸, Y. Okazaki ⁸⁶, M.W. O'Keefe ⁹¹, Y. Okumura ¹⁵²,
 A. Olariu ^{27b}, L.F. Oleiro Seabra ^{129a}, S.A. Olivares Pino ^{136e}, D. Oliveira Damazio ²⁹,
 D. Oliveira Goncalves ^{81a}, J.L. Oliver ¹⁵⁹, M.J.R. Olsson ¹⁵⁹, A. Olszewski ⁸⁵, J. Olszowska ^{85,*},
 Ö.O. Öncel ⁵⁴, D.C. O'Neil ¹⁴¹, A.P. O'Neill ¹⁹, A. Onofre ^{129a,129e}, P.U.E. Onyisi ¹¹,
 M.J. Oreglia ³⁹, G.E. Orellana ⁸⁹, D. Orestano ^{76a,76b}, N. Orlando ¹³, R.S. Orr ¹⁵⁴,
 V. O'Shea ⁵⁹, R. Ospanov ^{62a}, G. Otero y Garzon ³⁰, H. Otono ⁸⁸, P.S. Ott ^{63a}, G.J. Ottino ^{17a},
 M. Ouchrif ^{35d}, J. Ouellette ^{29,ak}, F. Ould-Saada ¹²⁴, M. Owen ⁵⁹, R.E. Owen ¹³³,
 K.Y. Oyulmaz ^{21a}, V.E. Ozcan ^{21a}, N. Ozturk ⁸, S. Ozturk ^{21d}, J. Pacalt ¹²¹, H.A. Pacey ³²,
 K. Pachal ⁵¹, A. Pacheco Pages ¹³, C. Padilla Aranda ¹³, G. Padovano ^{74a,74b}, S. Pagan Griso ^{17a},
 G. Palacino ⁶⁷, A. Palazzo ^{69a,69b}, S. Palazzo ⁵², S. Palestini ³⁶, M. Palka ^{84b}, J. Pan ¹⁷¹,
 T. Pan ^{64a}, D.K. Panchal ¹¹, C.E. Pandini ¹¹³, J.G. Panduro Vazquez ⁹⁴, H. Pang ^{14b}, P. Pani ⁴⁸,
 G. Panizzo ^{68a,68c}, L. Paolozzi ⁵⁶, C. Papadatos ¹⁰⁷, S. Parajuli ⁴⁴, A. Paramonov ⁶,
 C. Paraskevopoulos ¹⁰, D. Paredes Hernandez ^{64b}, T.H. Park ¹⁵⁴, M.A. Parker ³², F. Parodi ^{57b,57a},
 E.W. Parrish ¹¹⁴, V.A. Parrish ⁵², J.A. Parsons ⁴¹, U. Parzefall ⁵⁴, B. Pascual Dias ¹⁰⁷,
 L. Pascual Dominguez ¹⁵⁰, V.R. Pascuzzi ^{17a}, F. Pasquali ¹¹³, E. Pasqualucci ^{74a}, S. Passaggio ^{57b},
 F. Pastore ⁹⁴, P. Pasuwan ^{47a,47b}, P. Patel ⁸⁵, J.R. Pater ¹⁰⁰, T. Pauly ³⁶, J. Pearkes ¹⁴²,
 M. Pedersen ¹²⁴, R. Pedro ^{129a}, S.V. Peleganchuk ³⁷, O. Penc ³⁶, E.A. Pender ⁵², C. Peng ^{64b},
 H. Peng ^{62a}, K.E. Pensi ¹⁰⁸, M. Penzin ³⁷, B.S. Peralva ^{81d}, A.P. Pereira Peixoto ⁶⁰,
 L. Pereira Sanchez ^{47a,47b}, D.V. Perepelitsa ^{29,ak}, E. Perez Codina ^{155a}, M. Perganti ¹⁰,
 L. Perini ^{70a,70b,*}, H. Pernegger ³⁶, S. Perrella ³⁶, A. Perrevoort ¹¹², O. Perrin ⁴⁰, K. Peters ⁴⁸,
 R.F.Y. Peters ¹⁰⁰, B.A. Petersen ³⁶, T.C. Petersen ⁴², E. Petit ¹⁰¹, V. Petousis ¹³¹,
 C. Petridou ¹⁵¹, A. Petrukhin ¹⁴⁰, M. Pettee ^{17a}, N.E. Pettersson ³⁶, A. Petukhov ³⁷,
 K. Petukhova ¹³², A. Peyaud ¹³⁴, R. Pezoa ^{136f}, L. Pezzotti ³⁶, G. Pezzullo ¹⁷¹, T.M. Pham ¹⁶⁹,
 T. Pham ¹⁰⁴, P.W. Phillips ¹³³, M.W. Phipps ¹⁶¹, G. Piacquadio ¹⁴⁴, E. Pianori ^{17a},
 F. Piazza ^{70a,70b}, R. Piegai ³⁰, D. Pietreanu ^{27b}, A.D. Pilkington ¹⁰⁰, M. Pinamonti ^{68a,68c},
 J.L. Pinfeld ², B.C. Pinheiro Pereira ^{129a}, C. Pitman Donaldson ⁹⁵, D.A. Pizzi ³⁴,
 L. Pizzimento ^{75a,75b}, A. Pizzini ¹¹³, M.-A. Pleier ²⁹, V. Plesanovs ⁵⁴, V. Pleskot ¹³²,
 E. Plotnikova ³⁸, G. Poddar ⁴, R. Poettgen ⁹⁷, L. Poggioli ¹²⁶, I. Pogrebnyak ¹⁰⁶, D. Pohl ²⁴,
 I. Pokharel ⁵⁵, S. Polacek ¹³², G. Polesello ^{72a}, A. Poley ^{141,155a}, R. Polifka ¹³¹, A. Polini ^{23b},
 C.S. Pollard ¹²⁵, Z.B. Pollock ¹¹⁸, V. Polychronakos ²⁹, E. Pompa Pacchi ^{74a,74b},
 D. Ponomarenko ³⁷, L. Pontecorvo ³⁶, S. Popa ^{27a}, G.A. Popeneciu ^{27d},

D.M. Portillo Quintero [ID155a](#), S. Pospisil [ID131](#), P. Postolache [ID27c](#), K. Potamianos [ID125](#), I.N. Potrap [ID38](#),
 C.J. Potter [ID32](#), H. Potti [ID1](#), T. Poulsen [ID48](#), J. Poveda [ID162](#), M.E. Pozo Astigarraga [ID36](#),
 A. Prades Ibanez [ID162](#), M.M. Prapa [ID46](#), J. Pretel [ID54](#), D. Price [ID100](#), M. Primavera [ID69a](#),
 M.A. Principe Martin [ID98](#), R. Privara [ID121](#), M.L. Proffitt [ID137](#), N. Proklova [ID127](#), K. Prokofiev [ID64c](#),
 G. Proto [ID75a,75b](#), S. Protopopescu [ID29](#), J. Proudfoot [ID6](#), M. Przybycien [ID84a](#), J.E. Puddefoot [ID138](#),
 D. Pudzha [ID37](#), P. Puzo [ID66](#), D. Pyatiizbyantseva [ID37](#), J. Qian [ID105](#), D. Qichen [ID100](#), Y. Qin [ID100](#),
 T. Qiu [ID93](#), A. Quadt [ID55](#), M. Queitsch-Maitland [ID100](#), G. Quetant [ID56](#), G. Rabanal Bolanos [ID61](#),
 D. Rafanoharana [ID54](#), F. Ragusa [ID70a,70b](#), J.L. Rainbolt [ID39](#), J.A. Raine [ID56](#), S. Rajagopalan [ID29](#),
 E. Ramakoti [ID37](#), K. Ran [ID48,14d](#), N.P. Rapheeha [ID33g](#), V. Raskina [ID126](#), D.F. Rassloff [ID63a](#), S. Rave [ID99](#),
 B. Ravina [ID55](#), I. Ravinovich [ID168](#), M. Raymond [ID36](#), A.L. Read [ID124](#), N.P. Readioff [ID138](#),
 D.M. Rebuzzi [ID72a,72b](#), G. Redlinger [ID29](#), K. Reeves [ID45](#), J.A. Reidelsturz [ID170](#), D. Reikher [ID150](#),
 A. Reiss [ID99](#), A. Rej [ID140](#), C. Rembser [ID36](#), A. Renardi [ID48](#), M. Renda [ID27b](#), M.B. Rendel [ID109](#), F. Renner [ID48](#),
 A.G. Rennie [ID59](#), S. Resconi [ID70a](#), M. Ressegotti [ID57b,57a](#), E.D. Resseguie [ID17a](#), S. Rettie [ID36](#),
 B. Reynolds [ID118](#), E. Reynolds [ID17a](#), M. Rezaei Estabragh [ID170](#), O.L. Rezanova [ID37](#), P. Reznicek [ID132](#),
 E. Ricci [ID77a,77b](#), R. Richter [ID109](#), S. Richter [ID47a,47b](#), E. Richter-Was [ID84b](#), M. Ridel [ID126](#), P. Rieck [ID116](#),
 P. Riedler [ID36](#), M. Rijssenbeek [ID144](#), A. Rimoldi [ID72a,72b](#), M. Rimoldi [ID48](#), L. Rinaldi [ID23b,23a](#),
 T.T. Rinn [ID29](#), M.P. Rinnagel [ID108](#), G. Ripellino [ID143](#), I. Riu [ID13](#), P. Rivadeneira [ID48](#),
 J.C. Rivera Vergara [ID164](#), F. Rizatdinova [ID120](#), E. Rizvi [ID93](#), C. Rizzi [ID56](#), B.A. Roberts [ID166](#),
 B.R. Roberts [ID17a](#), S.H. Robertson [ID103,x](#), M. Robin [ID48](#), D. Robinson [ID32](#), C.M. Robles Gajardo [ID136f](#),
 M. Robles Manzano [ID99](#), A. Robson [ID59](#), A. Rocchi [ID75a,75b](#), C. Roda [ID73a,73b](#), S. Rodriguez Bosca [ID63a](#),
 Y. Rodriguez Garcia [ID22a](#), A. Rodriguez Rodriguez [ID54](#), A.M. Rodríguez Vera [ID155b](#), S. Roe [ID36](#),
 J.T. Roemer [ID159](#), A.R. Roepe-Gier [ID119](#), J. Roggel [ID170](#), O. Røhne [ID124](#), R.A. Rojas [ID164](#), B. Roland [ID54](#),
 C.P.A. Roland [ID67](#), J. Roloff [ID29](#), A. Romaniouk [ID37](#), E. Romano [ID72a,72b](#), M. Romano [ID23b](#),
 A.C. Romero Hernandez [ID161](#), N. Rompotis [ID91](#), L. Roos [ID126](#), S. Rosati [ID74a](#), B.J. Rosser [ID39](#),
 E. Rossi [ID4](#), E. Rossi [ID71a,71b](#), L.P. Rossi [ID57b](#), L. Rossini [ID48](#), R. Rosten [ID118](#), M. Rotaru [ID27b](#),
 B. Rottler [ID54](#), D. Rousseau [ID66](#), D. Rousso [ID32](#), G. Rovelli [ID72a,72b](#), A. Roy [ID161](#), A. Rozanov [ID101](#),
 Y. Rozen [ID149](#), X. Ruan [ID33g](#), A. Rubio Jimenez [ID162](#), A.J. Ruby [ID91](#), V.H. Ruelas Rivera [ID18](#),
 T.A. Ruggeri [ID1](#), F. Rühr [ID54](#), A. Ruiz-Martinez [ID162](#), A. Rummler [ID36](#), Z. Rurikova [ID54](#),
 N.A. Rusakovich [ID38](#), H.L. Russell [ID164](#), J.P. Rutherford [ID7](#), K. Rybacki [ID90](#), M. Rybar [ID132](#),
 E.B. Rye [ID124](#), A. Ryzhov [ID37](#), J.A. Sabater Iglesias [ID56](#), P. Sabatini [ID162](#), L. Sabetta [ID74a,74b](#),
 H.F-W. Sadrozinski [ID135](#), F. Safai Tehrani [ID74a](#), B. Safarzadeh Samani [ID145](#), M. Safdari [ID142](#),
 S. Saha [ID103](#), M. Sahinsoy [ID109](#), M. Saimpert [ID134](#), M. Saito [ID152](#), T. Saito [ID152](#), D. Salamani [ID36](#),
 G. Salamanna [ID76a,76b](#), A. Salnikov [ID142](#), J. Salt [ID162](#), A. Salvador Salas [ID13](#), D. Salvatore [ID43b,43a](#),
 F. Salvatore [ID145](#), A. Salzburger [ID36](#), D. Sammel [ID54](#), D. Sampsonidis [ID151](#), D. Sampsonidou [ID62d,62c](#),
 J. Sánchez [ID162](#), A. Sanchez Pineda [ID4](#), V. Sanchez Sebastian [ID162](#), H. Sandaker [ID124](#), C.O. Sander [ID48](#),
 J.A. Sandesara [ID102](#), M. Sandhoff [ID170](#), C. Sandoval [ID22b](#), D.P.C. Sankey [ID133](#), A. Sansoni [ID53](#),
 L. Santi [ID74a,74b](#), C. Santoni [ID40](#), H. Santos [ID129a,129b](#), S.N. Santpur [ID17a](#), A. Santra [ID168](#),
 K.A. Saoucha [ID138](#), J.G. Saraiva [ID129a,129d](#), J. Sardain [ID7](#), O. Sasaki [ID82](#), K. Sato [ID156](#), C. Sauer [ID63b](#),
 F. Sauerburger [ID54](#), E. Sauvan [ID4](#), P. Savard [ID154,ah](#), R. Sawada [ID152](#), C. Sawyer [ID133](#), L. Sawyer [ID96](#),
 I. Sayago Galvan [ID162](#), C. Sbarra [ID23b](#), A. Sbrizzi [ID23b,23a](#), T. Scanlon [ID95](#), J. Schaarschmidt [ID137](#),
 P. Schacht [ID109](#), D. Schaefer [ID39](#), U. Schäfer [ID99](#), A.C. Schaffer [ID66](#), D. Schaile [ID108](#),
 R.D. Schamberger [ID144](#), E. Schanet [ID108](#), C. Scharf [ID18](#), M.M. Schefer [ID19](#), V.A. Schegelsky [ID37](#),
 D. Scheirich [ID132](#), F. Schenck [ID18](#), M. Schernau [ID159](#), C. Scheulen [ID55](#), C. Schiavi [ID57b,57a](#),
 Z.M. Schillaci [ID26](#), E.J. Schioppa [ID69a,69b](#), M. Schioppa [ID43b,43a](#), B. Schlag [ID99](#), K.E. Schleicher [ID54](#),
 S. Schlenker [ID36](#), J. Schmeing [ID170](#), M.A. Schmidt [ID170](#), K. Schmieden [ID99](#), C. Schmitt [ID99](#),
 S. Schmitt [ID48](#), L. Schoeffel [ID134](#), A. Schoening [ID63b](#), P.G. Scholer [ID54](#), E. Schopf [ID125](#), M. Schott [ID99](#),
 J. Schovancova [ID36](#), S. Schramm [ID56](#), F. Schroeder [ID170](#), H-C. Schultz-Coulon [ID63a](#), M. Schumacher [ID54](#),

B.A. Schumm [ID135](#), Ph. Schune [ID134](#), A. Schwartzman [ID142](#), T.A. Schwarz [ID105](#), Ph. Schwemling [ID134](#),
 R. Schwienhorst [ID106](#), A. Sciandra [ID135](#), G. Sciolla [ID26](#), F. Scuri [ID73a](#), F. Scutti [ID104](#), C.D. Sebastiani [ID91](#),
 K. Sedlaczek [ID49](#), P. Seema [ID18](#), S.C. Seidel [ID111](#), A. Seiden [ID135](#), B.D. Seidlitz [ID41](#), T. Seiss [ID39](#),
 C. Seitz [ID48](#), J.M. Seixas [ID81b](#), G. Sekhniaidze [ID71a](#), S.J. Sekula [ID44](#), L. Selem [ID4](#),
 N. Semprini-Cesari [ID23b,23a](#), S. Sen [ID51](#), D. Sengupta [ID56](#), V. Senthilkumar [ID162](#), L. Serin [ID66](#),
 L. Serkin [ID68a,68b](#), M. Sessa [ID76a,76b](#), H. Severini [ID119](#), S. Sevova [ID142](#), F. Sforza [ID57b,57a](#), A. Sfyrla [ID56](#),
 E. Shabalina [ID55](#), R. Shaheen [ID143](#), J.D. Shahinian [ID127](#), D. Shaked Renous [ID168](#), L.Y. Shan [ID14a](#),
 M. Shapiro [ID17a](#), A. Sharma [ID36](#), A.S. Sharma [ID163](#), P. Sharma [ID79](#), S. Sharma [ID48](#), P.B. Shatalov [ID37](#),
 K. Shaw [ID145](#), S.M. Shaw [ID100](#), Q. Shen [ID62c,5](#), P. Sherwood [ID95](#), L. Shi [ID95](#), C.O. Shimmin [ID171](#),
 Y. Shimogama [ID167](#), J.D. Shinner [ID94](#), I.P.J. Shipsey [ID125](#), S. Shirabe [ID60](#), M. Shiyakova [ID38](#),
 J. Shlomi [ID168](#), M.J. Shochet [ID39](#), J. Shojaii [ID104](#), D.R. Shope [ID124](#), S. Shrestha [ID118,al](#), E.M. Shrif [ID33g](#),
 M.J. Shroff [ID164](#), P. Sicho [ID130](#), A.M. Sickles [ID161](#), E. Sideras Haddad [ID33g](#), A. Sidoti [ID23b](#),
 F. Siegert [ID50](#), Dj. Sijacki [ID15](#), R. Sikora [ID84a](#), F. Sili [ID89](#), J.M. Silva [ID20](#), M.V. Silva Oliveira [ID36](#),
 S.B. Silverstein [ID47a](#), S. Simion [ID66](#), R. Simoniello [ID36](#), E.L. Simpson [ID59](#), N.D. Simpson [ID97](#),
 S. Simsek [ID21d](#), S. Sindhu [ID55](#), P. Sinervo [ID154](#), V. Sinetckii [ID37](#), S. Singh [ID141](#), S. Singh [ID154](#),
 S. Sinha [ID48](#), S. Sinha [ID33g](#), M. Sioli [ID23b,23a](#), I. Siral [ID36](#), S.Yu. Sivoklov [ID37,*](#), J. Sjölin [ID47a,47b](#),
 A. Skaf [ID55](#), E. Skorda [ID97](#), P. Skubic [ID119](#), M. Slawinska [ID85](#), V. Smakhtin [ID168](#), B.H. Smart [ID133](#),
 J. Smiesko [ID36](#), S.Yu. Smirnov [ID37](#), Y. Smirnov [ID37](#), L.N. Smirnova [ID37,a](#), O. Smirnova [ID97](#),
 A.C. Smith [ID41](#), E.A. Smith [ID39](#), H.A. Smith [ID125](#), J.L. Smith [ID91](#), R. Smith [ID142](#), M. Smizanska [ID90](#),
 K. Smolek [ID131](#), A. Smykiewicz [ID85](#), A.A. Snesarev [ID37](#), H.L. Snoek [ID113](#), S. Snyder [ID29](#),
 R. Sobie [ID164,x](#), A. Soffer [ID150](#), C.A. Solans Sanchez [ID36](#), E.Yu. Soldatov [ID37](#), U. Soldevila [ID162](#),
 A.A. Solodkov [ID37](#), S. Solomon [ID54](#), A. Soloshenko [ID38](#), K. Solovieva [ID54](#), O.V. Solovyanov [ID37](#),
 V. Solovyev [ID37](#), P. Sommer [ID36](#), A. Sonay [ID13](#), W.Y. Song [ID155b](#), A. Sopczak [ID131](#), A.L. Sopio [ID95](#),
 F. Sopkova [ID28b](#), V. Sothilingam [ID63a](#), S. Sottocornola [ID72a,72b](#), R. Soualah [ID115b](#), Z. Soumami [ID35e](#),
 D. South [ID48](#), S. Spagnolo [ID69a,69b](#), M. Spalla [ID109](#), F. Spanò [ID94](#), D. Sperlich [ID54](#), G. Spigo [ID36](#),
 M. Spina [ID145](#), S. Spinali [ID90](#), D.P. Spiteri [ID59](#), M. Spousta [ID132](#), E.J. Staats [ID34](#), A. Stabile [ID70a,70b](#),
 R. Stamen [ID63a](#), M. Stamenkovic [ID113](#), A. Stampekis [ID20](#), M. Standke [ID24](#), E. Stanecka [ID85](#),
 M.V. Stange [ID50](#), B. Stanislaus [ID17a](#), M.M. Stanitzki [ID48](#), M. Stankaityte [ID125](#), B. Stapf [ID48](#),
 E.A. Starchenko [ID37](#), G.H. Stark [ID135](#), J. Stark [ID101,ab](#), D.M. Starko [ID155b](#), P. Staroba [ID130](#),
 P. Starovoitov [ID63a](#), S. Stärz [ID103](#), R. Staszewski [ID85](#), G. Stavropoulos [ID46](#), J. Steentoft [ID160](#),
 P. Steinberg [ID29](#), A.L. Steinhebel [ID122](#), B. Stelzer [ID141,155a](#), H.J. Stelzer [ID128](#), O. Stelzer-Chilton [ID155a](#),
 H. Stenzel [ID58](#), T.J. Stevenson [ID145](#), G.A. Stewart [ID36](#), M.C. Stockton [ID36](#), G. Stoicea [ID27b](#),
 M. Stolarski [ID129a](#), S. Stonjek [ID109](#), A. Straessner [ID50](#), J. Strandberg [ID143](#), S. Strandberg [ID47a,47b](#),
 M. Strauss [ID119](#), T. Strebler [ID101](#), P. Strizeneč [ID28b](#), R. Ströhmer [ID165](#), D.M. Strom [ID122](#), L.R. Strom [ID48](#),
 R. Stroynowski [ID44](#), A. Strubig [ID47a,47b](#), S.A. Stucci [ID29](#), B. Stugu [ID16](#), J. Stupak [ID119](#), N.A. Styles [ID48](#),
 D. Su [ID142](#), S. Su [ID62a](#), W. Su [ID62d,137,62c](#), X. Su [ID62a,66](#), K. Sugizaki [ID152](#), V.V. Sulin [ID37](#),
 M.J. Sullivan [ID91](#), D.M.S. Sultan [ID77a,77b](#), L. Sultanaliyeva [ID37](#), S. Sultansoy [ID3b](#), T. Sumida [ID86](#),
 S. Sun [ID105](#), S. Sun [ID169](#), O. Sunneborn Gudnadottir [ID160](#), M.R. Sutton [ID145](#), M. Svatos [ID130](#),
 M. Swiatlowski [ID155a](#), T. Swirski [ID165](#), I. Sykora [ID28a](#), M. Sykora [ID132](#), T. Sykora [ID132](#), D. Ta [ID99](#),
 K. Tackmann [ID48,w](#), A. Taffard [ID159](#), R. Tafirout [ID155a](#), J.S. Tafuya Vargas [ID66](#), R.H.M. Taibah [ID126](#),
 R. Takashima [ID87](#), K. Takeda [ID83](#), E.P. Takeva [ID52](#), Y. Takubo [ID82](#), M. Talby [ID101](#), A.A. Talyshev [ID37](#),
 K.C. Tam [ID64b](#), N.M. Tamir [ID150](#), A. Tanaka [ID152](#), J. Tanaka [ID152](#), R. Tanaka [ID66](#), M. Tanasini [ID57b,57a](#),
 J. Tang [ID62c](#), Z. Tao [ID163](#), S. Tapia Araya [ID80](#), S. Tapprogge [ID99](#), A. Tarek Abouelfadl Mohamed [ID106](#),
 S. Tarem [ID149](#), K. Tariq [ID62b](#), G. Tarna [ID101,27b](#), G.F. Tartarelli [ID70a](#), P. Tas [ID132](#), M. Tasevsky [ID130](#),
 E. Tassi [ID43b,43a](#), A.C. Tate [ID161](#), G. Tateno [ID152](#), Y. Tayalati [ID35e](#), G.N. Taylor [ID104](#), W. Taylor [ID155b](#),
 H. Teagle [ID91](#), A.S. Tee [ID169](#), R. Teixeira De Lima [ID142](#), P. Teixeira-Dias [ID94](#), J.J. Teoh [ID154](#),
 K. Terashi [ID152](#), J. Terron [ID98](#), S. Terzo [ID13](#), M. Testa [ID53](#), R.J. Teuscher [ID154,x](#), A. Thaler [ID78](#),

O. Theiner ⁵⁶, N. Themistokleous ⁵², T. Thevenaux-Pelzer ¹⁸, O. Thielmann ¹⁷⁰, D.W. Thomas⁹⁴, J.P. Thomas ²⁰, E.A. Thompson ⁴⁸, P.D. Thompson ²⁰, E. Thomson ¹²⁷, E.J. Thorpe ⁹³, Y. Tian ⁵⁵, V. Tikhomirov ^{37,a}, Yu.A. Tikhonov ³⁷, S. Timoshenko³⁷, E.X.L. Ting ¹, P. Tipton ¹⁷¹, S. Tisserant ¹⁰¹, S.H. Tlou ^{33g}, A. Tnourji ⁴⁰, K. Todome ^{23b,23a}, S. Todorova-Nova ¹³², S. Todt⁵⁰, M. Togawa ⁸², J. Tojo ⁸⁸, S. Tokár ^{28a}, K. Tokushuku ⁸², R. Tombs ³², M. Tomoto ^{82,110}, L. Tompkins ^{142,q}, K.W. Topolnicki ^{84b}, P. Tornambe ¹⁰², E. Torrence ¹²², H. Torres ⁵⁰, E. Torró Pastor ¹⁶², M. Toscani ³⁰, C. Tosciri ³⁹, M. Tost ¹¹, D.R. Tovey ¹³⁸, A. Traeet¹⁶, I.S. Trandafir ^{27b}, T. Trefzger ¹⁶⁵, A. Tricoli ²⁹, I.M. Trigger ^{155a}, S. Trincaz-Duvoid ¹²⁶, D.A. Trischuk ²⁶, B. Trocmé ⁶⁰, A. Trofymov ⁶⁶, C. Troncon ^{70a}, L. Truong ^{33c}, M. Trzebinski ⁸⁵, A. Trzuppek ⁸⁵, F. Tsai ¹⁴⁴, M. Tsai ¹⁰⁵, A. Tsiamis ¹⁵¹, P.V. Tsiarehka³⁷, S. Tsigaridas ^{155a}, A. Tsirigotis ^{151,u}, V. Tsiskaridze ¹⁴⁴, E.G. Tskhadadze^{148a}, M. Tsopoulou ¹⁵¹, Y. Tsujikawa ⁸⁶, I.I. Tsukerman ³⁷, V. Tsulaia ^{17a}, S. Tsuno ⁸², O. Tsur¹⁴⁹, D. Tsybychev ¹⁴⁴, Y. Tu ^{64b}, A. Tudorache ^{27b}, V. Tudorache ^{27b}, A.N. Tuna ³⁶, S. Turchikhin ³⁸, I. Turk Cakir ^{3a}, R. Turra ^{70a}, T. Turtuvshin ^{38,y}, P.M. Tuts ⁴¹, S. Tzamarias ¹⁵¹, P. Tzanis ¹⁰, E. Tzovara ⁹⁹, K. Uchida¹⁵², F. Ukegawa ¹⁵⁶, P.A. Ulloa Poblete ^{136c}, G. Unal ³⁶, M. Unal ¹¹, A. Undrus ²⁹, G. Unel ¹⁵⁹, J. Urban ^{28b}, P. Urquijo ¹⁰⁴, G. Usai ⁸, R. Ushioda ¹⁵³, M. Usman ¹⁰⁷, Z. Uysal ^{21b}, L. Vacavant ¹⁰¹, V. Vacek ¹³¹, B. Vachon ¹⁰³, K.O.H. Vadla ¹²⁴, T. Vafeiadis ³⁶, A. Vaitkus ⁹⁵, C. Valderanis ¹⁰⁸, E. Valdes Santurio ^{47a,47b}, M. Valente ^{155a}, S. Valentinetti ^{23b,23a}, A. Valero ¹⁶², A. Vallier ^{101,ab}, J.A. Valls Ferrer ¹⁶², T.R. Van Daalen ¹³⁷, P. Van Gemmeren ⁶, M. Van Rijnbach ^{124,36}, S. Van Stroud ⁹⁵, I. Van Vulpen ¹¹³, M. Vanadia ^{75a,75b}, W. Vandelli ³⁶, M. Vandenbroucke ¹³⁴, E.R. Vandewall ¹²⁰, D. Vannicola ¹⁵⁰, L. Vannoli ^{57b,57a}, R. Vari ^{74a}, E.W. Varnes ⁷, C. Varni ^{17a}, T. Varol ¹⁴⁷, D. Varouchas ⁶⁶, L. Varriale ¹⁶², K.E. Varvell ¹⁴⁶, M.E. Vasile ^{27b}, L. Vaslin⁴⁰, G.A. Vasquez ¹⁶⁴, F. Vazeille ⁴⁰, T. Vazquez Schroeder ³⁶, J. Veatch ³¹, V. Vecchio ¹⁰⁰, M.J. Veen ¹⁰², I. Veliscek ¹²⁵, L.M. Veloce ¹⁵⁴, F. Veloso ^{129a,129c}, S. Veneziano ^{74a}, A. Ventura ^{69a,69b}, A. Verbytskyi ¹⁰⁹, M. Verducci ^{73a,73b}, C. Vergis ²⁴, M. Verissimo De Araujo ^{81b}, W. Verkerke ¹¹³, J.C. Vermeulen ¹¹³, C. Vernieri ¹⁴², P.J. Verschuuren ⁹⁴, M. Vessella ¹⁰², M.C. Vetterli ^{141,ah}, A. Vgenopoulos ¹⁵¹, N. Viaux Maira ^{136f}, T. Vickey ¹³⁸, O.E. Vickey Boeriu ¹³⁸, G.H.A. Viehhauser ¹²⁵, L. Vigani ^{63b}, M. Villa ^{23b,23a}, M. Villaplana Perez ¹⁶², E.M. Villhauer⁵², E. Vilucchi ⁵³, M.G. Vincter ³⁴, G.S. Virdee ²⁰, A. Vishwakarma ⁵², C. Vittori ^{23b,23a}, I. Vivarelli ¹⁴⁵, V. Vladimirov¹⁶⁶, E. Voevodina ¹⁰⁹, F. Vogel ¹⁰⁸, P. Vokac ¹³¹, J. Von Ahnen ⁴⁸, E. Von Toerne ²⁴, B. Vormwald ³⁶, V. Vorobel ¹³², K. Vorobev ³⁷, M. Vos ¹⁶², J.H. Vosseveld ⁹¹, M. Vozak ¹¹³, L. Vozdecky ⁹³, N. Vranjes ¹⁵, M. Vranjes Milosavljevic ¹⁵, M. Vreeswijk ¹¹³, R. Vuillermet ³⁶, O. Vujinovic ⁹⁹, I. Vukotic ³⁹, S. Wada ¹⁵⁶, C. Wagner¹⁰², W. Wagner ¹⁷⁰, S. Wahdan ¹⁷⁰, H. Wahlberg ⁸⁹, R. Wakasa ¹⁵⁶, M. Wakida ¹¹⁰, V.M. Walbrecht ¹⁰⁹, J. Walder ¹³³, R. Walker ¹⁰⁸, W. Walkowiak ¹⁴⁰, A.M. Wang ⁶¹, A.Z. Wang ¹⁶⁹, C. Wang ^{62a}, C. Wang ^{62c}, H. Wang ^{17a}, J. Wang ^{64a}, R.-J. Wang ⁹⁹, R. Wang ⁶¹, R. Wang ⁶, S.M. Wang ¹⁴⁷, S. Wang ^{62b}, T. Wang ^{62a}, W.T. Wang ⁷⁹, X. Wang ^{14c}, X. Wang ¹⁶¹, X. Wang ^{62c}, Y. Wang ^{62d}, Y. Wang ^{14c}, Z. Wang ¹⁰⁵, Z. Wang ^{62d,51,62c}, Z. Wang ¹⁰⁵, A. Warburton ¹⁰³, R.J. Ward ²⁰, N. Warrack ⁵⁹, A.T. Watson ²⁰, H. Watson ⁵⁹, M.F. Watson ²⁰, G. Watts ¹³⁷, B.M. Waugh ⁹⁵, A.F. Webb ¹¹, C. Weber ²⁹, H.A. Weber ¹⁸, M.S. Weber ¹⁹, S.M. Weber ^{63a}, C. Wei^{62a}, Y. Wei ¹²⁵, A.R. Weidberg ¹²⁵, J. Weingarten ⁴⁹, M. Weirich ⁹⁹, C. Weiser ⁵⁴, C.J. Wells ⁴⁸, T. Wenaus ²⁹, B. Wendland ⁴⁹, T. Wengler ³⁶, N.S. Wenke¹⁰⁹, N. Wermes ²⁴, M. Wessels ^{63a}, K. Whalen ¹²², A.M. Wharton ⁹⁰, A.S. White ⁶¹, A. White ⁸, M.J. White ¹, D. Whiteson ¹⁵⁹, L. Wickremasinghe ¹²³, W. Wiedenmann ¹⁶⁹, C. Wiel ⁵⁰, M. Wielers ¹³³, N. Wieseotte⁹⁹, C. Wiglesworth ⁴², L.A.M. Wiik-Fuchs ⁵⁴, D.J. Wilbern¹¹⁹, H.G. Wilkens ³⁶, D.M. Williams ⁴¹, H.H. Williams¹²⁷, S. Williams ³², S. Willocq ¹⁰², P.J. Windischhofer ¹²⁵,

F. Winklmeier , B.T. Winter , J.K. Winter , M. Wittgen , M. Wobisch , R. Wölker , J. Wollrath , M.W. Wolter , H. Wolters , V.W.S. Wong , A.F. Wongel , S.D. Worm , B.K. Wosiek , K.W. Woźniak , K. Wraight , J. Wu , M. Wu , M. Wu , S.L. Wu , X. Wu , Y. Wu , Z. Wu , J. Wuerzinger , T.R. Wyatt , B.M. Wynne , S. Xella , L. Xia , M. Xia , J. Xiang , X. Xiao , M. Xie , X. Xie , S. Xin , J. Xiong , I. Xioidis , D. Xu , H. Xu , H. Xu , L. Xu , R. Xu , T. Xu , W. Xu , Y. Xu , Z. Xu , Z. Xu , B. Yabsley , S. Yacoob , N. Yamaguchi , Y. Yamaguchi , H. Yamauchi , T. Yamazaki , Y. Yamazaki , J. Yan , S. Yan , Z. Yan , H.J. Yang , H.T. Yang , S. Yang , T. Yang , X. Yang , X. Yang , Y. Yang , Z. Yang , W-M. Yao , Y.C. Yap , H. Ye , H. Ye , J. Ye , S. Ye , X. Ye , Y. Yeh , I. Yeletsikh , B.K. Yeo , M.R. Yexley , P. Yin , K. Yorita , S. Younas , C.J.S. Young , C. Young , M. Yuan , R. Yuan , L. Yue , X. Yue , M. Zaazoua , B. Zabinski , E. Zaid , T. Zakareishvili , N. Zakharchuk , S. Zambito , J.A. Zamora Saa , J. Zang , D. Zanzi , O. Zaplatilek , S.V. Zeibner , C. Zeitnitz , J.C. Zeng , D.T. Zenger Jr , O. Zenin , T. Ženiš , S. Zenz , S. Zerradi , D. Zerwas , B. Zhang , D.F. Zhang , G. Zhang , J. Zhang , J. Zhang , K. Zhang , L. Zhang , P. Zhang , R. Zhang , S. Zhang , T. Zhang , X. Zhang , X. Zhang , Y. Zhang , Z. Zhang , Z. Zhang , H. Zhao , P. Zhao , T. Zhao , Y. Zhao , Z. Zhao , A. Zhemchugov , X. Zheng , Z. Zheng , D. Zhong , B. Zhou , C. Zhou , H. Zhou , N. Zhou , Y. Zhou , C.G. Zhu , C. Zhu , H.L. Zhu , H. Zhu , J. Zhu , Y. Zhu , Y. Zhu , X. Zhuang , K. Zhukov , V. Zhulanov , N.I. Zimine , J. Zinsser , M. Ziolkowski , L. Živković , A. Zoccoli , K. Zoch , T.G. Zorbas , O. Zormpa , W. Zou , L. Zwalinski .

¹Department of Physics, University of Adelaide, Adelaide; Australia.

²Department of Physics, University of Alberta, Edmonton AB; Canada.

³(^a)Department of Physics, Ankara University, Ankara; (^b)Division of Physics, TOBB University of Economics and Technology, Ankara; Türkiye.

⁴LAPP, Université Savoie Mont Blanc, CNRS/IN2P3, Annecy; France.

⁵APC, Université Paris Cité, CNRS/IN2P3, Paris; France.

⁶High Energy Physics Division, Argonne National Laboratory, Argonne IL; United States of America.

⁷Department of Physics, University of Arizona, Tucson AZ; United States of America.

⁸Department of Physics, University of Texas at Arlington, Arlington TX; United States of America.

⁹Physics Department, National and Kapodistrian University of Athens, Athens; Greece.

¹⁰Physics Department, National Technical University of Athens, Zografou; Greece.

¹¹Department of Physics, University of Texas at Austin, Austin TX; United States of America.

¹²Institute of Physics, Azerbaijan Academy of Sciences, Baku; Azerbaijan.

¹³Institut de Física d'Altes Energies (IFAE), Barcelona Institute of Science and Technology, Barcelona; Spain.

¹⁴(^a)Institute of High Energy Physics, Chinese Academy of Sciences, Beijing; (^b)Physics Department, Tsinghua University, Beijing; (^c)Department of Physics, Nanjing University, Nanjing; (^d)University of Chinese Academy of Science (UCAS), Beijing; China.

¹⁵Institute of Physics, University of Belgrade, Belgrade; Serbia.

¹⁶Department for Physics and Technology, University of Bergen, Bergen; Norway.

¹⁷(^a)Physics Division, Lawrence Berkeley National Laboratory, Berkeley CA; (^b)University of California, Berkeley CA; United States of America.

- ¹⁸Institut für Physik, Humboldt Universität zu Berlin, Berlin; Germany.
- ¹⁹Albert Einstein Center for Fundamental Physics and Laboratory for High Energy Physics, University of Bern, Bern; Switzerland.
- ²⁰School of Physics and Astronomy, University of Birmingham, Birmingham; United Kingdom.
- ²¹(^a) Department of Physics, Bogazici University, Istanbul; (^b) Department of Physics Engineering, Gaziantep University, Gaziantep; (^c) Department of Physics, Istanbul University, Istanbul; (^d) Istinye University, Sariyer, Istanbul; Türkiye.
- ²²(^a) Facultad de Ciencias y Centro de Investigaciones, Universidad Antonio Nariño, Bogotá; (^b) Departamento de Física, Universidad Nacional de Colombia, Bogotá; Colombia.
- ²³(^a) Dipartimento di Fisica e Astronomia A. Righi, Università di Bologna, Bologna; (^b) INFN Sezione di Bologna; Italy.
- ²⁴Physikalisches Institut, Universität Bonn, Bonn; Germany.
- ²⁵Department of Physics, Boston University, Boston MA; United States of America.
- ²⁶Department of Physics, Brandeis University, Waltham MA; United States of America.
- ²⁷(^a) Transilvania University of Brasov, Brasov; (^b) Horia Hulubei National Institute of Physics and Nuclear Engineering, Bucharest; (^c) Department of Physics, Alexandru Ioan Cuza University of Iasi, Iasi; (^d) National Institute for Research and Development of Isotopic and Molecular Technologies, Physics Department, Cluj-Napoca; (^e) University Politehnica Bucharest, Bucharest; (^f) West University in Timisoara, Timisoara; (^g) Faculty of Physics, University of Bucharest, Bucharest; Romania.
- ²⁸(^a) Faculty of Mathematics, Physics and Informatics, Comenius University, Bratislava; (^b) Department of Subnuclear Physics, Institute of Experimental Physics of the Slovak Academy of Sciences, Kosice; Slovak Republic.
- ²⁹Physics Department, Brookhaven National Laboratory, Upton NY; United States of America.
- ³⁰Universidad de Buenos Aires, Facultad de Ciencias Exactas y Naturales, Departamento de Física, y CONICET, Instituto de Física de Buenos Aires (IFIBA), Buenos Aires; Argentina.
- ³¹California State University, CA; United States of America.
- ³²Cavendish Laboratory, University of Cambridge, Cambridge; United Kingdom.
- ³³(^a) Department of Physics, University of Cape Town, Cape Town; (^b) iThemba Labs, Western Cape; (^c) Department of Mechanical Engineering Science, University of Johannesburg, Johannesburg; (^d) National Institute of Physics, University of the Philippines Diliman (Philippines); (^e) University of South Africa, Department of Physics, Pretoria; (^f) University of Zululand, KwaDlangezwa; (^g) School of Physics, University of the Witwatersrand, Johannesburg; South Africa.
- ³⁴Department of Physics, Carleton University, Ottawa ON; Canada.
- ³⁵(^a) Faculté des Sciences Ain Chock, Réseau Universitaire de Physique des Hautes Energies - Université Hassan II, Casablanca; (^b) Faculté des Sciences, Université Ibn-Tofail, Kénitra; (^c) Faculté des Sciences Semlalia, Université Cadi Ayyad, LPHEA-Marrakech; (^d) LPMR, Faculté des Sciences, Université Mohamed Premier, Oujda; (^e) Faculté des sciences, Université Mohammed V, Rabat; (^f) Institute of Applied Physics, Mohammed VI Polytechnic University, Ben Guerir; Morocco.
- ³⁶CERN, Geneva; Switzerland.
- ³⁷Affiliated with an institute covered by a cooperation agreement with CERN.
- ³⁸Affiliated with an international laboratory covered by a cooperation agreement with CERN.
- ³⁹Enrico Fermi Institute, University of Chicago, Chicago IL; United States of America.
- ⁴⁰LPC, Université Clermont Auvergne, CNRS/IN2P3, Clermont-Ferrand; France.
- ⁴¹Nevis Laboratory, Columbia University, Irvington NY; United States of America.
- ⁴²Niels Bohr Institute, University of Copenhagen, Copenhagen; Denmark.
- ⁴³(^a) Dipartimento di Fisica, Università della Calabria, Rende; (^b) INFN Gruppo Collegato di Cosenza, Laboratori Nazionali di Frascati; Italy.

- ⁴⁴Physics Department, Southern Methodist University, Dallas TX; United States of America.
- ⁴⁵Physics Department, University of Texas at Dallas, Richardson TX; United States of America.
- ⁴⁶National Centre for Scientific Research "Demokritos", Agia Paraskevi; Greece.
- ⁴⁷(^a) Department of Physics, Stockholm University; (^b) Oskar Klein Centre, Stockholm; Sweden.
- ⁴⁸Deutsches Elektronen-Synchrotron DESY, Hamburg and Zeuthen; Germany.
- ⁴⁹Fakultät Physik, Technische Universität Dortmund, Dortmund; Germany.
- ⁵⁰Institut für Kern- und Teilchenphysik, Technische Universität Dresden, Dresden; Germany.
- ⁵¹Department of Physics, Duke University, Durham NC; United States of America.
- ⁵²SUPA - School of Physics and Astronomy, University of Edinburgh, Edinburgh; United Kingdom.
- ⁵³INFN e Laboratori Nazionali di Frascati, Frascati; Italy.
- ⁵⁴Physikalisches Institut, Albert-Ludwigs-Universität Freiburg, Freiburg; Germany.
- ⁵⁵II. Physikalisches Institut, Georg-August-Universität Göttingen, Göttingen; Germany.
- ⁵⁶Département de Physique Nucléaire et Corpusculaire, Université de Genève, Genève; Switzerland.
- ⁵⁷(^a) Dipartimento di Fisica, Università di Genova, Genova; (^b) INFN Sezione di Genova; Italy.
- ⁵⁸II. Physikalisches Institut, Justus-Liebig-Universität Giessen, Giessen; Germany.
- ⁵⁹SUPA - School of Physics and Astronomy, University of Glasgow, Glasgow; United Kingdom.
- ⁶⁰LPSC, Université Grenoble Alpes, CNRS/IN2P3, Grenoble INP, Grenoble; France.
- ⁶¹Laboratory for Particle Physics and Cosmology, Harvard University, Cambridge MA; United States of America.
- ⁶²(^a) Department of Modern Physics and State Key Laboratory of Particle Detection and Electronics, University of Science and Technology of China, Hefei; (^b) Institute of Frontier and Interdisciplinary Science and Key Laboratory of Particle Physics and Particle Irradiation (MOE), Shandong University, Qingdao; (^c) School of Physics and Astronomy, Shanghai Jiao Tong University, Key Laboratory for Particle Astrophysics and Cosmology (MOE), SKLPPC, Shanghai; (^d) Tsung-Dao Lee Institute, Shanghai; China.
- ⁶³(^a) Kirchhoff-Institut für Physik, Ruprecht-Karls-Universität Heidelberg, Heidelberg; (^b) Physikalisches Institut, Ruprecht-Karls-Universität Heidelberg, Heidelberg; Germany.
- ⁶⁴(^a) Department of Physics, Chinese University of Hong Kong, Shatin, N.T., Hong Kong; (^b) Department of Physics, University of Hong Kong, Hong Kong; (^c) Department of Physics and Institute for Advanced Study, Hong Kong University of Science and Technology, Clear Water Bay, Kowloon, Hong Kong; China.
- ⁶⁵Department of Physics, National Tsing Hua University, Hsinchu; Taiwan.
- ⁶⁶IJCLab, Université Paris-Saclay, CNRS/IN2P3, 91405, Orsay; France.
- ⁶⁷Department of Physics, Indiana University, Bloomington IN; United States of America.
- ⁶⁸(^a) INFN Gruppo Collegato di Udine, Sezione di Trieste, Udine; (^b) ICTP, Trieste; (^c) Dipartimento Politecnico di Ingegneria e Architettura, Università di Udine, Udine; Italy.
- ⁶⁹(^a) INFN Sezione di Lecce; (^b) Dipartimento di Matematica e Fisica, Università del Salento, Lecce; Italy.
- ⁷⁰(^a) INFN Sezione di Milano; (^b) Dipartimento di Fisica, Università di Milano, Milano; Italy.
- ⁷¹(^a) INFN Sezione di Napoli; (^b) Dipartimento di Fisica, Università di Napoli, Napoli; Italy.
- ⁷²(^a) INFN Sezione di Pavia; (^b) Dipartimento di Fisica, Università di Pavia, Pavia; Italy.
- ⁷³(^a) INFN Sezione di Pisa; (^b) Dipartimento di Fisica E. Fermi, Università di Pisa, Pisa; Italy.
- ⁷⁴(^a) INFN Sezione di Roma; (^b) Dipartimento di Fisica, Sapienza Università di Roma, Roma; Italy.
- ⁷⁵(^a) INFN Sezione di Roma Tor Vergata; (^b) Dipartimento di Fisica, Università di Roma Tor Vergata, Roma; Italy.
- ⁷⁶(^a) INFN Sezione di Roma Tre; (^b) Dipartimento di Matematica e Fisica, Università Roma Tre, Roma; Italy.
- ⁷⁷(^a) INFN-TIFPA; (^b) Università degli Studi di Trento, Trento; Italy.
- ⁷⁸Universität Innsbruck, Department of Astro and Particle Physics, Innsbruck; Austria.
- ⁷⁹University of Iowa, Iowa City IA; United States of America.

- ⁸⁰Department of Physics and Astronomy, Iowa State University, Ames IA; United States of America.
- ⁸¹(^a) Departamento de Engenharia Elétrica, Universidade Federal de Juiz de Fora (UFJF), Juiz de Fora; (^b) Universidade Federal do Rio De Janeiro COPPE/EE/IF, Rio de Janeiro; (^c) Instituto de Física, Universidade de São Paulo, São Paulo; (^d) Rio de Janeiro State University, Rio de Janeiro; Brazil.
- ⁸²KEK, High Energy Accelerator Research Organization, Tsukuba; Japan.
- ⁸³Graduate School of Science, Kobe University, Kobe; Japan.
- ⁸⁴(^a) AGH University of Science and Technology, Faculty of Physics and Applied Computer Science, Krakow; (^b) Marian Smoluchowski Institute of Physics, Jagiellonian University, Krakow; Poland.
- ⁸⁵Institute of Nuclear Physics Polish Academy of Sciences, Krakow; Poland.
- ⁸⁶Faculty of Science, Kyoto University, Kyoto; Japan.
- ⁸⁷Kyoto University of Education, Kyoto; Japan.
- ⁸⁸Research Center for Advanced Particle Physics and Department of Physics, Kyushu University, Fukuoka ; Japan.
- ⁸⁹Instituto de Física La Plata, Universidad Nacional de La Plata and CONICET, La Plata; Argentina.
- ⁹⁰Physics Department, Lancaster University, Lancaster; United Kingdom.
- ⁹¹Oliver Lodge Laboratory, University of Liverpool, Liverpool; United Kingdom.
- ⁹²Department of Experimental Particle Physics, Jožef Stefan Institute and Department of Physics, University of Ljubljana, Ljubljana; Slovenia.
- ⁹³School of Physics and Astronomy, Queen Mary University of London, London; United Kingdom.
- ⁹⁴Department of Physics, Royal Holloway University of London, Egham; United Kingdom.
- ⁹⁵Department of Physics and Astronomy, University College London, London; United Kingdom.
- ⁹⁶Louisiana Tech University, Ruston LA; United States of America.
- ⁹⁷Fysiska institutionen, Lunds universitet, Lund; Sweden.
- ⁹⁸Departamento de Física Teórica C-15 and CIAFF, Universidad Autónoma de Madrid, Madrid; Spain.
- ⁹⁹Institut für Physik, Universität Mainz, Mainz; Germany.
- ¹⁰⁰School of Physics and Astronomy, University of Manchester, Manchester; United Kingdom.
- ¹⁰¹CPPM, Aix-Marseille Université, CNRS/IN2P3, Marseille; France.
- ¹⁰²Department of Physics, University of Massachusetts, Amherst MA; United States of America.
- ¹⁰³Department of Physics, McGill University, Montreal QC; Canada.
- ¹⁰⁴School of Physics, University of Melbourne, Victoria; Australia.
- ¹⁰⁵Department of Physics, University of Michigan, Ann Arbor MI; United States of America.
- ¹⁰⁶Department of Physics and Astronomy, Michigan State University, East Lansing MI; United States of America.
- ¹⁰⁷Group of Particle Physics, University of Montreal, Montreal QC; Canada.
- ¹⁰⁸Fakultät für Physik, Ludwig-Maximilians-Universität München, München; Germany.
- ¹⁰⁹Max-Planck-Institut für Physik (Werner-Heisenberg-Institut), München; Germany.
- ¹¹⁰Graduate School of Science and Kobayashi-Maskawa Institute, Nagoya University, Nagoya; Japan.
- ¹¹¹Department of Physics and Astronomy, University of New Mexico, Albuquerque NM; United States of America.
- ¹¹²Institute for Mathematics, Astrophysics and Particle Physics, Radboud University/Nikhef, Nijmegen; Netherlands.
- ¹¹³Nikhef National Institute for Subatomic Physics and University of Amsterdam, Amsterdam; Netherlands.
- ¹¹⁴Department of Physics, Northern Illinois University, DeKalb IL; United States of America.
- ¹¹⁵(^a) New York University Abu Dhabi, Abu Dhabi; (^b) University of Sharjah, Sharjah; United Arab Emirates.
- ¹¹⁶Department of Physics, New York University, New York NY; United States of America.

- ¹¹⁷Ochanomizu University, Otsuka, Bunkyo-ku, Tokyo; Japan.
- ¹¹⁸Ohio State University, Columbus OH; United States of America.
- ¹¹⁹Homer L. Dodge Department of Physics and Astronomy, University of Oklahoma, Norman OK; United States of America.
- ¹²⁰Department of Physics, Oklahoma State University, Stillwater OK; United States of America.
- ¹²¹Palacký University, Joint Laboratory of Optics, Olomouc; Czech Republic.
- ¹²²Institute for Fundamental Science, University of Oregon, Eugene, OR; United States of America.
- ¹²³Graduate School of Science, Osaka University, Osaka; Japan.
- ¹²⁴Department of Physics, University of Oslo, Oslo; Norway.
- ¹²⁵Department of Physics, Oxford University, Oxford; United Kingdom.
- ¹²⁶LPNHE, Sorbonne Université, Université Paris Cité, CNRS/IN2P3, Paris; France.
- ¹²⁷Department of Physics, University of Pennsylvania, Philadelphia PA; United States of America.
- ¹²⁸Department of Physics and Astronomy, University of Pittsburgh, Pittsburgh PA; United States of America.
- ¹²⁹^(a)Laboratório de Instrumentação e Física Experimental de Partículas - LIP, Lisboa;^(b)Departamento de Física, Faculdade de Ciências, Universidade de Lisboa, Lisboa;^(c)Departamento de Física, Universidade de Coimbra, Coimbra;^(d)Centro de Física Nuclear da Universidade de Lisboa, Lisboa;^(e)Departamento de Física, Universidade do Minho, Braga;^(f)Departamento de Física Teórica y del Cosmos, Universidad de Granada, Granada (Spain);^(g)Departamento de Física, Instituto Superior Técnico, Universidade de Lisboa, Lisboa; Portugal.
- ¹³⁰Institute of Physics of the Czech Academy of Sciences, Prague; Czech Republic.
- ¹³¹Czech Technical University in Prague, Prague; Czech Republic.
- ¹³²Charles University, Faculty of Mathematics and Physics, Prague; Czech Republic.
- ¹³³Particle Physics Department, Rutherford Appleton Laboratory, Didcot; United Kingdom.
- ¹³⁴IRFU, CEA, Université Paris-Saclay, Gif-sur-Yvette; France.
- ¹³⁵Santa Cruz Institute for Particle Physics, University of California Santa Cruz, Santa Cruz CA; United States of America.
- ¹³⁶^(a)Departamento de Física, Pontificia Universidad Católica de Chile, Santiago;^(b)Millennium Institute for Subatomic physics at high energy frontier (SAPHIR), Santiago;^(c)Instituto de Investigación Multidisciplinario en Ciencia y Tecnología, y Departamento de Física, Universidad de La Serena;^(d)Universidad Andres Bello, Department of Physics, Santiago;^(e)Instituto de Alta Investigación, Universidad de Tarapacá, Arica;^(f)Departamento de Física, Universidad Técnica Federico Santa María, Valparaíso; Chile.
- ¹³⁷Department of Physics, University of Washington, Seattle WA; United States of America.
- ¹³⁸Department of Physics and Astronomy, University of Sheffield, Sheffield; United Kingdom.
- ¹³⁹Department of Physics, Shinshu University, Nagano; Japan.
- ¹⁴⁰Department Physik, Universität Siegen, Siegen; Germany.
- ¹⁴¹Department of Physics, Simon Fraser University, Burnaby BC; Canada.
- ¹⁴²SLAC National Accelerator Laboratory, Stanford CA; United States of America.
- ¹⁴³Department of Physics, Royal Institute of Technology, Stockholm; Sweden.
- ¹⁴⁴Departments of Physics and Astronomy, Stony Brook University, Stony Brook NY; United States of America.
- ¹⁴⁵Department of Physics and Astronomy, University of Sussex, Brighton; United Kingdom.
- ¹⁴⁶School of Physics, University of Sydney, Sydney; Australia.
- ¹⁴⁷Institute of Physics, Academia Sinica, Taipei; Taiwan.
- ¹⁴⁸^(a)E. Andronikashvili Institute of Physics, Iv. Javakhishvili Tbilisi State University, Tbilisi;^(b)High Energy Physics Institute, Tbilisi State University, Tbilisi;^(c)University of Georgia, Tbilisi; Georgia.

- ¹⁴⁹Department of Physics, Technion, Israel Institute of Technology, Haifa; Israel.
- ¹⁵⁰Raymond and Beverly Sackler School of Physics and Astronomy, Tel Aviv University, Tel Aviv; Israel.
- ¹⁵¹Department of Physics, Aristotle University of Thessaloniki, Thessaloniki; Greece.
- ¹⁵²International Center for Elementary Particle Physics and Department of Physics, University of Tokyo, Tokyo; Japan.
- ¹⁵³Department of Physics, Tokyo Institute of Technology, Tokyo; Japan.
- ¹⁵⁴Department of Physics, University of Toronto, Toronto ON; Canada.
- ¹⁵⁵(^a) TRIUMF, Vancouver BC; (^b) Department of Physics and Astronomy, York University, Toronto ON; Canada.
- ¹⁵⁶Division of Physics and Tomonaga Center for the History of the Universe, Faculty of Pure and Applied Sciences, University of Tsukuba, Tsukuba; Japan.
- ¹⁵⁷Department of Physics and Astronomy, Tufts University, Medford MA; United States of America.
- ¹⁵⁸United Arab Emirates University, Al Ain; United Arab Emirates.
- ¹⁵⁹Department of Physics and Astronomy, University of California Irvine, Irvine CA; United States of America.
- ¹⁶⁰Department of Physics and Astronomy, University of Uppsala, Uppsala; Sweden.
- ¹⁶¹Department of Physics, University of Illinois, Urbana IL; United States of America.
- ¹⁶²Instituto de Física Corpuscular (IFIC), Centro Mixto Universidad de Valencia - CSIC, Valencia; Spain.
- ¹⁶³Department of Physics, University of British Columbia, Vancouver BC; Canada.
- ¹⁶⁴Department of Physics and Astronomy, University of Victoria, Victoria BC; Canada.
- ¹⁶⁵Fakultät für Physik und Astronomie, Julius-Maximilians-Universität Würzburg, Würzburg; Germany.
- ¹⁶⁶Department of Physics, University of Warwick, Coventry; United Kingdom.
- ¹⁶⁷Waseda University, Tokyo; Japan.
- ¹⁶⁸Department of Particle Physics and Astrophysics, Weizmann Institute of Science, Rehovot; Israel.
- ¹⁶⁹Department of Physics, University of Wisconsin, Madison WI; United States of America.
- ¹⁷⁰Fakultät für Mathematik und Naturwissenschaften, Fachgruppe Physik, Bergische Universität Wuppertal, Wuppertal; Germany.
- ¹⁷¹Department of Physics, Yale University, New Haven CT; United States of America.
- ^a Also Affiliated with an institute covered by a cooperation agreement with CERN.
- ^b Also at An-Najah National University, Nablus; Palestine.
- ^c Also at Borough of Manhattan Community College, City University of New York, New York NY; United States of America.
- ^d Also at Bruno Kessler Foundation, Trento; Italy.
- ^e Also at Center for High Energy Physics, Peking University; China.
- ^f Also at Centro Studi e Ricerche Enrico Fermi; Italy.
- ^g Also at CERN, Geneva; Switzerland.
- ^h Also at Département de Physique Nucléaire et Corpusculaire, Université de Genève, Genève; Switzerland.
- ⁱ Also at Departament de Física de la Universitat Autònoma de Barcelona, Barcelona; Spain.
- ^j Also at Department of Financial and Management Engineering, University of the Aegean, Chios; Greece.
- ^k Also at Department of Physics and Astronomy, Michigan State University, East Lansing MI; United States of America.
- ^l Also at Department of Physics and Astronomy, University of Louisville, Louisville, KY; United States of America.
- ^m Also at Department of Physics, Ben Gurion University of the Negev, Beer Sheva; Israel.
- ⁿ Also at Department of Physics, California State University, East Bay; United States of America.
- ^o Also at Department of Physics, California State University, Sacramento; United States of America.

- p* Also at Department of Physics, King's College London, London; United Kingdom.
- q* Also at Department of Physics, Stanford University, Stanford CA; United States of America.
- r* Also at Department of Physics, University of Fribourg, Fribourg; Switzerland.
- s* Also at Department of Physics, University of Thessaly; Greece.
- t* Also at Department of Physics, Westmont College, Santa Barbara; United States of America.
- u* Also at Hellenic Open University, Patras; Greece.
- v* Also at Institutio Catalana de Recerca i Estudis Avancats, ICREA, Barcelona; Spain.
- w* Also at Institut für Experimentalphysik, Universität Hamburg, Hamburg; Germany.
- x* Also at Institute of Particle Physics (IPP); Canada.
- y* Also at Institute of Physics and Technology, Ulaanbaatar; Mongolia.
- z* Also at Institute of Physics, Azerbaijan Academy of Sciences, Baku; Azerbaijan.
- aa* Also at Institute of Theoretical Physics, Ilia State University, Tbilisi; Georgia.
- ab* Also at L2IT, Université de Toulouse, CNRS/IN2P3, UPS, Toulouse; France.
- ac* Also at Lawrence Livermore National Laboratory, Livermore; United States of America.
- ad* Also at National Institute of Physics, University of the Philippines Diliman (Philippines); Philippines.
- ae* Also at RWTH Aachen University, III. Physikalisches Institut A, Aachen; Germany.
- af* Also at Technical University of Munich, Munich; Germany.
- ag* Also at The Collaborative Innovation Center of Quantum Matter (CICQM), Beijing; China.
- ah* Also at TRIUMF, Vancouver BC; Canada.
- ai* Also at Università di Napoli Parthenope, Napoli; Italy.
- aj* Also at University of Chinese Academy of Sciences (UCAS), Beijing; China.
- ak* Also at University of Colorado Boulder, Department of Physics, Colorado; United States of America.
- al* Also at Washington College, Maryland; United States of America.
- am* Also at Yeditepe University, Physics Department, Istanbul; Türkiye.
- * Deceased